Expanding antibiotic chemical space through precursor-directed biosynthesis

Mahmud Tareq Morshed

Department of Chemistry and Biomolecular Sciences

Macquarie University

10th October, 2016

Abstract

The rapid emergence of multidrug-resistant microorganisms demands continuous development of new antibiotics with novel modes of action. However, very few candidates are currently in the pipeline. The present study addresses this challenge by combining natural product chemistry, precursor-directed biosynthesis and chemical derivatisation to expand the chemical space around nidulin, an antibiotic depsidone first isolated from *Aspergillus nidulans* in 1944. Initial optimisation of culture media led to two new fungal metabolites, 7-carboxyfolipastatin and unguinolic acid, as well as four previously reported compounds. In precursor-directed biosynthesis experiments, *Aspergillus unguis* was fed unnatural salicylic acid and orsellinic acid derivatives, which did not yield any new nidulin analogues. However, supplementing the culture medium with halide salts led to three new depsides, unguidepside A, unguidepside B and 5-bromoagonodepside B, and one new depsidone, 2-bromo-7-chlorounguinol. Finally, a semi-synthetic approach was employed to generate six nidulin analogues. All natural, unnatural and semi-synthetic compounds were screened for antibacterial, antifungal and cell cytotoxicity activities. Among the new depsides and depsidones, 2-bromo-7-chlorounguinol showed good antibacterial activity (IC_{50} 2.8 µg/mL), while 2,4-diiodo-1′,2′-dihydrounguinol exhibited the highest antibacterial activity (IC_{50} 0.99 µg/mL) against *Bacillus subtilis* among the all synthetic compounds. A structure-activity relationship for the nidulin pharmacophore was proposed.

Acknowledgements

Firstly, I would like to thank my supervisor, Dr Andrew Piggott, for his excellent advice, constant encouragement and reassurance throughout my MRes studies. His caring nature, calm attitude and patience with me throughout, helped me to complete this thesis. He stood by me during a very difficult time of my life. Thank you. I feel so lucky to have worked with him. Thanks also to my associate supervisor, Prof. Peter Karuso, for his feedback during group meetings.

Many thanks to Dr Ernest Lacey and other lab members, specially Daniel Vuong, Andrew Crombie and David Handler at Microbial Screening Technologies (MST) for support during my lab work. I really enjoyed working at MST.

I would like to thank the members of the Piggott Group, especially Dr Jenny Vo and Shalini for making the lab an enjoyable place to work. Many thanks to the Karuso Group members for helping me on numerous occasions.

I would also like to thank other members of the CBMS Department. I would especially like to thank Dr Erika Davies and Anthony Gurlica for their help and support.

Last but not least I would like to thank my wife, Tahira Foyzun Munia, my beloved son and my parents for their support, love and encouragement throughout this journey.

Finally, my thanks to Allah who made all things possible.

Declaration

I hereby declare that this thesis entitled ‘Expanding antibiotic chemical space through precursor-directed biosynthesis’ represents my own work entirely and has not previously been submitted for a degree to any other university or institution other than Macquarie University. In addition, I certify that all information sources and literature used are indicated in the thesis.

_____ _____

Mahmud Tareq Morshed Dated

Table of Contents

1 Introduction

1.1 Antibiotic resistance and global scenario

After the discovery of penicillin, antibiotics have been considered as a 'cure-all' drug for all types of infection regardless of the source[1]. During the golden era of antibiotic discovery, which spanned only between 1940-1960, a substantial number of antibiotics were discovered and soon after it was thought that infectious diseases would be eliminated[2]. However, due to the widespread use and misuse of antibiotics, microorganisms developed resistance quickly and in some cases, such as tetracycline and streptomycin, resistance was reported in the same year of their introduction for clinical use[3-4]. Following the golden era of antibiotic discovery, we passed through the medicinal chemistry era (1960-1990), where synthetic modifications of old scaffolds were performed with high success. We are now living in the antibiotics resistance (post antibiotics) era, where multiple drug resistant 'ESKAPE' organisms (*Enterococcus* spp., *Staphylococcus aureus*, *Klebsiella* spp., *Acinetobacter baumannii*, *Pseudomonas aeruginosa* and *Enterobacter* spp.) have become increasingly prevalent and we are unable to tackle many of these infection-causing organisms with existing antibiotics[5]. According to the European Centre for Disease Control (ECDC) and the US Centers for Disease Control and Prevention (CDC), every year around 25000 and 23000 people die in Europe and USA respectively from antibiotic-resistant organisms. The impact of antibiotic resistance is also high in terms of morbidity, mortality and healthcare costs[4] and the World Health Organization (WHO) has declared that antibiotic resistance is one of the greatest threats to global health[6].

Antibiotics may be bacteriostatic or bactericidal and when an organism develops resistance it is unable to stop or kill the microorganism at the concentration where susceptible microorganisms shows a response. Generally there are four well-understood mechanisms of resistance to antimicrobial agents, which include destruction of the antibiotic by enzymes (e.g. β-lactamase), antibiotic target modification by mutation, reduced uptake or active efflux of the antibiotic, or overproduction of the antibiotic target[7]. Apart from these mechanisms, new resistance mechanisms are also appearing and it is now generally accepted that antibiotic resistance cannot be prevented, but only controlled[8]. To address this global health crisis, immediate action is needed, including development of new antibiotic scaffolds with different modes of action, repurposing or reinvestigating the old and neglected antibiotics and searching an alternative to antibiotics for treating bacterial infections.

1.2 Microbial sources of antibiotics

Historically, natural products and their derivatives have played a vital role in the discovery of leads for the development of therapeutics. Over the last 30 years, 41% of drugs have come from natural products or their derivatives[9]. Microbes (bacteria and fungi) have proven to be a good source of

natural products for drug discovery and development compare to other sources[10]. Significantly the proportion of antiinfective agents, including antibacterials, antifungals, antivirals and antiparasitics that come from natural derivatives is high.

Secondary metabolites are highly chemically diverse molecules when compared to synthetic or combinatorial compounds. The extremely versatile biosynthetic pathways of microbial metabolite and unique combination of rare moieties and skeletons gives them uniqueness and potent activity. Apart from the natural structural diversity of secondary metabolites, other special characteristics of these compounds are the selectivity and specificity of their mechanisms of action[11].

1.3 Ways to expand antibiotics chemical space

Antibiotic drug discovery and development has evolved through two different and independent methods. Since the serendipitous discovery of penicillin, a widely used platform for antibiotic drug discovery was the 'Waksman Platform', invented by Selman Waksman in 1940[7]. This platform was mainly based on empirical screening of soil derived streptomycetes for antimicrobial activity without focusing on their mode of action. Using this platform, pharmaceutical companies had been working extensively from 1940 to 1960 and had identified most of the major classes of antibiotics that are currently using in the clinic[12-13]. As resistance to these antibiotic classes began to emerge, medicinal chemists began modifying their side chains whilst keeping the core antibiotic pharmacophore intact, resulting in several new generations of antibiotics. Despite the emergence of high-tech drug discovery approaches such as combinatorial chemistry and high throughput screening (HTS), synthetic chemistry has failed to supply new antibiotics, leading to a discovery vacuum. Moreover, it is noteworthy that over the past 40 years, only one new class of synthetic antibiotics drugs was developed, which was the oxazolidinones (linezolid), approved in the US in 2000. On the other hand, only two novel naturally derived antibiotics (daptomycin and retapamulin) were approved during the past 40 years [7, 14]. Against this back drop, there is an urgent need to develop antibiotics with new scaffolds, either from natural sources or using modern synthetic chemistry.

It is evident that the antibiotic drug discovery pipeline has almost dried up and most of these antibiotics are based on existing old scaffolds. Discovery of new antibiotic scaffolds or re-engineering of existing scaffolds is urgently needed to combat antibiotic resistance. The determination of the genome sequence of *Haemophilis influenzae* in 1995, followed by numerous other bacterial genome sequences has identified promising targets for new antibiotic development. The goal of this target-based approach is to identify a target for generations of new antibiotics that are not susceptible to existing mechanisms of resistance. However, two decades have passed and this approach has not delivered an antibiotic to the market[15]. The time has come to explore methods of expanding chemical

space around new and existing antibiotic natural products to deliver next-generation drugs capable of overcoming existing resistance mechanisms.

1.3.1 Cultivation of unculturable microorganisms

Environmental microbes are a major source of novel natural compounds and these compounds are highly diverse in terms of chemical structure. Metagenomic studies suggest that 99% of environmental microorganisms are unculturable using conventional laboratory conditions, leading to an enormous untapped reservoir of structural diversity[16]. Recently, some progress has been made to cultivate some of these unculturable organisms, such as employing simulated natural environment *in situ* and co-culture technique or culture cocktail. Lewis and his group recently isolated a new antibiotic, teixobactin[17], from *Eleftheria terrae*, using an iChip device[18-19]. Genomic analysis of *Eleftheria terrae* (based on 16s rDNA and *in silico* DNA/DNA hybridization) revealed that this organism belongs to a new genus related to *Aquabacteria*. Teixobactin has a different mode of action compared to the other antibiotics that are clinically used. Teixobactin inhibits peptidoglycan biosynthesis by binding to a highly conserved motif of lipid II (a precursor of peptidoglycan) and lipid III (a precursor of teichoic acid). Teixobactin is the first identified lipid II binding agent and is also structurally distinct from other antibiotics. Teixobactin is active against many Gram-positive organisms, including resistant pathogens, but ineffective against most of the Gram-negative pathogens. Significantly, the authors were unable to isolate any teixobactin-resistant *Staphylococcus aureus* and *Mycobacterium tuberculosis* when tested at four times the minimum inhibitory concentration (MIC), which suggest that it will take a longer time for teixobactin resistance to emerge compared to other currently used antibiotics[17].

1.3.2 Interspecies cross-talk or co-culturing

There are several methods to augment the chemodiversity of secondary metabolites produced by microorganisms including mutasynthesis, metabolic engineering, precursor-directed biosynthesis, and co-culture[20]. Mutasynthesis, metabolic engineering and precursor-directed biosynthesis require prior knowledge of the bacterial genome, while co-culture is a genome-independent method for increasing chemodiversity. Watanabe *et al*. in 1982 isolated an antibacterial polyketide, enacyloxine from *Gluconobacter* sp. by co-cultivation with another fungus *Aspergillus oryzae* (Figure 1.1). Since then, co-culture or co-cultivation of microbial species has gained popularity – particularly in the last 5-7 years – and is considered as a key method of new natural product discovery for pharmaceutical and agricultural applications[20-21].

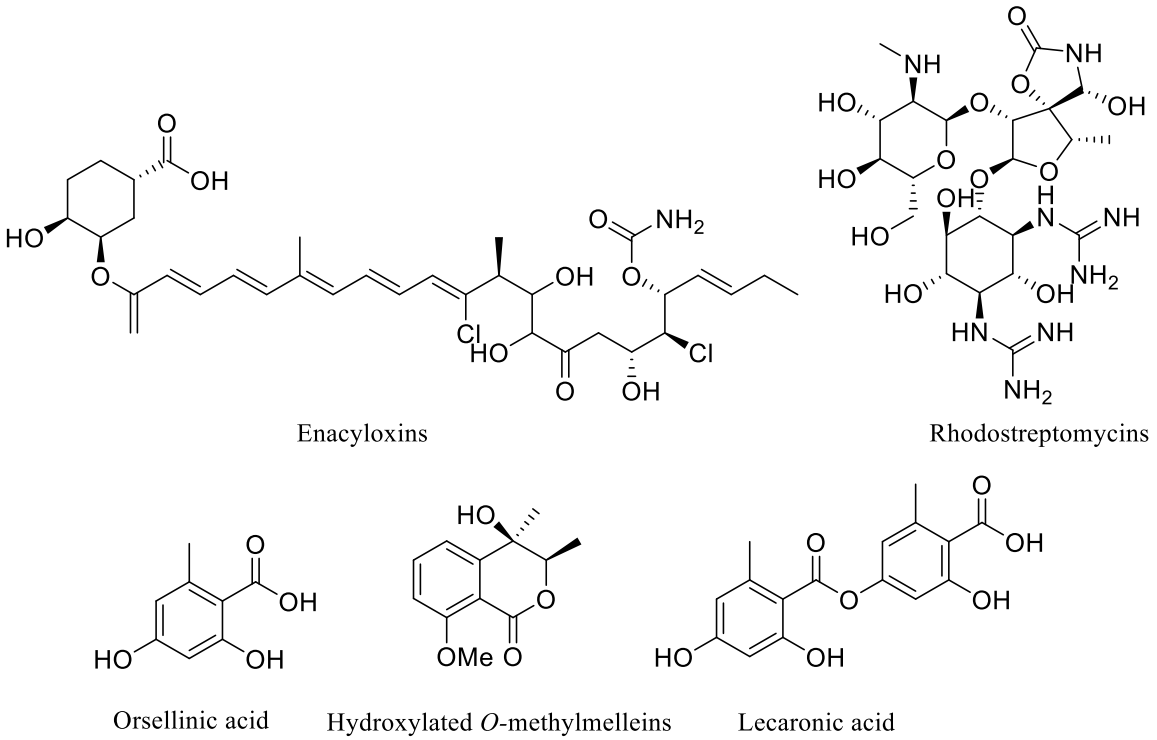

Figure 1.1: Selected compounds isolated via microbial co-culture technique

It should be noted that increased secondary metabolite production has been observed in 20% of cases in *Streptomyces* cross-feeding experiments[22]. Several groups have demonstrated co-culturing that has resulted in the activation of silent cryptic biosynthetic gene clusters in microorganisms, although the molecular mechanism of activation are unknown. Microbial co-culture can be: i) bacterium vs. bacterium; ii) fungus vs. fungus; iii) bacterium vs. fungus. One example of secondary metabolites produced in bacterium vs. bacterium co-culture on solid medium is rhodostreptomycins A and B (aminoglycosides) formed by *Rhodococcus fascians* in mixed cultured with *Streptomyces padanus*[23]. Another example of fungus vs. fungus (*Eutypa lata* and *Botryosphaeria obtuse*) interaction on solid media produced hydroxylated *O*-methylmelleins (polyketide)[24] (Figure 1.1). On the other hand, the bacterium vs. fungus interaction is very common and one good example of this co-culture is the accidental discovery of beta-lactam antibiotic, penicillin in an unintentional co-culture (contamination) of *Staphylococcus* sp. and *Penicillum* sp. by Fleming. This interaction is also exemplified by the isolation of orsellinic acid, lecanoric acid, and other polyketides from liquid media co-culture of *Aspergillus nidulans* and *Escherichia coli*[25].

1.3.3 Semi-synthetic approach

Semi-synthetic chemical and enzymatic modification or addition of functional groups at various sites on a core scaffold have been used in antibiotic drug development to overcome resistance, improve pharmacokinetics and reduce toxicity[26-27]. Since the semisynthetic production of dihydrostreptomycin and tetracycline, a pioneering work done by Merck/Squibb and Pfizer in 1946 and 1952 respectively,

this process enables the improvement of all the major classes of natural antibiotics to tackle resistant organisms[26]. Synthetic modification of existing antibiotic scaffolds is an effective and frequently employed tool in antibiotic discovery and development. One example of this semi-synthetic drug modification is amoxicillin, a broad spectrum β-lactam antibiotic. Modification of the 6-aminopenicilanic acid ring with *α*-amino-*p*-hydroxy-phenylacetic acid gave rise to amoxicillin with improved antibacterial activity and pharmacokinetic properties[28]. Another example of this approach is the second generation glycopeptides antibiotics. The extensive use of vancomycin for the treatment of a wide range of infections has seen the emergence of vancomycin-resistant *Staphylococcus aureus* (VRSA) and vancomycin-resistant enterococci (VRE)[29]. Second generation glycopeptides, such as telavancin, oritavancin and dalbavancin, were developed by semi-synthesis, with some unique features over vancomycin[30-31]. Pleuromutilin, a naturally occurring fungal metabolite, was first isolated by Kavanagh and coworkers in the early 1950s[32]. Later, Egger reported semi-synthetic derivatives of pleuromutilin with improved antimicrobial activity[33]. Currently, there are three pluromutilin analogues available on the market, namely valnemulin, tiamulin, and retapamulin. Valnemulin and tiamulin are used as veterinary drugs, whereas retapamulin is the first pleuromutilin antibiotic that has been approved for human use by FDA (2007)[34-35]. Tigecycline, a third generation semi-synthetic tetracycline, overcomes the traditional tetracycline resistance mechanisms, including efflux pumps and ribosomal protection[36].

1.3.4 Precursor-directed biosynthesis

One of the earliest approaches to expand chemodiversity, increase bioactivity and reduce toxicity of natural products is precursor-directed biosynthesis (PDB)[20]. PDB involves the generation of novel natural products by feeding the organism with unnatural precursor analogues, which are incorporated by existing biosynthetic pathway to produce unnatural analogues[37]. PDB exploits the substrate promiscuity of many biosynthetic enzymes and does not require any time-consuming genetic modification to generate mutant microorganisms (in mutasynthesis approach), nor enzyme inhibitors (in hybrid biosynthesis). However, there are two factors to be considered for successful implementation of PDB: i) Whether microorganism is cultivable or not (cultivation-dependence) ii) How the target natural product is assembled biosynthetically[38]. After careful selection of unnatural biosynthetic precursors for supplementation studies, there are several factors to be considered in PDB including: i) Are biosynthetic enzymes sufficiently flexibility to accept the unnatural precursor analogues[37]? ii) Will there be any unexpected toxic effects because these unnatural analogues have to be fed in high concentration for incorporation in biosynthetic pathway[38]? iii) Will the unnatural precursor be outcompeted by the natural precursor[39]?

One of the earliest examples of PDB is the production of phenoxymethylpenicillin (penicillin V) by adding phenoxyacetic acid to the *Penicillium chrysogenum* cultivation broth[40-41]. A recent elegant example of PDB was reported by Ritacco[42-43] and coworkers who generated unnatural rapamycin analogues (Figure 1.2). Rapamycin, isolated from *Streptomyces hygroscopicus*, is a polyketide polyene that demonstrates antifungal, immunosuppressive, and antitumour activities[43]. Rapamycin is biosynthesised by both a polyketide synthase and a nonribosomal peptide synthase. Rapamycin has an unusual mechanism of macrocyclic ring formation where L-pipecolate is incorporated in the macrocyclic ring with the help of pipecolate-incorporating enzyme (PIE). By feeding the organism unnatural thia-analogues of L-pipecolate, the authors were able to generate two new thiarapamycins. Though these thiarapamycins have less immunosuppressive activity compared to rapamycin, this study provided deeper insights into the SAR of rapamycin.

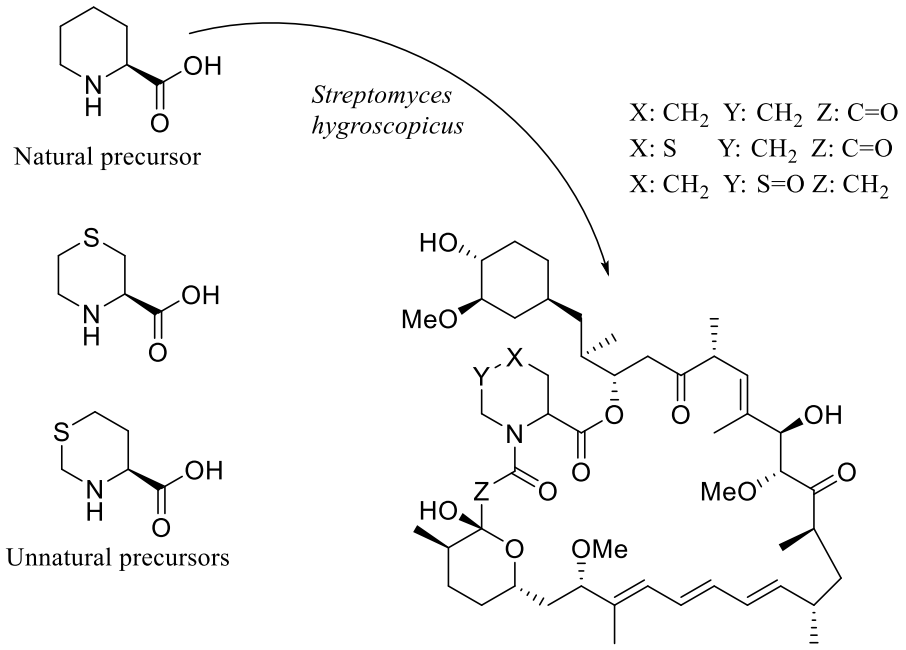

Figure 1.2: Precursor-directed biosynthesis of novel rapamycin analogues

Borrelidin, isolated from several species of *Streptomyces* sp., is an 18-membered polyketide macrolide. The diverse biological activities demonstrated by borrelidin including antibacterial[44], antifungal[45], antimalarial[46], antiangiogenesis and cytotoxic activities[47], have generated significant interest in accessing analogues of the parent compound. Moss and coworkers[48] reported a number of novel borrelidin analogues by PDB using a mutant actinomycetes, *Streptomyces parvulus*, where more than 40 mono- and dicarboxylic acids were added to the culture media. Among the several cyclic dicarboxylic acids investigated, only *trans*-cyclobutane-1,2-dicarboxylic acid produced a novel compound in high yield. Other novel compounds were isolated when 2-methyl- and 2,3-dimethylsuccinic acids were added to the medium (Figure 1.3). All the novel compounds showed

inferior cytotoxicity compare to borrelidin. However, this study successfully decoupled the cytotoxic and antiangiogenic activities of borrelidin.

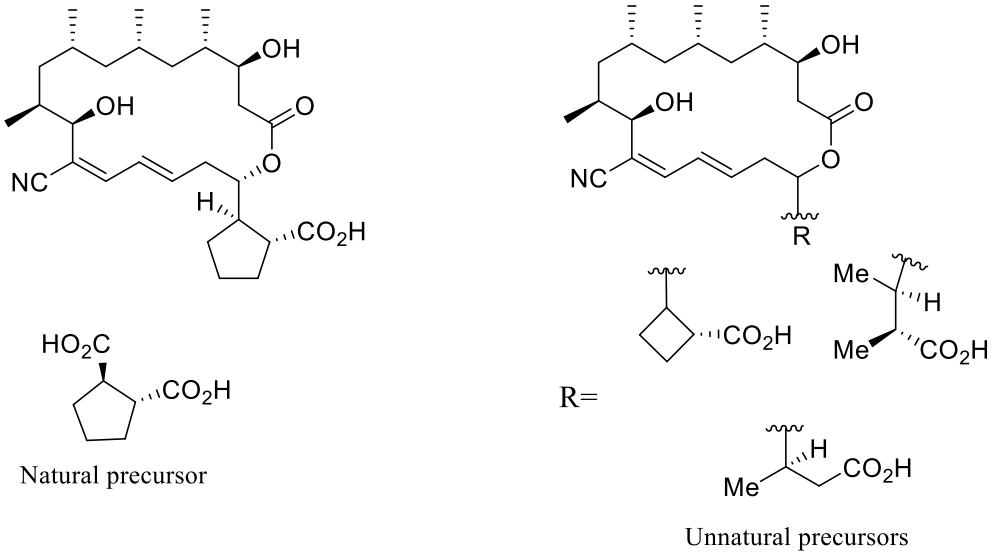

Figure 1.3: Novel borrelidin analogues generated by PDB using *Streptomyces parvulus*

Beauvericin, isolated from several different fungal species including *Beauveria* sp., *Paecilomyces* sp., and *Fusarium* sp., is a cyclohexadepsipeptide formed by a nonribosomal peptide synthetase. Beauvericin has antibacterial, antifungal, antimalarial and insecticidal activities[49]. Two different groups isolated novel beauvericin analogues using PDB by feeding with L-isoleucine and D-isoleucine in the cultivation medium (Figure 1.4). Beauvericin A and allobeauvericin A were isolated in higher concentration than beauvericin and the compounds showed slightly increased cytotoxicity[50]. Xu and coworkers reported six novel beauvericin analogues (beauvericins G_{1-3}, beauvericins H_{1-3}) by feeding different D-2-hydroxyisovalerate (such as DL-2-hydroxybutyrate) and L-phenylanaline (such as DL-3-fluorophenylalanine) analogues respectively. The authors reported that when the branched side chains of D-2-hydroxyisovalerate in beauvericin were replaced step by step by 2-hydroxybutyrate moieties, new analogues beauvericin G_{1-3} lost cytotoxicity activities. Conversely, replacement of the methyl group of L-phenylanaline in beauvericin with fluorine improved the cytotoxic activities of the new beauvericin analogues, beauvericin H_{1-3}[51].

Korkormicins are another example of cyclic depsipeptide antitumour antibiotics isolated from *Micromonospora* sp. Korkormicins exist as a complex mixture of seven compounds (korkormicin A-G) with korkormicin A being the major component. However, by feeding with L-valine in cultivation media, korkormicin A production increased 3-fold compared to the control and it also suppressed the growth of other minor compounds[52]

Rumbrin is a fungal polyketide containing an unusual chloropyrrole moiety, produced by a number of fungi from the order Onygenales. Rumbrin possesses several interesting biological activities, including anticancer[53], cytoprotective, and lipid peroxidation inhibitory activities[54]. Biosynthetic

studies on rumbrin reveals that pyrrole-2-carboxylic acid acts as a precursor during the formation of rumbrin[55]. Clark and coworkers exploited this to produce novel derivatives of rumbrin by feeding

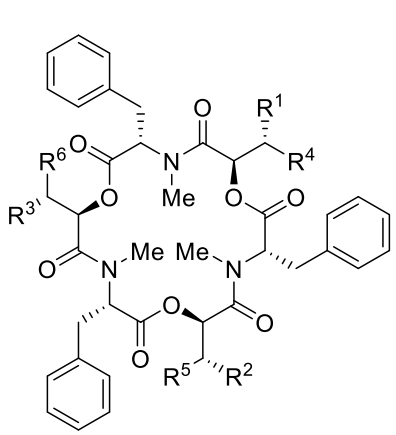

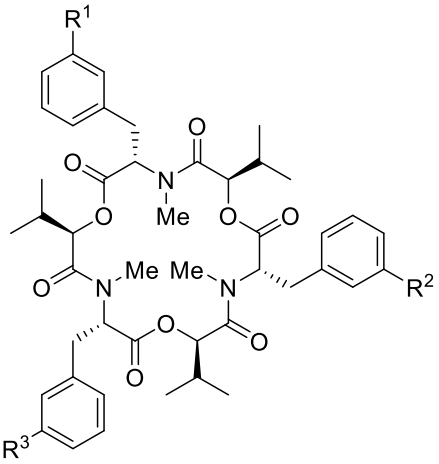

Compounds	R_1	R_2	R_3	R_4	R_5	R_6
Beauericin	Me	Me	Me	H	H	H
Beauvericin A	Et	Me	Me	Me	Me	Me
Allobeauvericin	Me	Me	Me	Et	Me	Me
Beauericin G_1	H	Me	Me	H	H	H
Beauericin G_2	H	H	Me	H	H	H
Beauericin G_3	H	H	H	H	H	H

Compounds	R_1	R_2	R_3	R_4	R_5	R_6
Beauericin H_1	Me	Me	Me	F	H	H
Beauericin H_2	Me	Me	Me	F	F	H
Beauericin H_3	Me	Me	Me	F	F	F

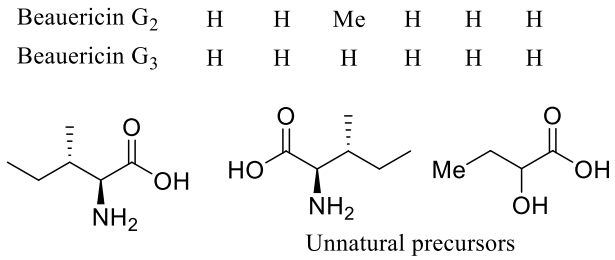

Unnatural precursors

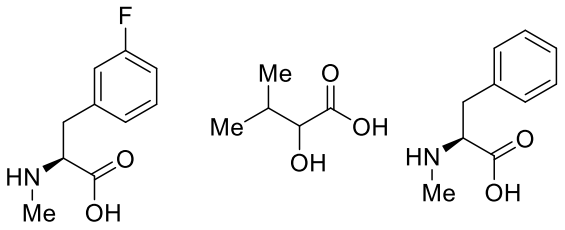

Natural precursors

Figure 1.4: Structure of beauvericin analogues isolated by feeding unnatural precursors

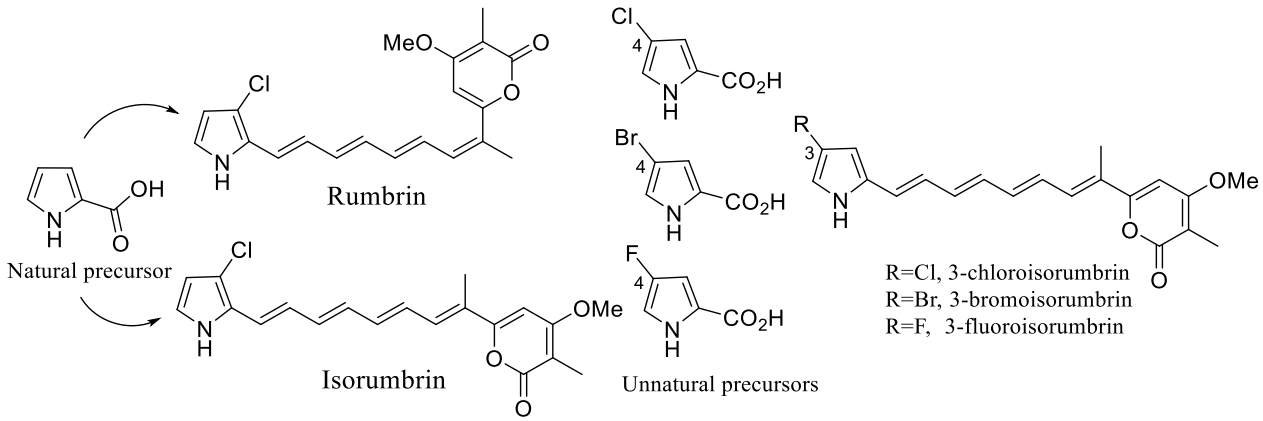

Figure 1.5: Rumbrin, isorumbrin and halogenated derivatives of isorumbrin generated by PDB

Auxarthron umbrinum with a series of substituted pyrrole-2-carboxylic acids[56]. Among the several mono- and di-substituted pyrrole-2-carboxylic acids, selected 4-halo-pyrrole-2-carboxylic acids were incorporated into the biosynthetic pathway sufficiently and generated rumbrin analogues such as 3-fluoro-, 3-chloro- and 3-bromo-isorumbrin, which were isolated from cultivation media in milligram quantities Figure 1.5. Cytotoxicity assays revealed these new isorumbrin compounds shows more

potent activity compared to rumbrin. This experiment demonstrates the potential to customise the pyrrole moiety by synthetic or engineered biosynthetic processes to obtain improved anticancer drugs.

Ammosamides A-F are a group of naturally occurring alkaloids containing a pyrroloquinoline core and produced by marine-derived *Streptomyces* sp. such as *Streptomyces variabilis*. Pan *et al*. made a library of ammosamides G-P, by PDB by supplementing different aryl amines (such as 2-aminobenzoic acid, 4-chloroaniline, benzoimidazole-2-amine) and alkyl amines (such as hexylamine, cyclohexylamine, isopropylamine) to the culture media[57] (Figure 1.6). Among the all ammosamide analogues, ammosamides M and L showed improved cytotoxic activity against non-small cell lung cancer (NSCLC) cell lines.

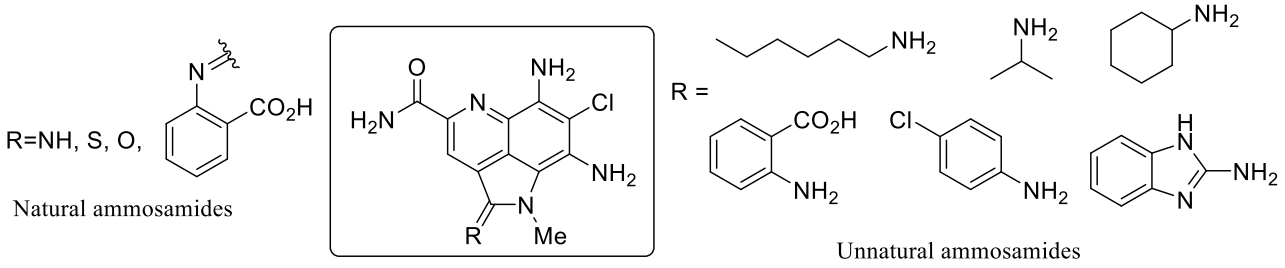

Figure 1.6: Natural ammosamides and unnatural ammosamides by precursor-directed biosynthesis

Micacocidin is another example of a hybrid polyketide and nonribosomal peptide antibiotic isolated from *Ralstonia solanacearum*[58]. Hexanoic acid is the starter unit of micacocidin, which is activated by fatty acid AMP-ligase (FAAL). Biochemical studies confirmed the plasticity of this enzyme to accept different substrates[59]. This finding prompted Kreutzer and coworkers to generate a micacocidin library by PDB. In this study, seven different saturated and unsaturated carboxylic acids were fed to the culture medium. These precursors were previously tested against FAAL to minimise the failure rate of the directed biosynthesis process[58]. This PDB study yielded six unnatural micacocidin analogues, micacocidin $P_{1\text{-}6}$ (Figure 1.7), which showed good activity against *Mycoplasma pneumoniae*, except for the pentenoic acid derivative. Thus, PDB is an effective method to improve the biological activity of natural compounds.

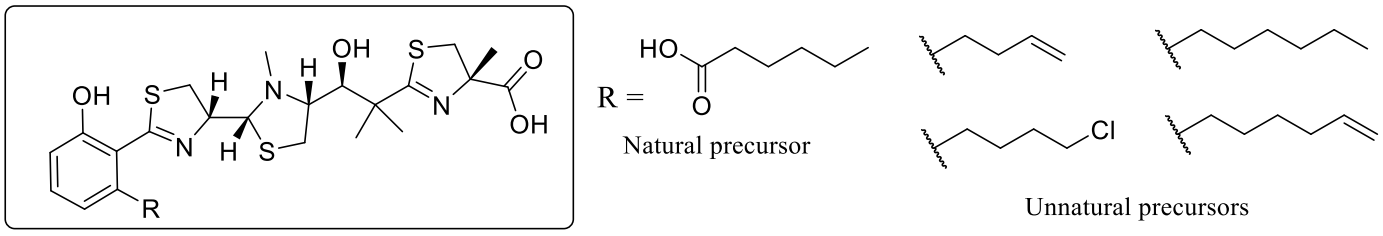

Figure 1.7: Chemical structure of micacocidin and its PDB-derived analogues

Dithiolopyrrolones belong to the pyrrothine class of antibiotics, which possess a unique pyrrolinonodithiole nucleus and exhibit antibacterial, antifungal, antiprotozoal, larvicidal, insecticidal and anticancer activities. There are approximately 30 naturally occurring dithiolopyrrolone

compounds reported to date[60]. These dithiolopyrrolone antibiotics are produced by certain *Streptomyces* spp., and other bacteria such as *Xenorhubdus* sp., the marine bacterium *Alteromonas rava,* and *Saccharothrix algeriensis*[61]. *Saccharothrix algeriensis* produces at least five thiolutin-type dithiolopyrrolones with different branched chains, which suggests there may be enzyme flexibility in the biosynthetic pathway. Later, Bouras *et al.* reported three novel unnatural dithiolopyrrolones (valeryl-pyrrothine, benzoyl-pyrrothine and dimethyl-benzoyl-pyrrothine) by feeding *Saccharothrix algeriensis* with different organic acids such valeric acid and benzoic acid[62] (Figure 1.8).

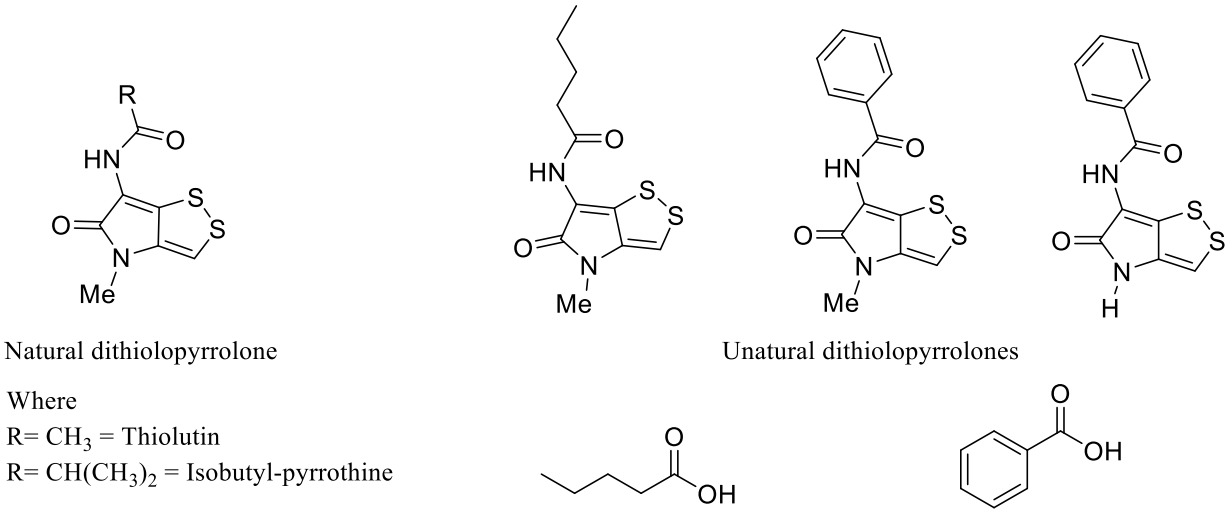

Figure 1.8: Structure of new dithiolopyrrolone derivatives induced by feeding alternative starter unit *via* PDB

Diazepinomicin (a farnesylated trihydroxy-dibenzodiazepinone) is a novel microbial metabolite, isolated from several *Micromonospora* strains. It shows modest antibacterial, anti-inflammatory, and anticancer activities[63]. Biosynthetic studies of diazepinomicin by labeled substrate feeding revealed that ring A of diazepinomicin is formed either from 3-hydroxyanthranilate or from tryptophan[64]. Based on this biosynthetic experiment result, Ratnayake and coworkers added halogenated derivatives of anthranilate (such as, 5-F, 5-Cl, and 5-Br anthranilate) and tryptophan (such as 4-, 5-, or 6- monofluorinated tryptophan) to growing *Micromonospora* culture media. 5- and 6- fluorinated tryptophan and only 5-F anthranilate were assimilated by the microorganism to produce fluoro derivatives of diazepinomicin (Figure 1.9). These fluoro derivatives showed modest antibacterial activity against Gram-positive cocci[63].

Production of synerazol analogues such as fluorosynerazols is an another example of the application of PDB[65]. In this experiment, feeding fluorophenylalanine to the culture medium of *Aspergillus fumigatus* led to the production of novel 19- and 20-fluorosynerazols along with other other fluorinated compounds (Figure 1.9). Bioactivity assays revealed that 19- and 20-fluorosynerazol exhibit more potent antiangiogenic effects than synerazol. Though halogenated secondary metabolites are common, fluorinated secondary metabolites are extremely rare in nature[66]. Thus, PDB

acts as an effective tool in replacement of hydrogen by fluorine in natural products by feeding different fluoroderivative biosynthetic precursors. Similarly, new fluoroderivatives of communesin and iturins were produced by feeding 6-fluorotryptophan and 3-fluorotyrosine to strains of *Penicillium* sp. and *Bacillus subtilis* respectively[67-68].

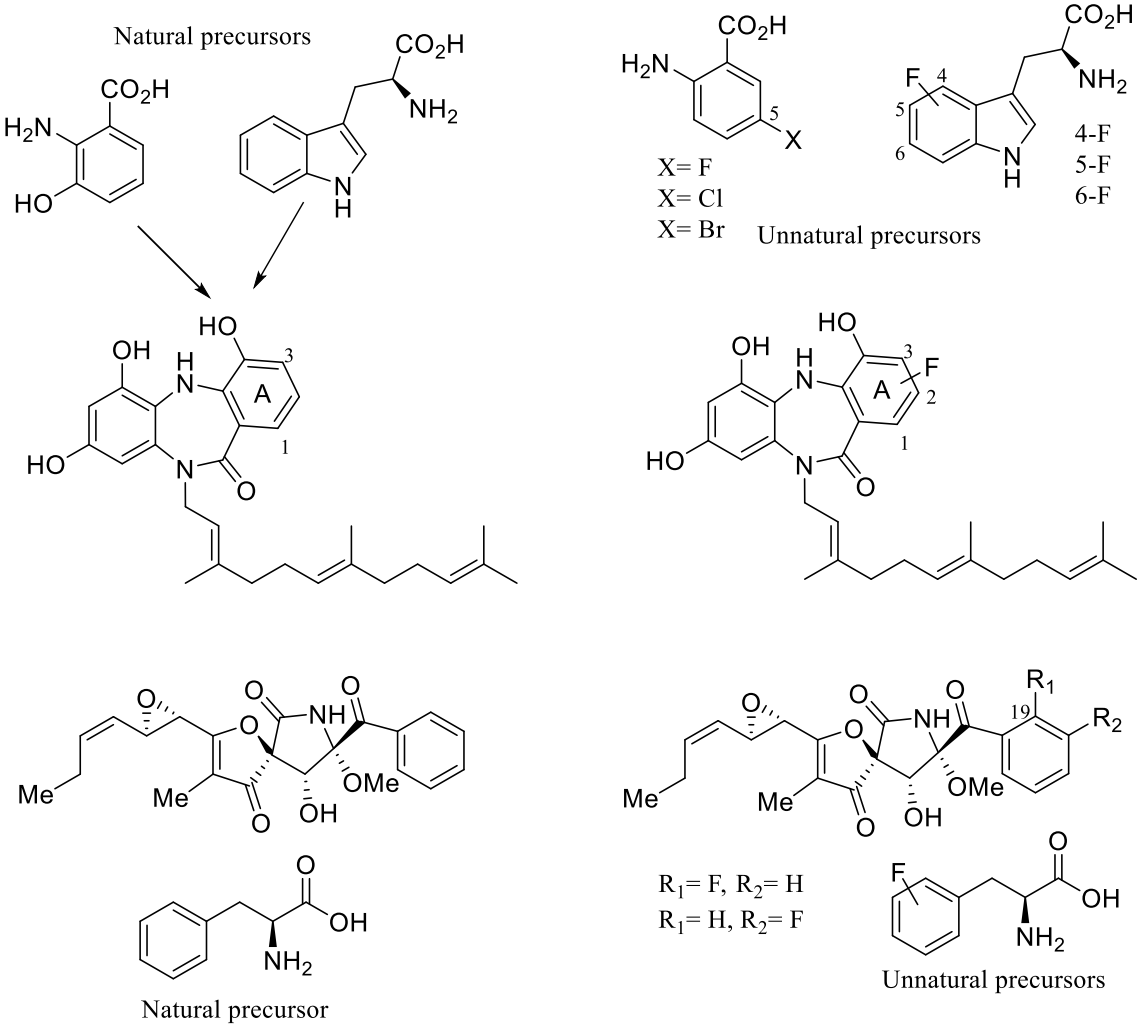

Figure 1.9: Fluorinated derivatives of unnatural products generated by PDB

1.4 Discovery of nidulin and nidulin analogues

In 1944, Kurung isolated a mould, *Aspergillus nidulans* (*Aspergillus unguis*) and demonstrated that the metabolites of this mould inhibit the growth of *Mycobacterium* sp. *in vitro*[69]. Later, in 1946, Hogeboom and Craig first isolated two compounds from the same mould[70]. However, Dean *et al.* reinvestigated all these metabolites and isolated another new compound from the same mould and named these three compounds as nidulin (**1**), nornidulin (**2**) and dechloronidulin (**6**) (Figure 1.10). Furthermore, this group established their structures and confirmed the presence of a depsidone nucleus in these compound in a series of articles[71-73]. In 1963, Beach and Richard confirmed the nidulin structure by classical degradation methods[74]. Recently, it has been reported that nidulin and

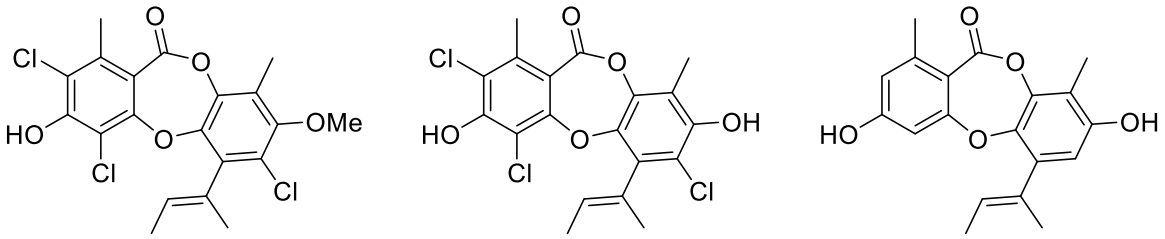

Figure 1.10: Structure of nidulin, nornidulin and unguinol

nornidulin are highly selective and effective against methicillin-resistant *Staphylococcus aureus* (MRSA) with MIC values of 4 and 2 µg/mL respectively[75].

Depside- and depsidone- containing secondary metabolites have been isolated mainly from lichens. However, many depsidones have been isolated from non-lichen sources including, garcidepsidones, leaves of *Garcinia parvifolia*[76]; excelsione, from an endophytic fungus[77]. These naturally occurring depsides and depsidone have broad biological activities, including antibacterial activity against *Mycobacterim* sp. and multidrug-resistant S*taphylococcus aureus* (lecanoric acid, protocetraric acid, norstictic acid, lobaric acid)[78-79] cytotoxic (atranorin, salazinic acid, vicanicin)[80], antioxidant (norstictic and fumarprotocetraric acids)[81] and antiviral (virensic acid and physodic acid)[82] activity. It is hypothesised that depsides are formed by two units of phenolic acids (such as salicylic acid and phenol) via a condensation reaction. Depsidone is biosynthesised from depside via oxidative coupling to form a seven-membered lactone[83].

Aspergillus nidulans grows well in Czapek-Dox medium, which contain 0.05% potassium chloride. Interestingly when this organism was allowed to grow in salt free Czapek-Dox medium, a new chlorine free metabolite was formed. Sierankiewicz and Gatenbeck isolated this compound and named it unguinol (**3**) (*tris*-dechloronornidulin)[84]. Later, it was reported that unguinol has potent herbicidal activity, weak cytotoxic activity[85], and animal growth permittant activity[86]. In 1988, a Japanese group, Nobuo Kawahara and co-workers, isolated 2-chlorounguinol (**5**) from *Emericella unguis* (anamorph: *Aspergillus unguis*)[87] and its structure was confirmed by spectroscopic methods and X-ray crystallography. In the same year, Kawahara and co-workers reported three novel depsidones from the same fungus and named them emeguisins A (**11**), B (**12**) and C (**13**)[88]. Bioassay of these depsidones revealed that emeguisin A (**11**) has monoamine oxidase (MAO) and sterol *O*-acyltransferase (a potential target for anti-atherosclerotic drugs) inhibitory activity and antibacterial activity against *Bacillus subtilis* where emeguisin B has only MAO inhibitory effect. Folipastatin (**4**), another depsidone isolated from *Aspergillus unguis*, was reported in 1992 along with the known compound unguinol and *in vitro* assay revealed, it has phospholipase A_2 inhibitory activity and anti-

inflammatory activity when applied topically[89]. Recently, a new depsidone, asperlide (**25**), was isolated from soil derived fungus *Aspergillus unguis*, along with known depsidones (Figure 1.11).

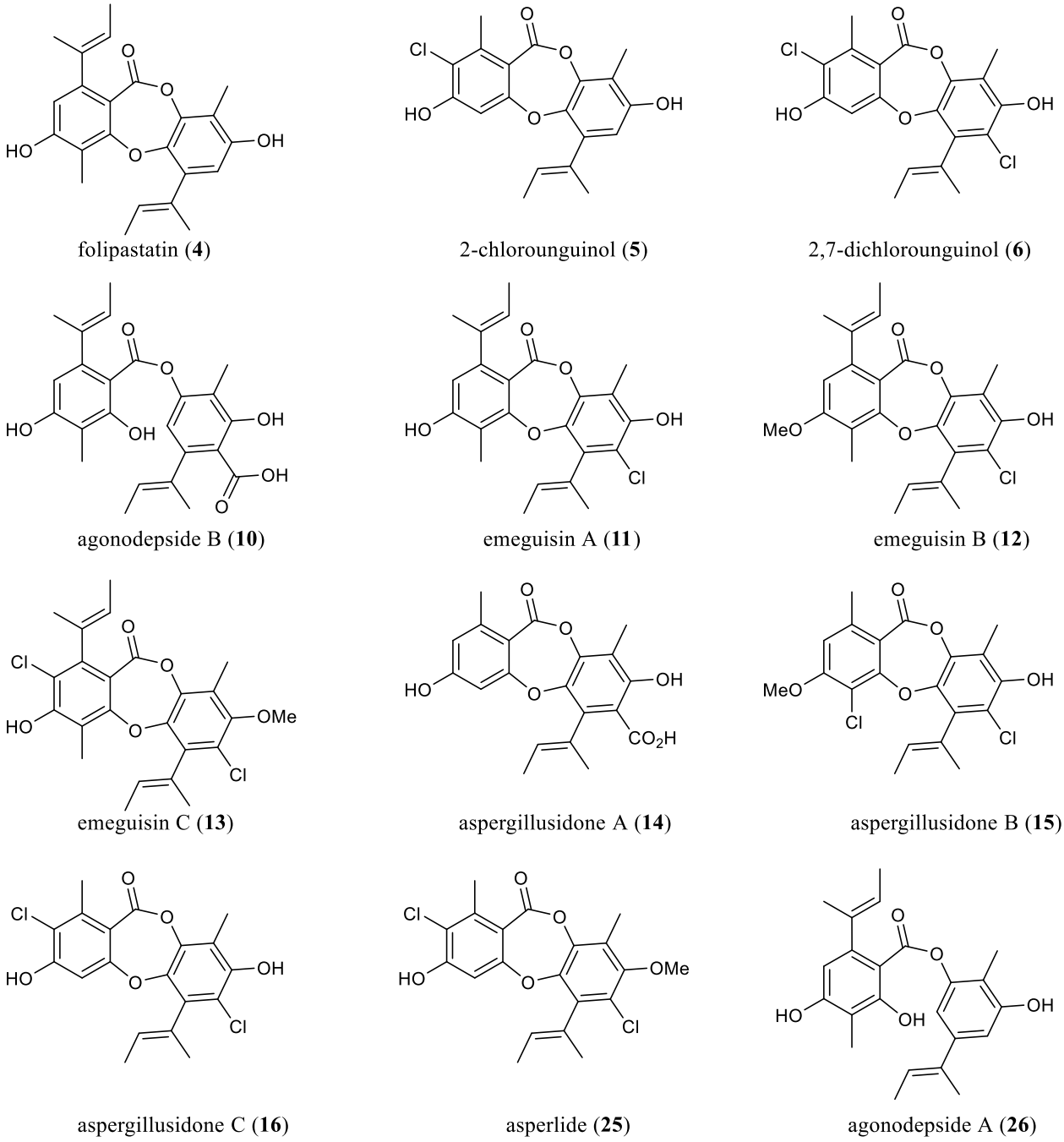

Figure 1.11: Structure of depsidones and depsides isolated from *Aspergillus nidulans*

Guisinol (**23**) is the first non-lichen depside isolated from a marine-derived strain of *Emericella unguis*[90] (Figure 1.12). Later, another two depsides, agonodepside A (**26**) and B (**10**), were isolated from this fungus[91]. Sureram *et al.* recently reported depsidones from *Aspergillus unguis* with potent aromatase-inhibitory activity, which is an important therapeutic target of breast cancer treatment[92]. Thus, Sureram and co-workers isolated three new depsidones (aspergillusidone A (**14**), B (**15**) and C (**16**)) and one methyl ester derivative of nidulin (aspergillusether A, **24**) along with three known compounds (nidulin, nornidulin, and 2-chlorounguinol) (Figure 1.11). All compounds exhibited

aromatase inhibition except aspergillusether A (**24)**, with aspergillusidone C (**16**) being the most potent (IC_{50}:0.7µM). Aspergillusidone C (**16**), is also active against MRSA (2 µg/mL), while

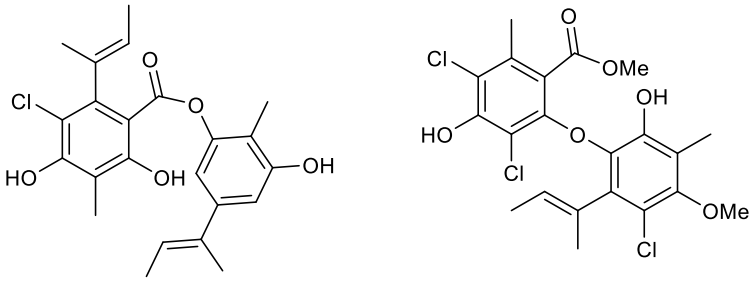

guisinol (**23**) aspergillusether A (**24**)

Figure 1.12: Structure of depside (guisinol) and methyl ester derivative isolated from *Aspergillus nidulans*

aspergillusether A (**24**) did not show any biological activity. Thus, it is appeared that for bioactivity the depsidone nucleus is essential [75, 92]. The same group conducted PDB to obtain unnatural analogues by feeding the culture media of *Aspergillus unguis* with KBr, KI, and KF. The group isolated three unnatural depsidones (aspergillusidone D (**20**), E (**21**) and F (**22**)) (Figure 1.13) along with nidulin, nornidulin and unguinol. Aromatase inhibitory assay revealed that aspergillusidones D-F exhibited higher activity compared to aspergillusidones A-C[85].

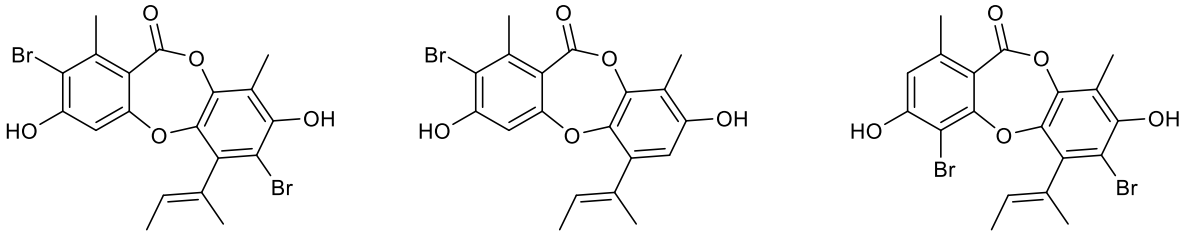

aspergillusidone D (**20**) aspergillusidone E (**21**) aspergillusidone F (**22**)

Figure 1.13: Unnatural depsidone isolated from *Aspergillus nidulans* by PDB

1.5 Aims

Antibiotic chemical space is quite distinct from other drugs and currently clinically approved antibiotics are based on only four basic scaffolds – cephalosporins, penicillins, quinolones, and macrolides[93-94]. However, precursor-directed biosynthesis, synthetic and semi-synthetic approach are frequently used to expand the antibiotic chemical space around the basic scaffold, improve the draggability of lead compounds and bioactivity. The work presented in this thesis aims to combine all these approaches to expand the nidulin pharmacophore by accessing new nidulin analogues. All the nidulin analogues were screened for antibacterial, antifungal and cell cytotoxicity activities and a structure activity relationship was proposed for the nidulin pharmacophore.

2 Optimisation of cultivation conditions for *Aspergillus unguis*

2.1 Introduction

For fungal growth and isolation of metabolites in the laboratory, there is a general dilemma between achieving maximum microbial growth rates and obtaining maximum metabolite yields as culture conditions promoting faster growth could be unfavourable to metabolite production[95-96]. Nonetheless, it is well known that variations in the cultivation conditions and media have a significant impact on quantity and diversity of the secondary metabolite profiles of fungi[97-99]. In the present study, the fungus *Aspergillus unguis* was selected as a known nidulin producer and it is interesting to note that genome analysis of this fungus demonstrated that it has the potential to generate 32 polyketides, 14 non-ribosomal peptide and two indole alkaloids[100]. Out of these, only 50% of secondary metabolites have been isolated. Therefore, by changing media composition, it should be possible to isolate new metabolites from this fungus. Thus, this chapter describes the optimisation of culture media for *Aspergillus unguis* and studies of metabolic profile of this fungus in presence of different carbon and nitrogen sources. Based on the optimisation result, one medium was selected for scaling up cultivation and metabolite isolation. This optimisation led to the identification of two new metabolites produced by this fungus and previously reported compounds. This chapter also describes the isolation and structure elucidation of these compounds.

2.2 Optimisation of culture media of *Aspergillus unguis*

The fungus *Aspergillus unguis* (*A. unguis*) was obtained from CSIRO FRR collection and was originally sourced from CBS Netherlands (collection code CBS 132.55). It was isolated from shoe leather and deposited by NRRL (NRRL 2393). Optimisation of culture media for *A. unguis* was carried out using a wide range of agar, liquid and grain based media. The agars; Glycerol Casein Agar (GCA), Czapek-Dox Agar (CZA), Malt Extract Agar (MEA), Oatmeal Agar (OMA), Yeast Extract and Sucrose Agar (YES) and the liquid media; Glycerol Casein (GCL), Czapek-Dox (CZL), Malt Extract (MEL), Oatmeal (OML), Yeast Extract Sucrose (YESL), were prepared according to the recipes presented in the Supplementary Material. Pearl barley, rice (Jasmine and Basmati) and cracked wheat were the grains selected.

2.2.1 Effect of different media on metabolic profile of *A. unguis*

Metabolic profiles of *A. unguis* were assessed on thirteen different solid, liquid and grain media by analysing the subsampling data by LCMS at day 7 and day 14. A representative HPLC trace of the

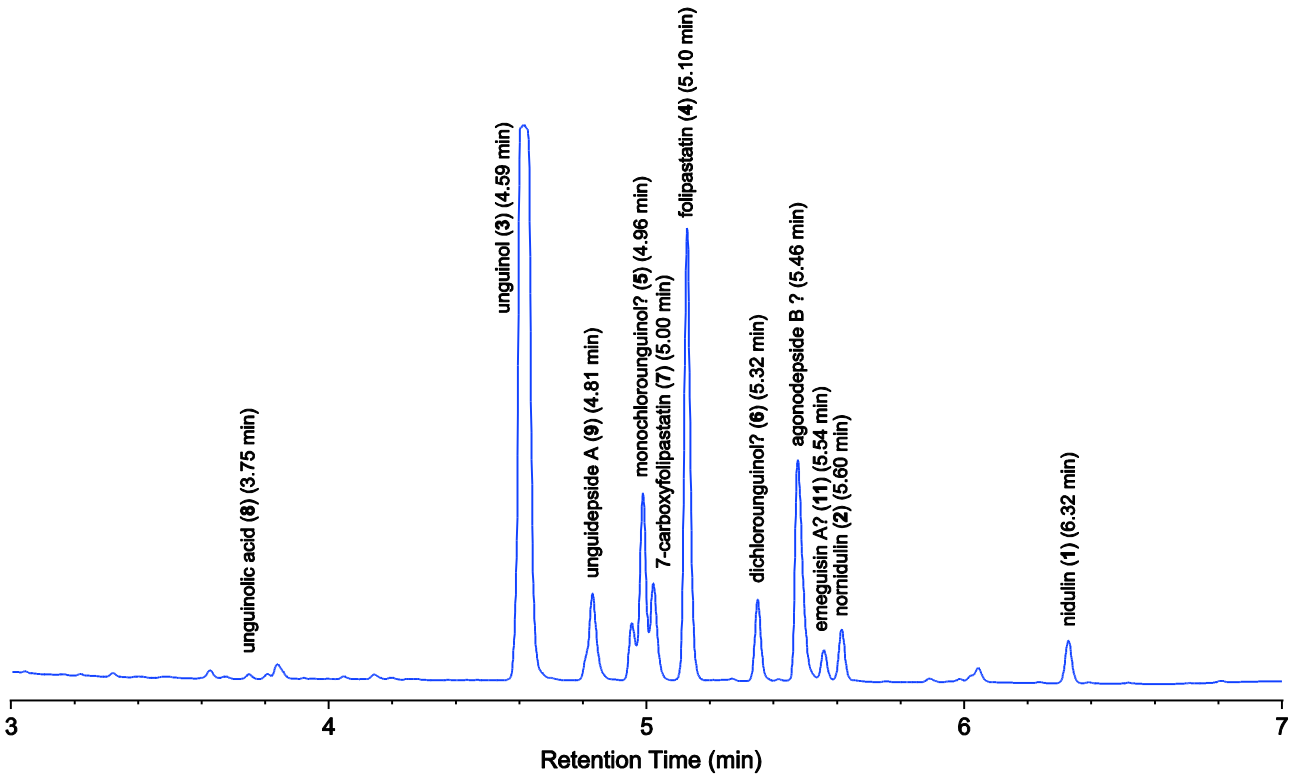

Figure 2.1: HPLC trace of crude extract of *A. unguis* after cultivation in YESL media for 14 days. ? = Tentative assignment based on molecular weight and ESIMS isotopic pattern

metabolic profile of *A. unguis* is shown in Figure 2.1. It was observed that at day 14, the abundance of all metabolites was higher than at day 7 (Figure 2.2). However, after analysing the day 14 subsampling data, it was revealed that *A. unguis* produced two different classes of metabolites (depsides and depsidones) in three different media and that none of the single media was ideal for the production of all secondary metabolites. It is noteworthy that in grain media *A. unguis* produced only one type of metabolite (depsidones) and therefore, for further optimisation, only liquid and agar media were considered.

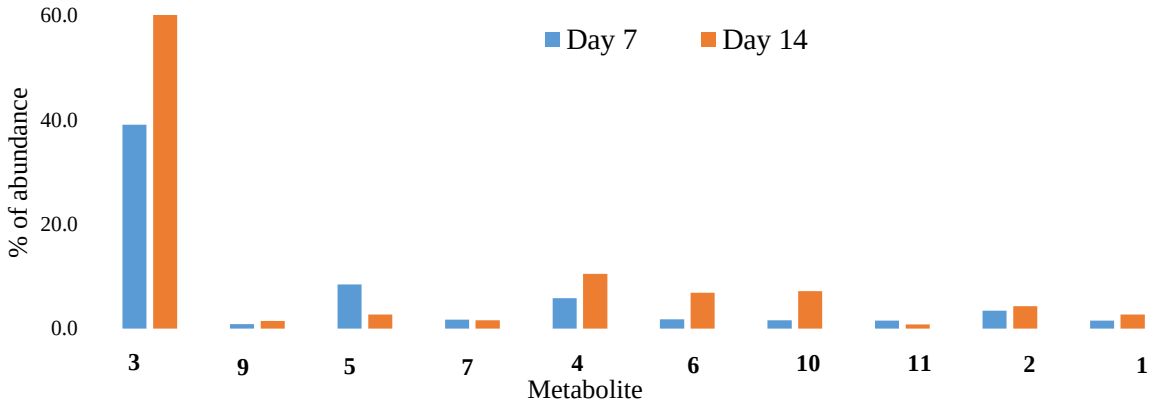

Figure 2.2: Percentage abundance of *A. unguis* metabolites after cultivation in YESL media for 7 and 14 days

2.2.1.1 Agar media

Five different agar media based on different carbon and nitrogen source were selected. In all media, it was observed that the six major metabolites (unguinol (**3**), folipastatin (**4**), nidulin (**1**), nornidulin (**2**), chlorounguinol (**5**) and dichlorounguinol (**6**)) (Table 2.1) were produced. Among all the solid media, *A. unguis* produced predominantly unguinol (**3**) (60%) in OMA media, while in CZA media the percentage of abundance of unguinol was 4.5% (Table 2.1). Conversely, in the latter media nornidulin (**2**) was the predominant metabolite (40%). This result suggested that production of nornidulin and nidulin depend on the availability of chlorine in media as CZA contains KCl. Moreover, folipastatin (**4**), an unchlorinated nidulin family depsidone, is produced in the highest amount (35%) in YES media.

Table 2.1: Relative metabolite abundance of *A. unguis* at day 14 in five agar media

Compound ID	Retention Time (min)	Relative Abundance (%)				
		GCA	CZA	MEA	OMA	YES
unguinol (**3**)	4.59	12.9	4.5	4.5	60.5	11.6
unguidepside A (**9**)	4.81	4.3	9.5	19.2	4.0	3.7
monochlorounguinol ? (**5**)	4.96	9.4	1.3	5.0	1.8	1.0
7-carboxyfolipastatin (**7**)	5.00	0.7	1.9	0.6	1.4	7.7
folipastatin (**4**)	5.10	5.3	0.0	0.2	11.6	35.2
dichlorounguinol (**6**)	5.32	29.8	5.4	11.6	3.1	2.3
agonodepside B ? (**10**)	5.46	3.2	6.7	4.0	5.6	13.4
emeguisin A (**11**)	5.54	8.4	4.1	4.8	2.1	2.1
nornidulin (**2**)	5.60	18.0	40.0	20.8	2.5	3.5
nidulin (**1**)	6.32	0.2	3.2	0.2	1.4	0.9

? = Tentative assignment based on molecular weight and ESIMS isotopic pattern

2.2.1.2 Liquid media

As for the agar media, five different liquid media were chosen and the effect of these liquid media on metabolic profile of *A. unguis* was observed in two different conditions (static liquid media and liquid media with shaking). After analysing the subsampling data by LCMS, it was revealed that in both conditions, *A. ungis* showed a consistent metabolic profile, with six major peaks although their percentage abundance varied significantly. In shaking condition, except the YESL media, the abundance of all major metabolites dropped. For example, in shaking condition the percentage of abundance of unguinol (**3**), folipastatin (**4**), nornidulin (**2**) and chlorounguinol (**5**), have been decreased by 67%, 80%, 85% and 87% respectively in MEL (Figure 2.3). In static condition, unguinol (**3**) production rate was 14% which was increased to 68% when this organism was cultured in shaking condition in YESL media.

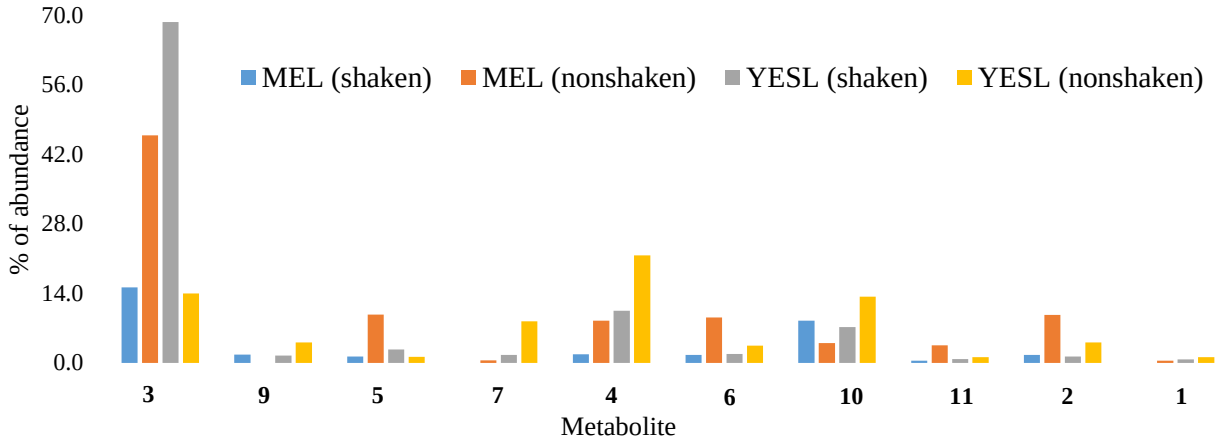

Figure 2.3: Percentage abundance of *A. unguis* metabolites after cultivation for 14 days in MEL and YESL media in shaking and static condition

After analysing the optimisation results, it was evident that *A. unguis* grows well in rich media and produces high levels of secondary metabolites and that different media selectively produce different analogues of the nidulin family. Significantly, in rich media such as OMA and YESL, *A. unguis* produced depsidone-class metabolites in large amounts, and this was the most important factor for selection of media for scaling up cultivation and metabolite isolation. Among all the culture media, YESL media (shaking condition) produced unguinol (**3**) and folipastatin (**4**) in the highest percentage of abundance (~80%) (Figure 2.4) and therefore this media was used for scaling up of cultivation, metabolite isolation and directed biosynthesis experiments.

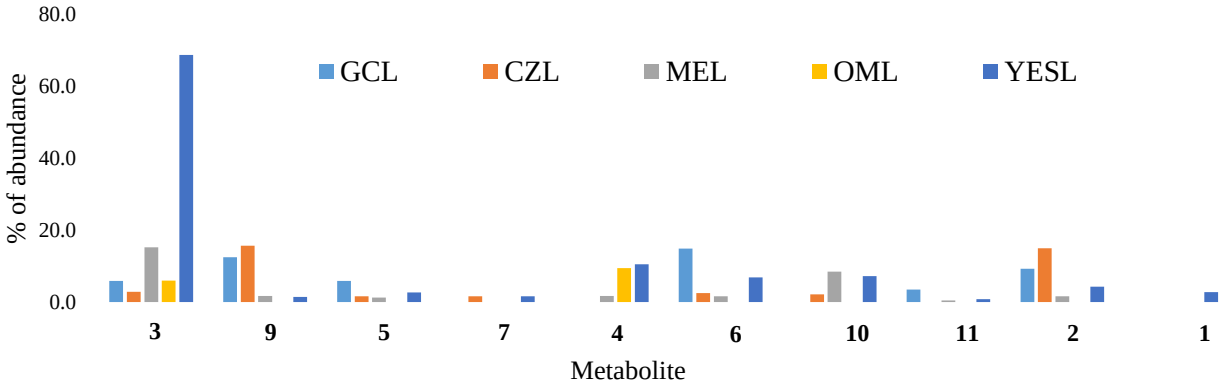

Figure 2.4: Percentage of abundance of *A. unguis* metabolites after cultivation in different liquid media for 14 days (with shaking)

2.3 Cultivation, extraction and fractionation of *A. unguis*

A. unguis was cultivated in yeast extract sucrose media for 14 days with continuous shaking and by this time the fungus turned a greenish colour. The whole cultivation was extracted with acetone to make a slurry. The slurry was partitioned against ethyl acetate, evaporated, extracted with hexane to remove the fat then with 10% water in methanol to prepare the crude extract. The fractionation of crude extract by C_{18} preparative HPLC followed by semi-preparative purification yielded two new

compounds, 7-carboxyfolipastatin (**7**) and unguinolic acid (**8**), as well as the previously reported compounds, unguinol (**3**), folipastatin (**4**), nidulin (**1**) and nornidulin (**2**).

2.4 New metabolites isolated from *A. unguis*

7-carboxyfolipastatin (**7**) was isolated as colourless powder. HR-ESI(+)-MS analysis of **7** revealed a quasimolecular ion ($[M+H]^+$ *m/z* 425.1593) indicative of a molecular formula $C_{24}H_{24}O_7$ requiring 13 double bond equivalents (DBEs). The mass of **7** was 44 amu more than that of reported compound folipastatin (**4**) (molecular formula $C_{23}H_{24}O_5$), which suggested that **7** was a carboxy derivative of **4**. The ^1H and ^{13}C NMR data for **7** and **4** were also very similar. However, **7** had an additional signal in ^{13}C NMR at δ_C 169.7 providing further evidence of presence of carboxylic acid.

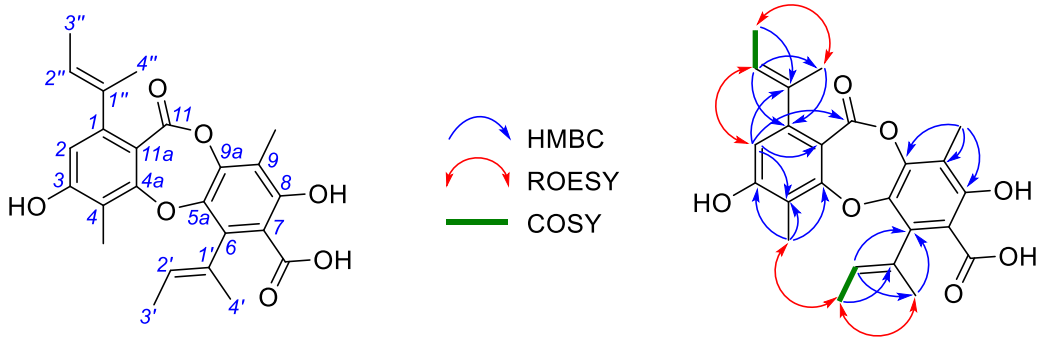

Figure 2.5: Key 2D NMR correlations observed in 7-carboxyfolipastatin (**7**)

The ^1H NMR spectrum of folipastatin (**4**) showed two aromatic protons at δ_H 6.53 (H-2) and 6.40 (H-7), while in **7** the aromatic proton H-7 (δ_H 6.40, s) was absent, suggesting the carboxylate moiety is located on C-7 (Figure 2.5). Moreover, in ^{13}C NMR spectrum, C-7 chemical shift for **4** and **7** (δ_C 111.0, 114.6 for **4** and **7** respectively) were different, which also suggested that H-7 in **4** has been replaced by a carboxylic acid in **7** (see Supplementary Material, Table S1). A diagnostic ROESY correlation between H_3-4 and H_3-3′ established the regiochemistry of the ether and ester linkages between the two subunits. Therefore, analysis of 2D NMR spectra, as well as the data correlation with those of folipastatin led to the assignment of protons and carbons in 7-carboxyfolipastatin (**7**) and secured the structure.

Unguinolic acid (**8**) was isolated as brown powder. HR-ESI(+)-MS analysis of **8** revealed an adduct ion ($[M+Na]^+$ *m/z* 367.1158) indicative of a molecular formula $C_{19}H_{20}O_6$, requiring 10 DBEs. Examination of the ^1H and ^{13}C NMR spectra of **8** revealed resonances for all 20 protons and 19 carbons, suggesting that the molecule is asymmetric. The ^1H and ^{13}C NMR data of **8** (see Supplementary Material, Table S2) were similar to those of unguinol (**3**) showing two meta-coupled aromatic protons at δ_H 6.22 (1H, d, *J* = 2.3) and δ_H 5.76 (1H, d, *J* = 2.3) with one singlet aromatic proton at δ_H 6.20 (1H, s) as well as two aromatic methyl protons (δ_H 2.22, s; 1.95, s). A set of signals at δ_H 5.48 (1H, qq, *J* = 6.8, 1.4), 1.56 (3H, dq, *J* = 6.8, 0.9) and 1.75 (3H, dq, *J* = 1.4, 0.9) with

corresponding carbon signals at δ_C 124.0, 13.8 and 16.6 is typical of a 1-methyl-1-propenyl unit. From the HMBC spectrum of **8** the location of 1-methyl-1-propenyl unit was confirmed as C-5′ by correlations from H-2″ and H-4″ to C-5′. The singlet at δ_H 6.20 was assigned to be H-4′ on the basis of HMBC correlation with C-1″ (δ_C 133.2), C-2′ (δ_C 110.3) and C-6′ (δ_C 131.6) (Figure 2.6).

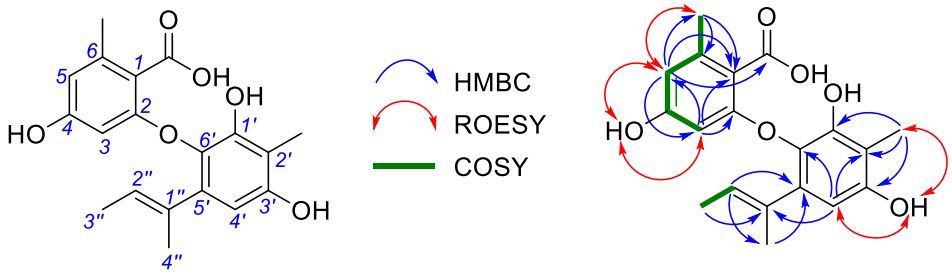

Figure 2.6: Key 2D NMR correlations observed in unguinolic acid (**8**)

The ^{13}C NMR resonance at δ_C 169.0 suggested the presence of carboxylic acid group. The two meta-coupled aromatic protons showed HMBC correlations from H-5 to C-1 (δ_C 114.9), C-3 (δ_C 99.1), 1-CO_2H (δ_C 169.0) and 6-Me (δ_C 19.8) and from H-3 to C-1 (δ_C 114.9) and C-5 (δ_C 110.5), which confirmed the position of H-5 and H-3 as well as carboxylic acid group. On the basis of these data, the structure of unguinolic acid (**8**) was established as the hydrolysed derivative of unguinol (**3**).

2.5 Isolation of previously reported compounds

Nidulin (**1**), nornidulin (**2**), unguinol (**3**) and folipastatin (**4**) were isolated along with the previously discussed new compounds and were identified by detailed spectroscopic analysis and comparison to literature data.

2.6 Summary

This chapter described the media optimisation of *A. ungis*, which was essential for assessment of metabolite profile as well as profiles of the metabolite produced in each media. Utilising these media optimisation results led to the further scaling up of cultivation and eventually the isolation and structure elucidation of two new compounds. 7-carboxyfolipastatin (**7**) is a unique compound because other folipastatin derivatives that were isolated from this fungus, such as emeguisin A, contain chlorine at the 7-position. On the other hand, unguinolic acid (**8**) is also a novel compound because it contains an ether linkage between the two aromatic rings, and a free carboxylic acid at C-1. This free carboxylic acid gave room for semi-synthetic modification of these two compounds and may be used as a lead compound for drug discovery.

3 Precursor-directed biosynthesis of nidulin analogues

3.1 Introduction

From the optimisation studies presented in Chapter 2, it was observed that changing the different carbon and nitrogen sources led to varied secondary metabolic profiles of *A. unguis*. Moreover, the optimisation studies also suggested that in YESL medium, *A. unguis* produces higher amounts of depsidones. Using this information, precursor-directed biosynthesis experiments of *A. unguis* were performed in YESL medium by feeding different unnatural biosynthetic building blocks (salicylic acid derivatives and orsellinic acid derivatives) to obtain unnatural products. While this strain of *A. unguis* did not accept any of these building blocks, supplementation of the media with halide salts (NaCl and KBr) led to the formation of several new unnatural analogues of nidulin.

3.2 Precursor-directed biosynthesis with orsellinic and salicylic acids

All nidulin family metabolites contain either a depside or depsidone nucleus. Depside and depsidone containing secondary metabolites have been isolated mainly from lichens and the biosynthesis of these lichen metabolites has been widely studied[101]. It is generally accepted that depsidones are derived from depsides, formed by either condensation of two molecules of orsellinic acid or by condensation of one molecule of an orsellinic acid and one molecule of an orcinol, and these depsidones are linked by both ester and ether bonds. Recently, Sureram and coworkers proposed the biosynthetic pathway of nidulin family depsidones (Figure 3.1) which were isolated by their groups through directed biohalogenation[85].

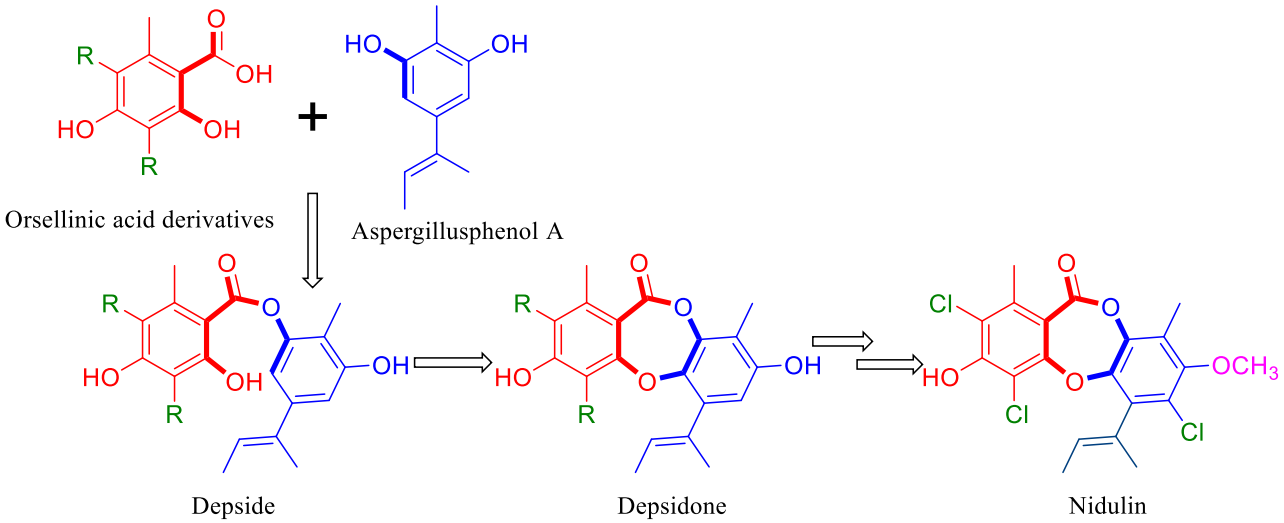

Figure 3.1: Proposed biosynthetic pathway of nidulin depsidone pharmacophore

In precursor-directed biosynthesis, novel natural product analogues are synthesised from unnatural building blocks by existing biosynthetic enzymes. However, it is necessary to understand the behaviour of organisms in the presence of unnatural building blocks when they were fed. To

understand this, in the present study the organism, *A. unguis*, was supplemented with orsellinic acid and 2-methylresorcinol (0.05%), as simple analogues of aspergillusphenol A. Subsampling at day 14 revealed that in presence of orsellinic acid, the metabolic profile of the fungus was not changed compared to the control, while 2-methylresorcinol inhibited the biosynthesis of depsidones, even when 2-methylresorcinol was supplemented with orsellinic acid (Figure 3.2). Antifungal assays confirmed that the growth of *A. unguis* was not affected by addition of these compounds. Therefore, this study suggested only orsellinic acid derivatives may be suitable for precursor-directed biosynthesis studies.

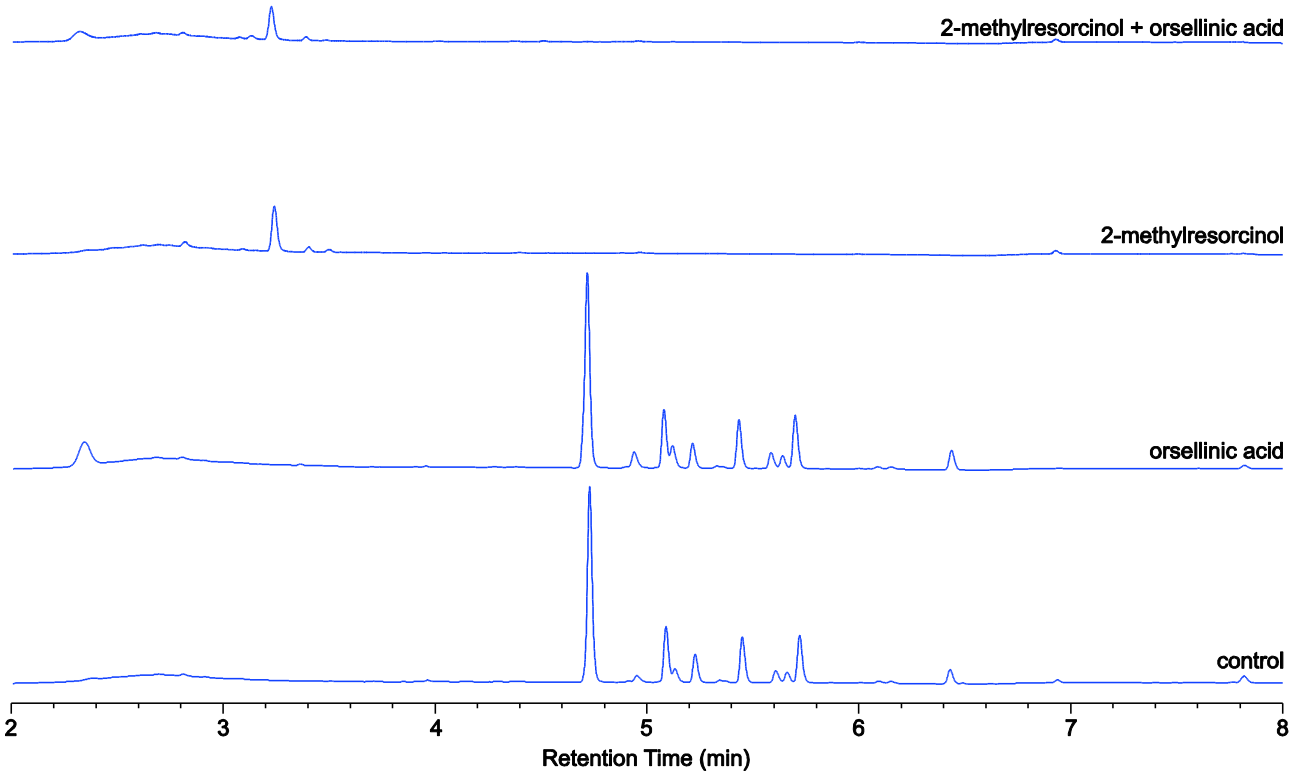

Figure 3.2: Metabolic profile of *A. unguis* in YESL media supplemented with orsellinic acid, 2-methylresorcinol and both compounds.

In the next experiment, *A. unguis* was fed with different unnatural biosynthetic building blocks categorised into two different classes – orsellinic acid derivatives and salicylic acid derivatives. Three orsellinic acid derivatives, 3-methylorsellinic acid, 3-isopropylorsellinic acid and orsellinic acid dimethyl ether, and four salicylic acid derivatives, 6-methylsalicylic acid, 6-methoxysalicylic acid, 2,4-dihydroxybenzoic acid and 6-fluorosalicylic acid, were selected for feeding studies (Figure 3.3).

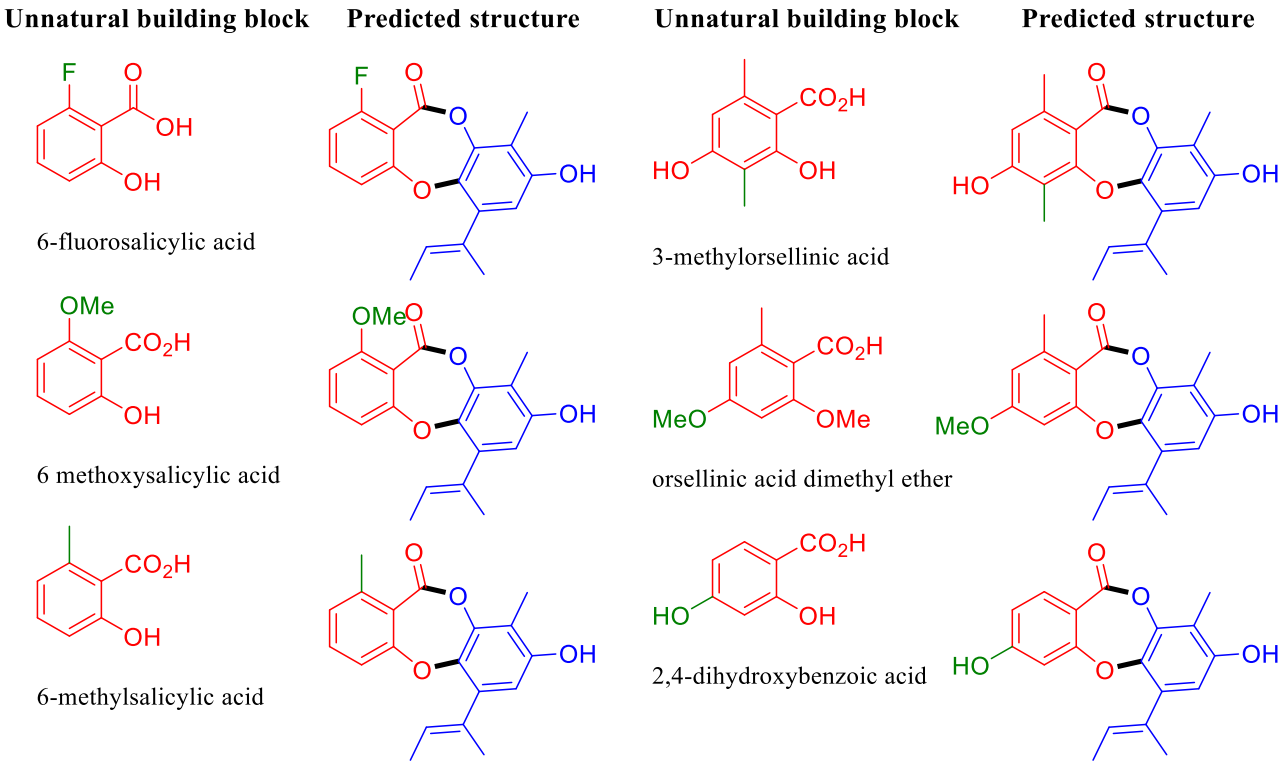

Figure 3.3: Unnatural building blocks and their corresponding predicted products after incorporation.

Before commencing feeding studies, these building blocks were also tested for antifungal activity against *A. unguis* to ensure they did not have any effect on growth. Of the building blocks listed in Figure 3.3, only 3-isopropylorsellinic acid inhibited the growth of *A. unguis*. Thus, except 3-isopropylorsellinic acid, all the unnatural building blocks were fed at 0.05% concentration in YESL media. *A. unguis* was cultivated for 14 days and subsampling was performed at day 7 and 14. To understand the level of incorporation of these building blocks, the resulting cultures were analysed by LCMS. LCMS analysis of metabolic profile of *A. unguis* revealed that none of the building blocks were incorporated by this organism. However, when the organism was supplemented with salicylate derivatives, the metabolic profile was not changed compare to the control experiment. It is interesting to note that in presence of unnatural salicylate building blocks, the relative abundance of major metabolite decreased moderately, e.g. unguinol (**3**), folipastatin (**4**) and nornidulin (**2**) production decreased by 20%, 28% and 42% respectively, while nidulin (**1**) production increased in presence of salicylate building blocks by 53% (Figure 3.4). Conversely, when *A. unguis* was fed orsellinic acid derivatives in YESL, these unnatural building blocks changed the metabolic profile of *A. unguis* completely and LCMS data revealed that organism did not produce any depsides and depsidones.

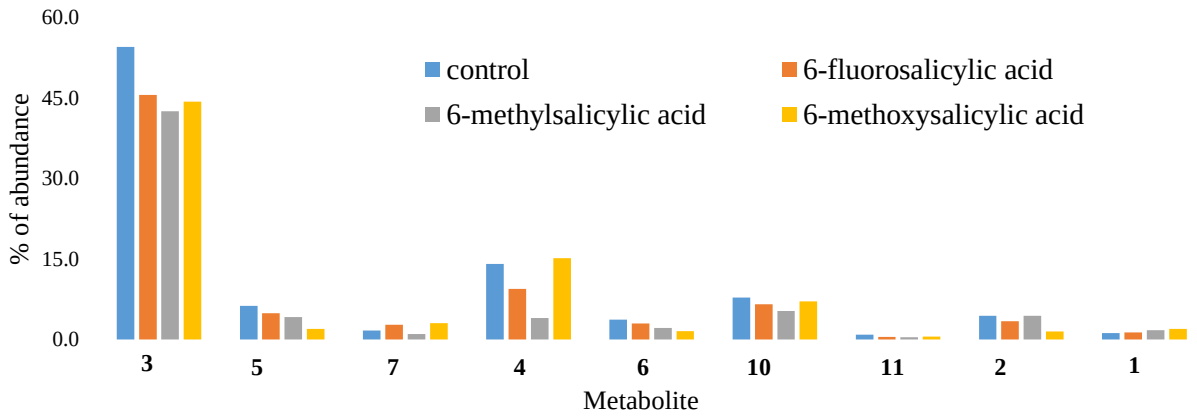

Figure 3.4: Metabolic profile of *A. unguis* after cultivation for 14 days in presence of unnatural salicylic acid derivatives at 0.05%

3.3 Precursor-directed biosynthesis of *A. unguis* with halides (NaCl and KBr)

3.3.1 Optimisation of salt concentration for directed biosynthesis

During the optimisation of culture studies of *A. unguis*, it was observed that the fungus produced varied amounts of nidulin and nidulin analogues in different media. In Czapek Dox medium, *A. unguis* produced nornidulin and nidulin (chlorinated depsidones), suggesting that the fungus took advantage of this media composition containing 1% KCl. In the present study *A. unguis* was supplemented with different concentrations of NaCl and KBr in YESL media to observe the effects on metabolic profiles. Initially, the fungus was inoculated in YESL media with 2.5%, 5% and 10% of NaCl. Subsampling and visual observation at day 7 revealed that that at 2.5% concentration *A. unguis* grew well but did not produce any secondary metabolite, whereas at 5% and 10% salt concentration the fungal growth and metabolite production were completely suppressed. Conversely, when the organism was cultivated at lower salt (NaCl and KBr) concentration (0.5%, 1% and 2%) subsampling revealed that the metabolic profile of *A. unguis* was similar to the control experiment. However, it was evident from this study that *A. unguis* was relatively salt intolerant and produced high levels of secondary metabolite in rich media.

3.3.2 Precursor-directed biosynthesis with NaCl

A. unguis was cultivated for 14 days in YESL media supplemented with 0.5%, 1% and 2% NaCl. During cultivation, subsampling was performed on day 7 and day 14. Subsampling data were analysed by LCMS and showed the metabolic profile of *A. unguis* has not changed and the major metabolites unguinol (**3**), folipastatin (**4**), nidulin (**1**) and nornidulin (**2**) were produced along with other metabolites. However, when *A. unguis* was fed with NaCl at different concentrations, the percentage of abundance of different metabolites in the media was changed markedly. The percentage of abundance of unguinol (**3**) and folipastatin (**4**), two major metabolites for control experiment, had decreased from 44% to 2.7% and from 17% to 1.3% respectively compared to the control (Figure

3.5). Conversely, a higher percentage of abundance of nornidulin (**2**) and dichlorounguinol (**6**) was observed. The nornidulin (**2**) and nidulin (**1**) production increased from 2% to 46% and from 3% to 18% respectively. It was evident that production of nornidulin (**2**), dichlorounguinol (**6**) and other chlorine-containing nidulin analogues was dependent on the availability of chlorine in the media as well as the efficacy of chlorination through biosynthetic pathways. Interestingly, the abundance of nidulin production did not change significantly (from 1.9% to 2.6%) when the organism was fed with different concentrations of NaCl.

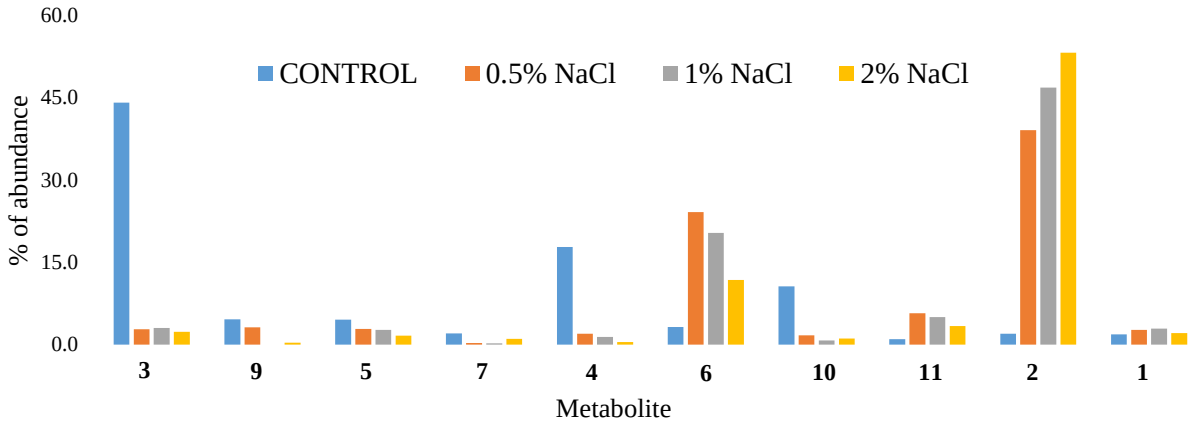

Figure 3.5: Percentage of abundance of metabolites of *A. unguis* after cultivation for 14 days in YESL media when supplemented with NaCl at different concentration.

3.3.3 Precursor-directed biosynthesis with KBr

Precursor-directed biosynthesis of *A. unguis* with NaCl revealed that the organism efficiently utilised the supplemented NaCl and the abundance of chlorinated depsidones was increased compared to the control. Following on from this result, *A. unguis* was also cultivated in YESL media with 0.5%, 1% and 2% KBr. Subsampling on day 7 and 14 revealed that the metabolite profile of *A. unguis* was changed completely compared to the control. By feeding *A. unguis* with KBr, the organism produced a new unnatural 'mixed' chloro/bromo depsidone and unnatural brominated depsides, as well as previously reported brominated depsidones. Nidulin-family depsidones (chlorounguinol (**5**), dichlorounguinol (**6**) and nidulin (**1**)) were replaced by bromine-containing depsidones (aspergillusidones D (**20**), E (**21**) and F (**22**)). Aspergillusidones D (**20**) and F (**22**) were the major metabolites when *A. unguis* was cultivated in YESL media treated with KBr and the percentage of abundance of unguinol (**3**) and folipastatin (**4**) dropped significantly (by 90% and 98% respectively) compared to the control experiment. However, based on LCMS data, it was found that when *A. unguis* was cultivated with 1% KBr in YESL media, the abundance of all unnatural metabolites was higher than for 0.5% and 2% KBr treatment (Figure 3.6). Thus, for scaling up cultivation to facilitate these new unnatural metabolites, *A. unguis* was supplemented with 1% KBr in YESL media.

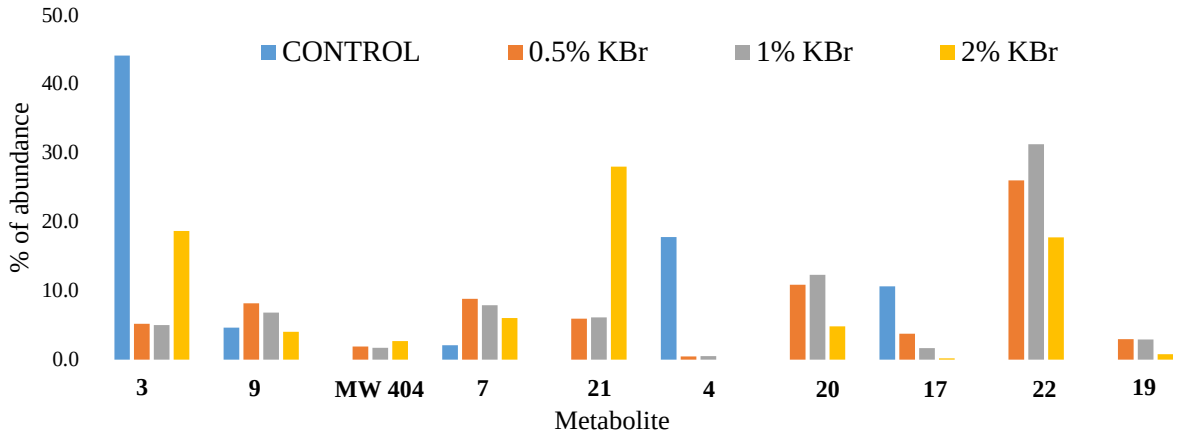

Figure 3.6: Relative abundance of metabolites of *A. unguis* cultivated for 14 days when supplemented with KBr at different concentration in YESL media.

3.3.4 New depsidone and depsides isolated by precursor-directed biosynthesis

2-bromo-7-chlorounguinol (**17**) was isolated as colourless powder. HR-ESI(+)-MS analysis of **17** revealed a quasimolecular ion ($[M+H]^+$ *m/z* 438.9948) indicative of a molecular formula $C_{19}H_{16}{}^{79}Br^{35}ClO_5$ requiring 12 DBEs. The positive and negative mass spectra of **17** showed isotope pattern at *m/z* $[M+H]^+$ 439/441/443 and $[M–H]^-$ 437/439/441 (in the ratio of 3:3:1), indicating the presence of one bromine and one chlorine atom. ^1H and ^{13}C NMR spectra of **17** (see Supplementary Material, Table S4) were nearly identical with aspergillusidone D (**20**) showing typical signal of 1-methyl-1-propenyl unit and two singlet methyls (1-Me and 9-Me) attached to aromatic ring and H-4 aromatic proton suggesting that **17** was a depsidone derivative. Given the similarity in NMR spectra, it is most likely that compared to aspergillusidone D (**20**), one of the bromine atoms was replaced by a chlorine atom in **17**.

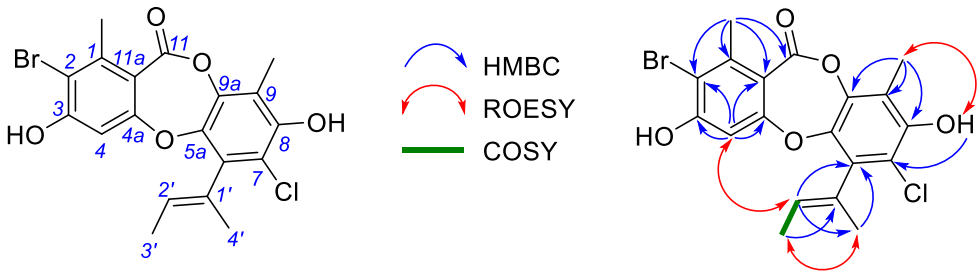

Figure 3.7: Key 2D NMR correlations observed in 2-bromo-7-chlorounguinol (**17**)

In the ^{13}C NMR spectra, the C-2 chemical shifts for aspergillusidone D (**20**) (δ_C 111.1) and 2-bromo-7-chlorounguinol (**17**) (δ_C 113.0) were very similar, while the C-7 chemical shifts (δ_C 108.2 vs 117.0) for these compounds were quite different, which suggested that the chlorine atom was attached at C-7 position in 2-bromo-7-chlorounguinol (**17**). The 2-Br/7-Cl regiochemistry was confirmed by correlations from H_3-1 to C-2 (δ_C 113.0), and 8-OH to C-7 (δ_C 117.0) in the HMBC spectrum of **17** (Figure 3.7). The C-7 carbon chemical shift of nornidulin (**2**) (δ_C 116.4) and nidulin (**1**) (δ_C 123.0) provided further evidence for the chlorine position in 2-bromo-7-chlorounguinol (**17**). A singlet H-4

(δ_H 6.58) aromatic proton in the ^{1}H NMR spectrum exhibited HMBC correlations with C-2, C-3, C-4a and C-11a. A diagnostic ROESY correlation between H-4 and H-2′ established the regiochemistry of the ether and ester linkages between the two subunits. Therefore, analysis of 2D spectra, as well as the data comparison with those of aspergillusidone D (**20**) led to the assignment of protons and carbons in 2-bromo-7-chlorounguinol (**17**) and established the structure as shown in Figure 3.7.

Unguidepside A (**9**) was isolated as light yellow coloured powder. HR-ESI(+)-MS analysis of **9** revealed a quasimolecular ion ([M+H]$^+$ *m/z* 373.1272) indicative of a molecular formula $C_{20}H_{20}O_7$ requiring 11 DBEs. Examination of the ^{1}H and ^{13}C NMR spectra of **9** (see Supplementary Material, Table S3) revealed resonances for all 20 protons and 20 carbons, suggesting that the molecule is asymmetric and it contains two carbonyl carbons at δ_C 166.9 and 171.7. The ^{1}H NMR spectrum of **9** showed two meta-coupled aromatic protons at δ_H 6.22 (1H, d, *J* = 2.4) and δ_H 6.21 (1H, d, *J* = 2.4) with one singlet aromatic proton at δ_H 6.45 (1H, s). A set of proton signals at δ_H 5.30 (1H, qq, *J* = 6.7, 1.4), 1.65 (3H, dq, *J* = 6.7, 1.1) and 1.85 (3H, dq, *J* = 1.4, 1.1) correlated with carbon signals at δ_C 121.5, 13.7 and 18.1 respectively is typical of the presence of a 1-methyl-1-propenyl unit in **9**. From the HMBC spectrum of **9**, the location of 1-methyl-1-propenyl unit was confirmed by correlations from H-2″ to C-6′ and from H-4″ to C-6′. Thus the location of 1-methyl-1-propenyl unit was confirmed at C-6′. Like aspergillusidone A (**14**), two meta-coupled aromatic protons showed correlations from H-3 to C-1, C-2, and C-5 and from H-5 to C-3, C-4, C-7 and 6-Me. HMBC correlations were also observed from 6-Me to C-1, C-5, C-6 and C-7 (Figure 3.8). The HMBC spectrum of **9** showed correlations from two meta-coupled aromatic proton H-3 and H-5 and from H_3-6 to the C-7 ester carbonyl, confirming the ester position in **9**. The appearance of the carbonyl chemical shift downfield (δ_C 166.9, for **9**) rather than upfield (δ_C 163.0 for **14**)[92, 102] indicated that the molecule was a depside.

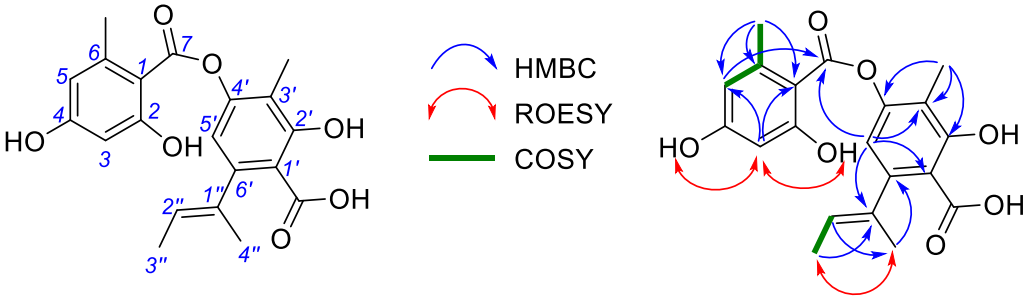

Figure 3.8: Key 2D NMR correlations observed in unguidepside A (**9**)

The remaining 8 DBEs and comparison with aspergillusidone A (**14**) (mass 370), suggested unguidepside A (**9**) to be a hydrogenated depside. The presence of a new aromatic signal (δ_H 6.45) and an additional hydroxylic proton signal (δ_H 10.34, s) indicated the absence of an ether linkage. This was also supported by the downfield carbon signal (δ_C 140.5, C-5a) in **14** being replaced by an

upfield signal (δ_C 114.0) in **9**. In addition, this additional aromatic proton displayed three bond correlations with C-1′, C-3′ and C-1″ in the HMBC spectrum. Moreover, in HMBC spectrum the C-2 was flanked by both hydroxylic group at C-4 and C-2 (Figure 3.8) confirmed the C-3 position and extra hydroxyl group at C-2. An HMBC correlation from H-5′ to C-7 established the regiochemistry of the ester linkage. It was therefore concluded that the position of the carboxylic acid in unguidepside A (**9**) was at C-1′. The positions of remaining substituents were determined from detailed analysis of the 2D NMR data.

Unguidepside B (**18**) was isolated as light yellow coloured powder. HR-ESI(–)-MS analysis of **18** revealed a quasimolecular ion ($[M–H]^-$ *m/z* 449.0240) indicative of a molecular formula $C_{20}H_{19}{}^{79}BrO_7$ requiring 11 DBEs. The positive and negative mass spectra of **18** showed isotope patterns at *m/z* $[2M+Na]^+$ 923/925 and $[M–H]^-$ 449/451 (in the ratio of 1:1), indicating the presence of one bromine. Examination of the ^1H and ^{13}C NMR spectra of **18** (see Supplementary Material, Table S5) revealed resonances for all 19 protons and 20 carbons, suggesting that the molecule is asymmetric and it contains two carbonyl carbons at δ_C 167.8 and 171.6. The ^1H NMR spectrum of **18** showed two aromatic protons at δ_H 6.50 (1H, s) and δ_H 6.57 (1H, s) as well as a set of signals at δ_H 5.32 (1H, qq, *J* = 6.8, 1.4), 1.65 (3H, dq, *J* = 6.8, 1.0) and 1.85 (3H, dq, *J* = 1.4, 1.0) correlated with carbon signals at δ_C 121.7, 13.7 and 18.0 respectively. This typical set of signals represents the presence of a 1-methyl-1-propenyl unit in **18**. From the HMBC spectrum of **18** the location of the 1-methyl-1-propenyl unit was confirmed by correlations from H-2″ to C-6′ and from H-4″ to C-6′. Thus the location of 1-methyl-1-propenyl unit was confirmed at position C-6′.

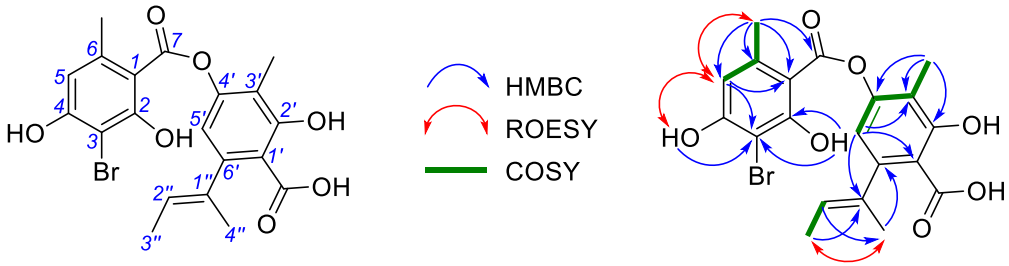

Figure 3.9: Key 2D NMR correlations observed in unguidepside B (**18**)

The remaining 8 DBEs, and comparison with aspergillusidone A (**14**) (mass 370), suggested unguidepside B (**18**) to be a hydrogenated depside with one bromine. The presence of a new aromatic proton (δ_H 6.57) and an additional hydroxylic proton signal (δ_H 11.16, s) indicated the absence of an ether linkage. This was also supported by the downfield carbon signal (δ_C 140.5, C-5a) in aspergillusidone A being replaced by upfield signal (δ_C 114.0) in **18**. The substitution patterns of the aromatic rings were confirmed by detailed analysis of HMBC data. Two aromatic proton signals at δ_H 6.57 and 6.50 were assigned to H-5 and H-5′ based on three-bond coupling with C-1, C-3, 6-Me and C-1′, C-3′, C-1″ respectively. The position of bromine atom could be either C-3 or C-1′. However,

the upfield carbon chemical shift of C-4 (δ_C 96.0) suggested that the bromine was located on C-3. Moreover, in the HMBC spectrum, both hydroxylic groups at C-4 and C-2 were coupled to C-3, confirming the C-3 bromine position (Figure 3.9). The location of bromine atom on the A-ring was supported by ESIMS fragmentation pattern. Hunneck *et al*. reported that depsides exhibit a prominent molecular ion in the mass spectrum along with concomitant cleavage of depside bond forming two fragments. The mass spectrum of **18** exhibited a peak at *m/z* 229/231 (1:1 ratio) confirming the presence of bromine atom in the A-ring that is carbonyl fragment. A prominent peak at *m/z* 221 corresponded to the remaining fragment, which also confirmed the position of the carboxylic group at C-1′. Given the lack of diagnostic HMBC correlations between the two aromatic subunits, the regiochemistry of the ester linkage was tentatively assigned to be the same as **9**. The positions of the remaining substituents were determined by detailed analysis of HMBC data. Based upon these data, the structure of **18** was established as the 3-bromo derivative of unguidepside A (**9**).

5-bromoagonodepside B (**19**) was isolated as colourless powder. HR-ESI(+)-MS analysis of **19** revealed a quasimolecular ion ($[M+H]^+$ *m/z* 505.0852) indicative of a molecular formula $C_{24}H_{25}{}^{79}BrO_7$ requiring 12 DBEs. The positive and negative mass spectra of **19** showed isotope patterns at *m/z* $[M+H]^+$ 505/507 and $[M–H]^-$ 503/505 (in the ratio of 1:1), indicating the presence of one bromine. Moreover, the mass 504 of **19** was 78 amu more than that of reported compound agonodepside B (**10**) ($C_{24}H_{26}O_7$), which suggested that **19** was a monobromo derivative of **10**. In the proton NMR spectrum of **19** (See Supplementary Material, Table S6) three hydroxyl singlets (δ_H 9.42, br s, 9.69, s and 11.41, br s), one aromatic singlet (1H, s, δ_H 6.30) and two aromatic methyl singlets, (3H, s, δ_H 2.12; 3H, s, δ_H 1.99) were observed. In addition, the aryl coupled methyl/olefinic proton pair at δ_H 1.84~5.30 and 1.87~5.31 which are coupled with methyl protons at δ_H 1.65 and 1.66 respectively suggests two sets of 1-methyl-1-propenyl groups. In the HMBC spectrum of **19**, both H-2‴ and H-4‴ correlated with C-6 (δ_C 142.5), which is the carbon bearing one of the 1-methyl-1-propenyl groups.

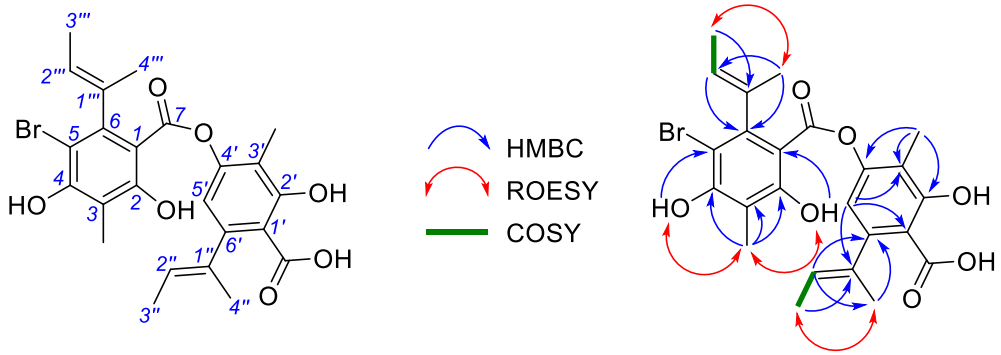

Figure 3.10: Key 2D NMR correlations observed in 5-bromoagonodepside B (**19**)

The aromatic methyl at δ_H 2.12 (3-Me) correlated with C-2 (δ_C 154.5), C-3 (δ_C 112.7) and C-4 (δ_C 154.4). The ROESY spectrum of **19** showed that 3-Me was flanked by two hydroxyl groups (Figure 3.10). The carbon chemical shift of C-4 (δ_C 154.4) and C-2 (δ_C 154.2) also indicated that these carbons were oxygenated. In addition, the HMBC spectrum showed 4-OH coupled with C-3, C-4 and C-5 and 2-OH with C-1 and C-2 respectively. Comparison of the molecular formula of **19** with that of agonodepside B (**10**) revealed that one hydrogen atom in **10** was replaced with a bromine atom in **19**. The carbon chemical shift that appeared upfield (δ_C 103.2) in **19** rather than downfield (δ_C 108.4) in **10** indicated that aromatic proton was replaced by one bromine atom. In addition, the location of bromine atom on the A-ring was supported by mass spectrum fragmentation pattern[103] as described for **18**. The mass spectrum of **19** exhibited a peak at *m/z* 283/285 (1:1 ratio) confirming the presence of bromine atom in A-ring that is carbonyl fragment. Thus, part I of the molecule was determined as hexa-substituted benzoate. Similarly, the substituents at C-2′, C-3′ and C-6′ in ring B were determined to be hydroxyl, methyl and 1-methyl-1-propenyl groups respectively. One aromatic proton in ring B (δ_H 6.30, s) showed correlations with C-1′, C-3′, C-1″ and C-1′carboxylic acid group. The latter correlation confirmed the carboxylic acid group attached at C-1′. The negative mass spectrum of **19** exhibited a significant peak at *m/z* 221 that corresponded to part-II. Thus part-I and part-II were connected via an ester linkage (δ_C 165.9, C-7). The appearance of the carbonyl group at downfield (δ_C 165.9) rather than upfield (δ_C 163.0)[92, 102] indicated that the molecule was a depside. Analysis of 2D NMR spectra, as well as the data correlation with those of agonodepside B (**10**), led to the assignment of protons and carbons in **19** and confirmed that **19** was the 5-bromo derivative of **10**.

3.4 Proposed biosynthetic pathway of carboxy depsides and depsidones

Biosynthetic pathways of nidulin family depsidones are quite interesting due to their origin from fungi rather than lichens. Previously, two research groups have studied the biosynthetic pathways of nidulin family depsidones and concluded that nidulin family depsidones may be formed from two separate aromatic polyketides rather than from a single polyketide chain[85, 104]. The first polyketide unit is orsellinic acid, which is derived from one acetate and three malonate units, while the second polyketide is orcinol, derived from one acetate and four malonate units. These two polyketide units condense to form a depside and this depside then forms a depsidone by oxidative coupling involving a one-step dehydrogenation reaction. Recently, Sureram and coworkers isolated an orsellinic acid derivative (3,5-dibromo-2,4-dihydroxy-6-methylbenzoic acid methyl ester) and orcinol derivatives (aspergillusphenol A and B) from the media of a marine-derived *A. unguis*, which may suggest that nidulin family depsidones are biosynthesised from orsellinic acids and orcinols[85].

In the present study, one new carboxy depsidone and three new carboxy depsides were isolated. It is hypothesised that these isolated structures arise from two orcinol derivatives, such as

aspergillusphenol A carboxylic acid, which are cyclodimerised under the loss of two molecules of water and form depsidone via oxidative coupling of the depside (Figure 3.11). The carboxy depsides could be formed from one unit of orsellinic acid and one unit of aspergillusphenol A carboxylic acid to yield the respective depside (Figure 3.12). From the literature review and compounds that were isolated in the present study, nidulin family depsidones and depsides were categorised into four main groups, as summarised in Figure 3.13.

.

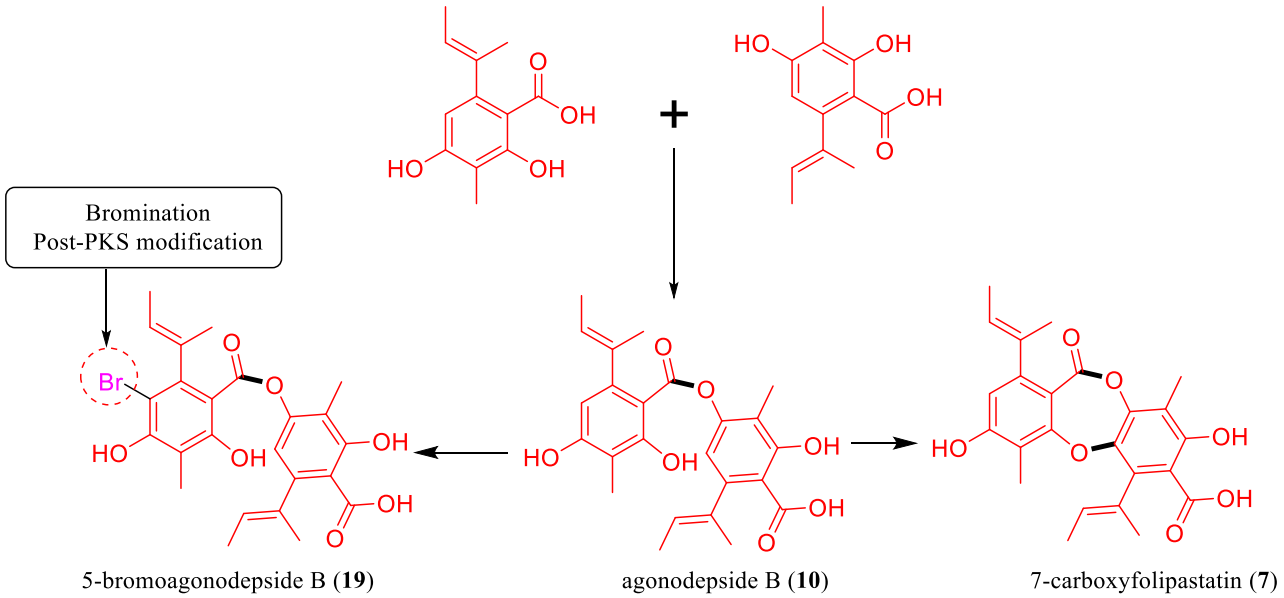

Figure 3.11: Plausible biosynthetic pathway of carboxy depside and depsidone (Group 2).

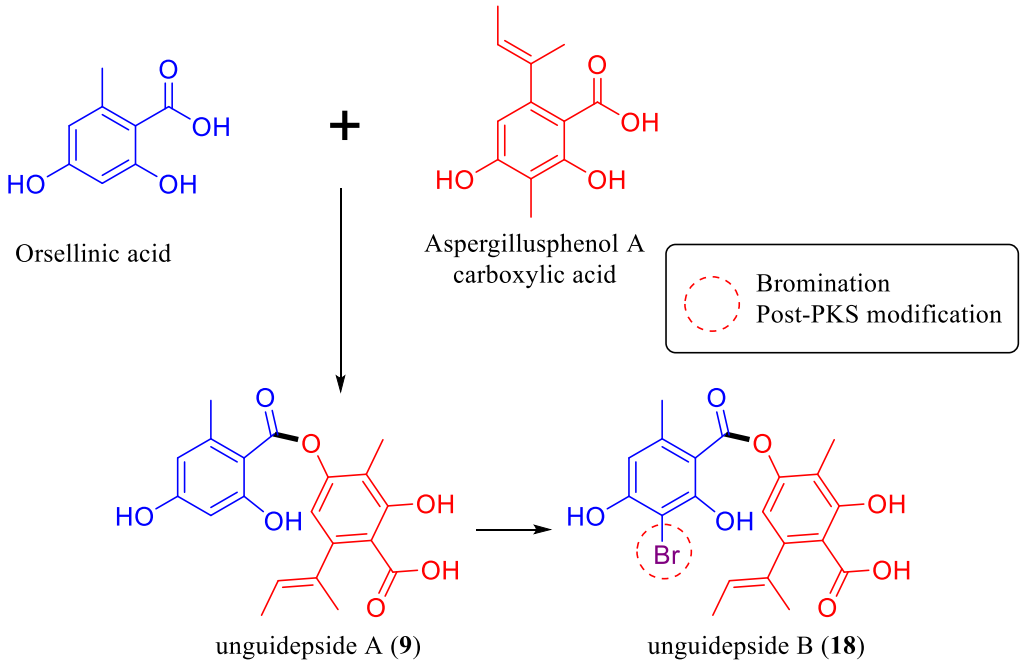

Figure 3.12: Plausible biosynthetic pathway of carboxy depside (Group 3)

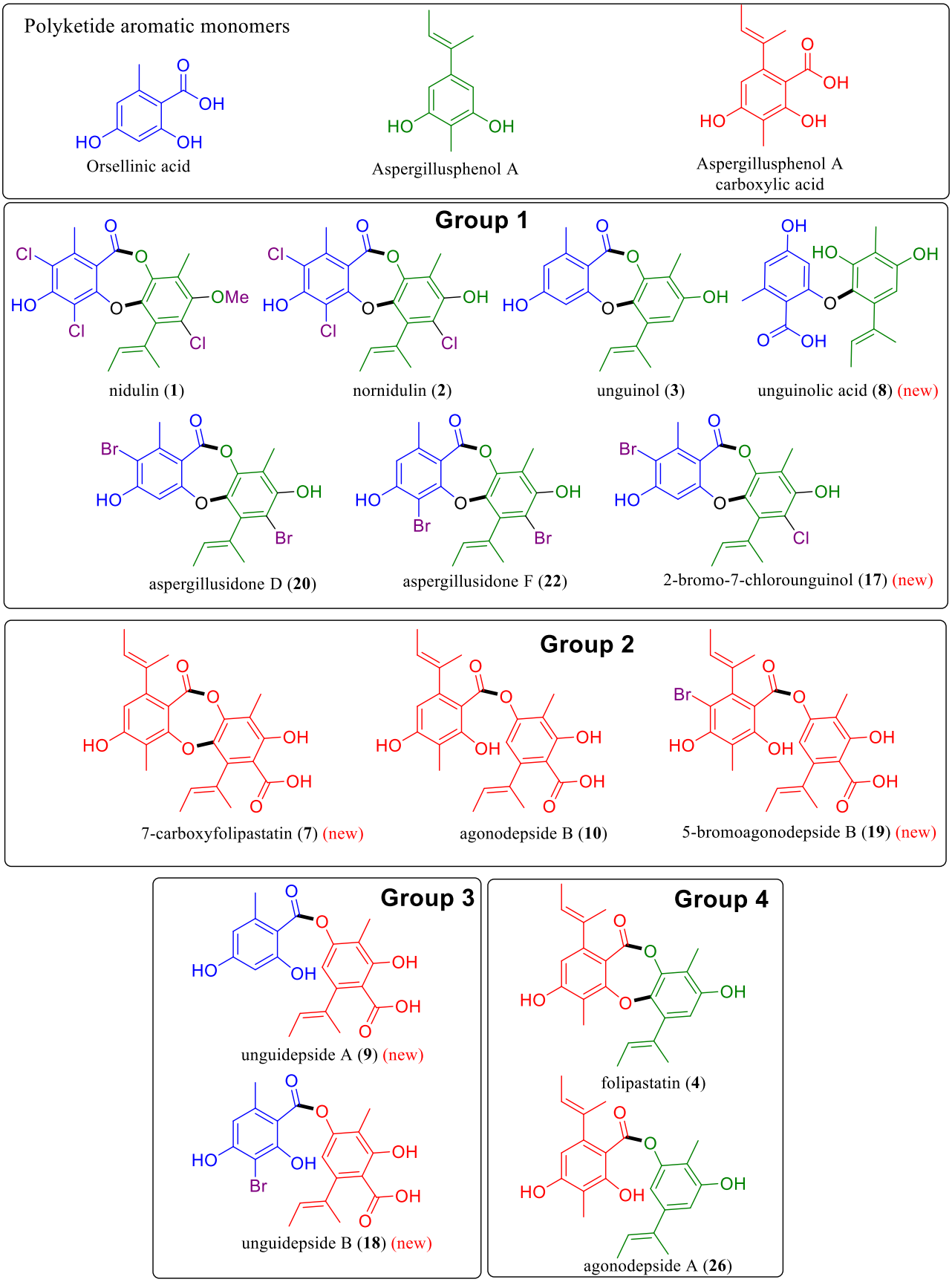

Figure 3.13: Nidulin family depsides and depsidones are biosynthesised from different polyketide aromatic monomers

3.5 Summary

By feeding *A. unguis* with salicylates and orsellinic acid derivatives it was clear that biosynthetic enzymes for nidulin family metabolites are not flexible and the organism did not accept the artificial building blocks. Limitations of precursor-directed biosynthesis mainly arise from restrictions in substrate tolerance of biosynthetic enzymes, regulatory influence of artificial precursors on biosynthetic pathway or toxicity. However, the salicylic acid derivative precursor may also compete with natural precursors, leading to the decreased percentage of all metabolites in the medium. It is also noteworthy that the natural precursors generally have intrinsic advantages over supplemented precursors[38]. On the other hand, in presence of orsellinic acid derivatives, *A. unguis* grows but unfortunately these artificial precursors block the biosynthetic machinery. This non-predictable effect of supplemented building blocks is a significant drawback of PDB[38].

In the present study, the strain of fungus used may be not suitable for directed biosynthesis experiments. Results from one strain cannot necessarily be transferred to other producing organism, even if it produces the same metabolic profile. For example, cyclosporin, produced by *Tolypocladium inflatum* allows incorporation of added amino acids to generate the derivatives of cyclosporin[105], while another cyclosporin-producing strain does not incorporate artificial building blocks when supplemented in the culture medium[106]. Therefore, changing the strain of *A. unguis* or changing to an alternative nidulin-producing species, may be suitable alternatives to overcome this failure.

In the present study, the feeding compounds were added at the beginning of the cultivation as an ingredient of the medium. However, addition of feeding material can also be performed at a later time with the beginning of production of the secondary metabolites. This would eliminate any unexpected toxic effects from the supplemented compounds in the lag and log phases of cell growth. Moreover, repeated feeding of lower doses of the supplemented compounds in the cultivation broth throughout cultivation period may also avoid any toxic effects of the artificial building blocks.

A. unguis produces an array of depsides and depsidones. Selection of appropriate target secondary metabolites is also important for successful operation of PDB. However, the biosynthetic pathway of nidulin synthesis is not well studied. A well-established metabolic pathway can prove useful in identifying enzymes that are not flexible enough to handle unnatural analogues, as is evident by the build-up of intermediates. Therefore, identification of biosynthetic enzymes of the nidulin family can be another alternative for successful operation of directed biosynthesis of this fungus. The use of mutant strains can be another alternative way to overcome limitations of PDB. Mutant strain can be developed by modifying their genes, such as gene disruption or gene exchange, which mediate the synthesis of biosynthetic precursor of nidulin. Such an approach would eliminate the intrinsic competition of the natural substrates over artificial building blocks.

By competing with natural substrate, PDB attempts to exploit the natural biosynthetic pathways to give unnatural products. In the present study, directed biosynthesis experiment with NaCl and KBr revealed that halogenation enzymes used these salts as substrates and effectively produced chlorodepsidones, bromodepsidones and bromodepsides. It is well known that $FADH_2$-dependent halogenases are responsible for halogenation of many aromatic compounds[107-108]. Moreover, Sureram and coworkers recently isolated three brominated depsidones through directed biohalogenation using marine derived fungus *A. unguis* and they also suggested that this halogenation is from the activity of $FADH_2$-dependant halogenase enzyme. Thus, after analysing the metabolic profile of this fungus, it was revealed that in control YESL media, nonchlorinated depsidones (unguinol and folipastatin) were the major products, whereas when this organism was supplemented with halide salts, chlorodepsidones (nornidulin, nidulin), bromodepsidones and bromodepsides (aspergillusidones D, E, F and unguidepside B) were the major products. It is noteworthy to mention that halogenated depsides (particularly chlorinated) are common in nature and most of these depsides have been isolated from lichen sources[109]. Conversely, halogenated depsides from fungal sources are rare and only three depsides, guisinol, agonodepsides A and B, have been reported from fungal sources to date. The present work demonstrates that unnatural brominated depsides can be readily produced by this fungus using a precursor-directed biosynthetic approach.

4 Semi-synthesis of nidulin analogues

4.1 Introduction

In Chapter 3, precursor-directed biosynthesis through biohalogenation was used to introduce halogen atoms into depsidone nucleus at different positions to generate novel depsides and depsidones. However, incorporation of other halogen atom like iodine and modification of other functional group in nidulin pharmacophore would provide additional valuable information towards generating a structure activity relationship for the nidulin pharmacophore. Therefore, in this chapter using unguinol as a starting material, a semi-synthetic approach was applied to generate a small library of nidulin analogues. This chapter describes the method of preparation of these derivatives and their structure elucidation using spectroscopic methods.

4.2 Unguinol

Unguinol (**3**), is the major metabolite of the nidulin family produced by *A. unguis*. Unguinol is the nonchlorinated analogue of nidulin (**1**) and has two free hydroxyl groups at C-3 and C-8. Due to the limited amount of unguinol available, all chemical reactions were conducted on a small scale (10 mg). The reaction schemes used to synthesise unguinol analogues are shown in Figure 4.1.

4.3 Semi-synthetic derivatives of unguinol

4.3.1 1′,2′-dihydrounguinol (27)

1′,2′-dihydrounguinol (**27**) was obtained by catalytic hydrogenation of the butenyl side chain (between C-1′ and C-2′) of unguinol (**3**). This reduction reaction was carried out in presence of Pd on carbon catalyst. The mixture of unguinol and catalyst was subjected to hydrogenation overnight and the reaction product was used without any further purification. In the ^{1}H NMR spectrum, two methylene protons (δ_H 1.50) and one methine proton (δ_H 3.25) as multiplet indicated the presence of two extra hydrogens in **27**. Analysis of 2D NMR spectra (see Supplementary Material, Table S7) as well as the data comparison with those of unguinol, led to the assignment of protons and carbons in **27**.

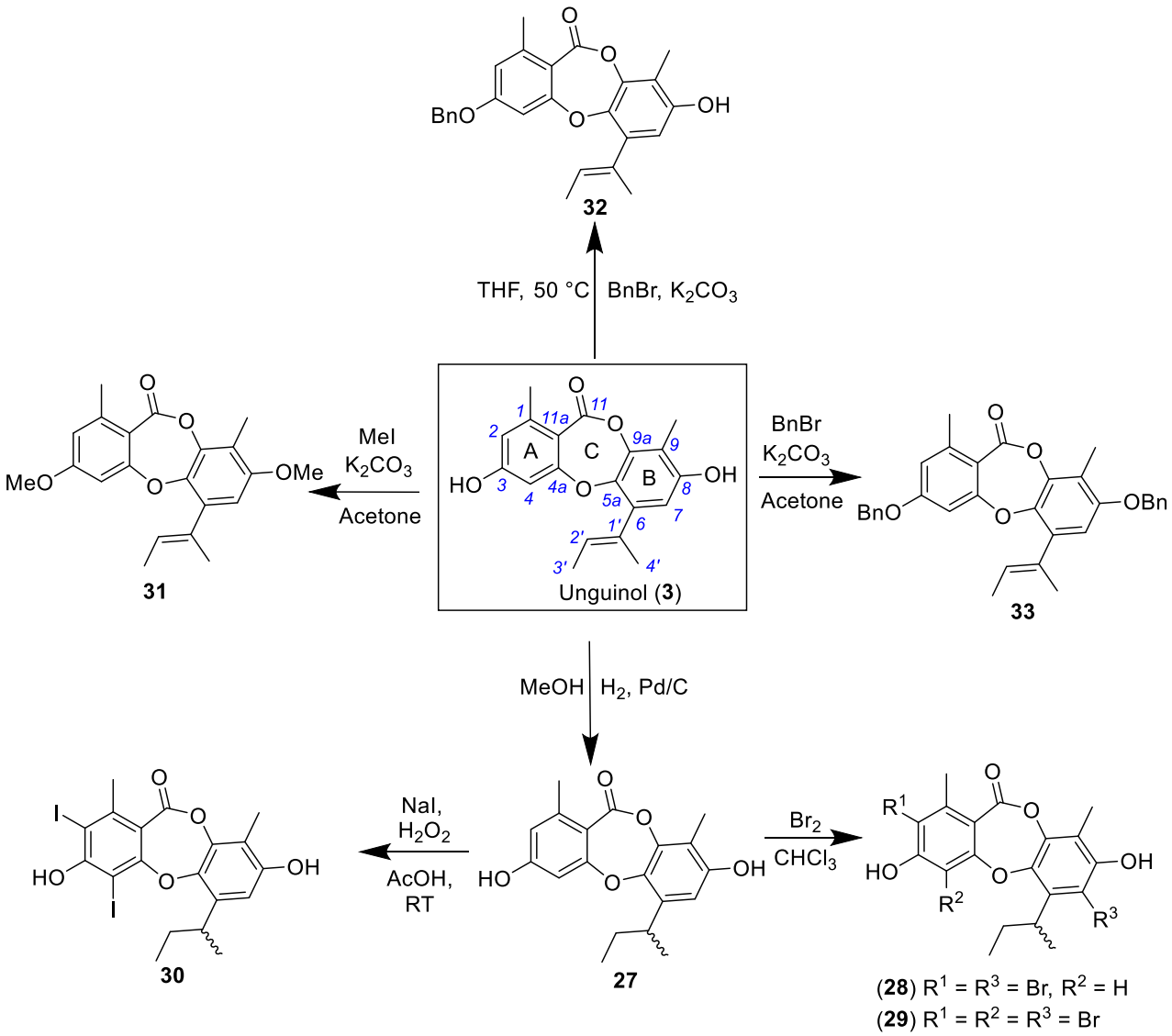

Figure 4.1: Reaction schemes for preparation of unguinol analogues

4.3.2 Bromination of 1′,2′-dihydrounguinol

1′,2′-dihydrounguinol (**27**) is a suitable for electrophilic substitution reaction. Thus, when **27** and bromine solution were kept in methanol overnight it gave a mixture of 2,7-dibromo-1′,2′-dihydrounguinol (**28**) and 2,4,7-tribromo-1′,2′-dihydrounguinol (**29**) and these synthetic compounds were separated by HPLC and their structures were confirmed by NMR (see Supplementary Material, Tables S8 and S9 respectively).

4.3.2.1 2,7-dibromo-1',2'-dihydrounguinol (28)

In unguinol (**3**), both aromatic rings A and B bear two electron-donating hydroxyl groups at positions 3 and 8 hence facilitating the occurrence of electrophilic substitution reactions. By analysing the product obtained it is clear that the positions 2 and 7 in aromatic rings A and B respectively were the preferred sites of bromination. The ESI positive and negative mass spectra of 2,7-dibromo-1′,2′-dihydrounguinol (**28**) showed isotope patterns at *m/z* $[M+H]^+$ 487/489/491 and $[M–H]^–$ 485/487/489 (in the ratio of 1:3:1) indicating the presence of two bromine atoms in the molecule. The structure of

28 was confirmed by analysis of NMR spectroscopic data. The ^{1}H NMR spectrum showed one singlet resonance in aromatic region (δ_H 6.86) which revealed that the compound was dibromo substituted analogue **27** (Figure 4.2). In the ^{13}C NMR spectrum, the carbon chemical shift of C-2 (δ_C 111.3) and C-4 (δ_C 104.6) was similar to the unnatural brominated depsidone, aspergillusidone D (**20**) (C-2 δ_C 111.1, C-4 δ_C 104.8), suggesting that two bromine atoms are attached to C-2 and C-7, while C-4 is underivatised. It is noteworthy to mention that the C-7 and C-5a resonances were not observed in the ^{13}C NMR spectrum due to peak broadening, possibly resulting from restricted rotation caused by the bulky bromine atoms. On the basis of these data, as well as detailed analysis of the 2D NMR data (Figure 4.2), the structure **28** was established to be 2,7-dibromo-1′,2′ dihydrounguinol.

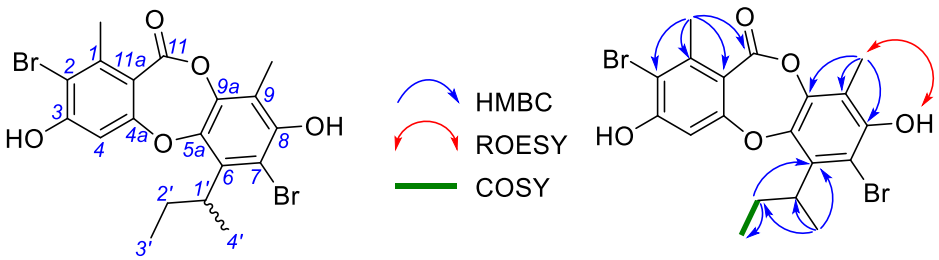

Figure 4.2: Key 2D NMR correlations observed in 2,7-dibromo-1′,2′ dihydrounguinol (**28**)

*4.3.2.2 2,4,7-tribromo-1',2'-dihydrounguinol (**29**)*

All the aromatic protons of **27** were substituted by bromine atoms to yield 2,4,7-triibromo-1′,2′-dihydrounguinol (**29**). The ESI negative mass spectrum of **29** showed an isotope pattern at *m/z* $[M–H]^-$ 562/564/566/568 (in the ratio of 1:3:3:1) indicating the presence of three bromine atom in the molecule. The structure of **29** was confirmed by detailed analysis of the NMR data (see Supplementary Material, Table S9). In the ^{1}H NMR spectrum, it was revealed that all the aromatic protons of 1′,2′-dihydrounguinol (**27**) had been replaced by bromine atoms, which confirmed **29** as 2,4,7-tribromo-1′,2′-dihydrounguinol.

4.3.3 Iodination of 1′,2′-dihydrounguinol

*4.3.3.1 2,4-diiodo-1',2'-dihydrounguinol (**30**)*

1′,2′-dihydrounguinol (**27**) was dissolved in acetic acid and NaI was added. H_2O_2 was added dropwise and reaction mixture kept for overnight to give **30**[110]. The structure of **30** was confirmed by detailed analysis of the ^{1}H and ^{13}C NMR data (see Supplementary Material, Table S10). The ^{1}H NMR spectrum of **30** showed one singlet aromatic proton at δ_H 6.52 (δ_C 108.3). Moreover, in the HMBC spectrum, 8-OH displayed correlations with C-7 (δ_C 108.3), C-8 (δ_C 153.4) and C-9 (δ_C 113.9), confirming the position of H-7 (Figure 4.3). In the ^{13}C NMR spectrum, chemical shifts for C-2 (δ_C 92.3) and C-4 (δ_C 76.9) were considerably more upfield than in **27** (C-2 δ_C 115.6; C-4 δ_C 104.4), suggesting that iodination occurred at the C-2 and C-4 positions. Therefore, on the basis of these data, the structure of **27** was confirmed as 2,4-diiodo-1′,2′-dihydrounguinol.

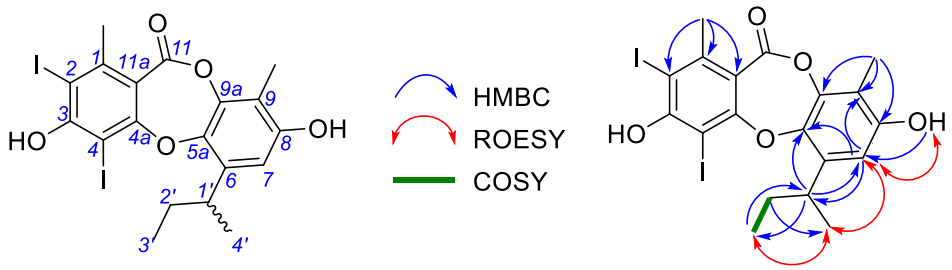

Figure 4.3: Key 2D NMR correlations observed in 2,4-diiodo-1′,2′-dihydrounguinol (**30**)

4.3.4 Methylation of unguinol

*4.3.4.1 3,8-di-O-methylunguinol (**31**)*

Unguinol (**3**) has two free phenolic groups at C-3 and C-8. Thus, adding methyl iodide to unguinol in the presence of base (K_2CO_3) gave 3,8-di-*O*-methylunguinol (**31**). After purification, the structure of **31** was confirmed by NMR (see Supplementary Material, Table S11). HR-ESI(+)-MS analysis of **31** revealed a quasimolecular ion ($[M+H]^+$ *m/z* 355.1535) indicative of a molecular formula $C_{21}H_{22}O_5$. Analysis of the ^1H and ^{13}C NMR spectra of **31** indicated the presence of two almost identical OMe groups (δ_H 3.77, δ_C 55.7; δ_H 3.76, δ_C 56.0). The HMBC spectrum showed correlations from the OMe protons at δ_H 3.77 and δ_H 3.76 to C-3 (δ_C 162.8) and C-8 (δ_C 154.3) respectively, indicating that it was a C-3 and C-8 dimethyl ether. Moreover, the ROESY spectrum of **31** showed that both 3-OMe and 8-OMe displayed a correlation with H-2 and H-7 aromatic protons respectively. On the basis of these data, the structure of **31** was established as 3,8-di-*O*-methylunguinol.

4.3.5 Benzylation of unguinol

*4.3.5.1 3-O-benzylunguinol (**32**)*

Mono-benzylation of unguinol (**3**) at the C-3 hydroxyl was achieved with benzyl bromide in the presence of K_2CO_3 at 50 °C where THF was used as solvent. Under these reaction conditions, 3-*O*-benzylunguinol was formed as the major product. HR-ESI(+)-MS analysis of **32** revealed a quasimolecular ion ($[M+H]^+$ *m/z* 417.1689) indicative of a molecular formula $C_{26}H_{24}O_5$. The position of the benzyl group was confirmed by NMR (see Supplementary Material, Table S12). Analysis of ^1H and ^{13}C NMR spectra of **32** indicated the two methylene protons on the benzyl group as a singlet at δ_H 5.14 (δ_C 69.6), with all benzyl aromatic ring proton at δ_H 7.31-7.40 appearing as a multiplet. The HMBC spectrum of **32** showed correlations from the benzyl methylene protons to C-3 (δ_C 161.7) and in the ROESY spectrum, these methylene protons demonstrated correlations with the H-2 aromatic proton (Figure 4.4). Therefore, these spectroscopic data confirmed the position of benzyl group. On the basis of these data, the structure of **32** was established as 3-*O*-benzylunguinol.

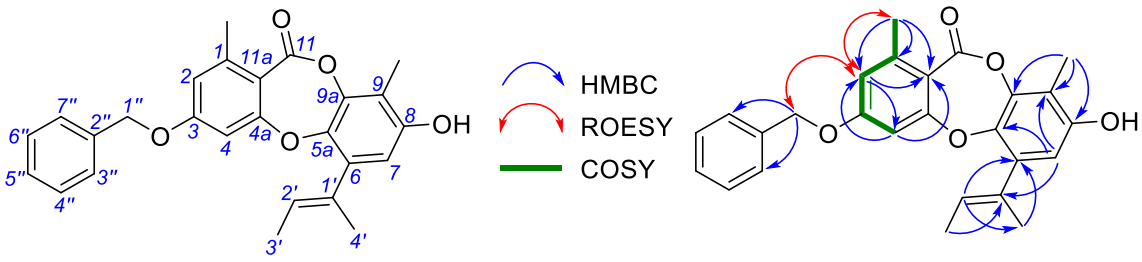

Figure 4.4: Key 2D NMR correlations observed in 3-*O*-benzylunguinol (**32**)

*4.3.5.2 3,8-di-O-benzylunguinol (**33**)*

Dibenzylation of **3** at the C-3 and C-8 hydroxyls was performed with benzyl bromide in the presence of K_2CO_3 and acetone at room temperature. After purification, the structure of **33** was confirmed by analysis of the NMR data (see Supplementary Material, Table S13). HR-ESI(+)-MS analysis of **33** revealed an adduct ion ($[M+H]^+$ *m/z* 507.2162) indicative of a molecular formula $C_{33}H_{30}O_5$. Analysis of the ^1H and ^{13}C NMR spectra of **33** revealed two sets of benzyl methylene protons as singlets at δ_H 5.15 (δ_C 69.6) and δ_H 5.08 (δ_C 69.9) respectively, with ten aromatic ring protons at δ_H 7.29-7.42 as a multiplet. The HMBC spectrum of 3,8-di-*O*-benzylunguinol (**33**) showed correlations from both 1″ and 1‴ methylene protons to C-3 (δ_C 161.8) and C-8 (δ_C 153.3) respectively. Moreover, ROESY correlations from H-2 and H-4 to 1″ methylene protons and from H-7 to 1‴ methylene protons were also observed. Therefore, on the basis of these data, the structure of **33** was established as 3,8-di-*O*-benzylunguinol.

4.4 Summary

This chapter described the semi-synthesis of six unguinol analogues. The structures of all derivatives were confirmed by 2D NMR spectra. In the next chapter, these derivatives were used to develop a structure activity relationship (SAR) of the nidulin pharmacophore to explore their full potential as antibiotic drug leads.

5 Bioassay and SAR

5.1 Introduction

To explore the bioassay profile of the nidulin pharmacophore, all natural and semi-synthetic nidulin derivatives were tested in antibacterial, antifungal and cell cytotoxicity assays. The *in vitro* antibacterial susceptibility of these compounds was tested against both Gram-positive (*Bacillus subtilis* and *Staphylococcus aureus*) and Gram-negative (*Escherichia coli*) organisms, while antifungal activity was assessed against *Candida albicans* and *Saccharomyces cerevisiae*. Cell cytotoxicity was assessed against mouse NS-1 myeloma cells.

5.2 Antibacterial activity of isolated natural compounds

Two new depsidones, 7-carboxyfolipastatin (**7**) and 2-bromo-7-chlorounguinol (**17**), along with four previously reported depsidones, were isolated in the present study. Isolated depsides and depsidones showed a wide range of activities (IC_{50} 0.7-9.5 µg/mL) against Gram-positive bacteria and no activity against Gram-negative *E. coli*. IC_{50} values of all the isolated natural compounds are summarised in Table 5.1. Nidulin (**1**) had the highest antibacterial activity (IC_{50} 0.70 µg/mL) against *B. subtilis* among the all the depsides and depsidones produced by *A. unguis*. Out of the two new depsidones, 2-bromo-7-chlorounguinol (**17**) was two-fold more potent than unguinol (**3**) (IC_{50} 6.1 µg/mL) against *B. subtilis* (IC_{50} 2.8 µg/mL) and four-fold more potent against *S. aureus* (IC_{50} 3.2 µg/mL), which indicated that a halogen atom is required for improved antibacterial activity. Folipastatin (**4**) showed good antibacterial activity against *Bacillus subtilis* and *S. aureus*, (IC_{50} 1.3 and 1.6 µg/mL respectively) while activity was lost following introduction of a carboxy group at C-7 in 7-carboxyfolipastatin (**7**).

Three new depsides were isolated in the present study, and out of these three depsides, only 5-bromoagonodepside B (**19**) showed moderate antibacterial activity (IC_{50} 9.5 µg/mL), while the other two showed very weak antibacterial activity (Table 5.1). Unguidepside B (**18**) is a brominated analogue of unguidepside A (**9**), and although unguidepside B (**18**) contains one bromine at C-3, it showed very weak antibacterial activity. On the other hand, 5-bromoagonodepside B (**19**) also contains one bromine atom at C-5 but showed moderate antibacterial activity, which suggests that the position of the bromine is important for antibacterial activity. Guisinol (**23**), the chloro analogue of 5-bromoagonodepside B, has been reported to show antibacterial activity against the Gram-negative bacterium *Vibrio parahaemolyticus*[90]. From the antibacterial assay, it was clear that a halogen is required for maximum antibacterial activity of nidulin family metabolites. Additionally, the location of the halogen on the aromatic ring is also an important factor for antibacterial activity. In the present study, it was revealed that when halogen atoms are present at C-2 and C-7 in the depsidone ring

Table 5.1: Antimicrobial activity of nidulin analogues

Compounds	IC_{50} (µg/mL)		
	B. subtilis	*S. aureus*	*S. cerevisiae*
nidulin (**1**)	0.70 ± 0.01	1.2 ± 0.1	> 50
nornidulin (**2**)	3.5 ± 0.1	Not tested	> 50
unguinol (**3**)	6.1 ± 0.1	11.6 ± 0.2	24.3 ± 0.5
folipastatin (**4**)	1.3 ± 0.3	1.65 ± 0.08	> 100
7-carboxyfolipastatin (**7**)	> 100	40.2 ± 0.4	> 100
unguinolic acid (**8**)	> 100	Not tested	
unguidepside A (**9**)	40.9 ± 0.4	> 100	> 100
2-bromo-7-chlorounguinol (**17**)	2.81 ± 0.02	3.25 ± 0.08	2.5 ± 0.2
unguidepside B (**18**)	37.3 ± 0.7	> 100	44 ± 3
5-bromoagonodepside B (**19**)	9.5 ± 0.2	46.6 ± 0.9	27 ± 3
aspergillusidone D (**20**)	2.4 ± 0.1	20.8 ± 0.5	2.4 ± 0.2
aspergillusidone F (**22**)	4.5 ± 0.2	5.94 ± 0.01	2.4 ± 0.1
1′,2′-dihydrounguinol (**27**)	3.1 ± 0.1	Not tested	> 100
2,7-dibromo-1′,2′-dihydrounguinol (**28**)	1.03 ± 0.02	2.03 ± 0.7	1.73 ± 0.03
2,4,7-tribromo-1′,2′-dihydrounguinol (**29**)	1.15 ± 0.02	7.3 ± 0.4	> 50
2,4-diiodo-1′,2′-dihydrounguinol (**30**)	0.99 ± 0.01	3.2 ± 0.1	4.7 ± 0.1
3,8-di-*O*-methylunguinol (**31**)	> 50	> 50	> 50
3-*O*-benzylunguinol (**32**)	7.2 ± 0.7	0.17 ± 0.01	> 50
3,8-di-*O*-benzylunguinol (**33**)	> 50	> 50	> 50
Ampicillin	0.14 ± 0.01		-
Clotrimazole	-	-	0.7 ± 0.2

(2-bromo-7-chlorounguinol (**17**), aspergillusidone-D (**20**), 2,7-dibromo-1′,2′-dihydrounguinol (**28**)) the compounds showed improved antibacterial activity compared to C-4 and C-7 position substituents (aspergillusidone F). Previous studies have indicated that 2,7-dichlorounguinol also shows activity against *Staphylococcus aureus* (MIC 16 mm)[111].

5.3 Antibacterial activity of semi-synthetic nidulin derivatives

The semi-synthetic nidulin analogues exhibited a wide range of activities against Gram-positive bacteria but no activity against Gram-negative *Escherichia coli.* The IC_{50} values for all of the semi-synthetic unguinol analogues are summarised in Table 5.1. Unguinol (**3**) contains two free hydroxyl groups at C-3 and C-8. However, when the both hydroxyl groups were methylated, antibacterial activities against *B. subtilis* and *S. aureus* were dramatically decreased. Benzylation of only the 3-OH in unguinol (3-*O*-benzylunguinol (**32**)) revealed that the antibacterial activity against *B. subtilis* was IC_{50} 7.2 µg/mL, which is similar to unguinol (IC_{50} 6.1 µg/mL). Benzylation of both hydroxyls led to the complete loss of antibacterial activity. These bioassay results suggest that one of these hydroxyl group is necessary for antibacterial activity. When the double bond of the butenyl side chain was hydrogenated, the resulting compound, 1′,2′-dihydrounguinol (**27**), showed two-fold higher

antibacterial activity against *B. subtilis* (IC_{50} 3.1 ± 0.1) than unguinol (**3**). Nidulin (**1**) contains three chlorine atoms at C-2, C-4 and C-8. In the present study, aromatic hydrogens of 1′,2′-dihydrounguinol (**27**) were replaced by bromine and iodine. Among the halosubstituted unguinol derivatives, 2,4-diiodo-1′,2′-dihydrounguinol (**30**) showed potent antibacterial activity against *B. subtilis* and *S. aureus* (IC_{50} 0.99 and 3.2 µg/mL respectively), which is almost equivalent to nidulin antibacterial activity (IC_{50} 0.70 and 1.2 µg/mL respectively). 2,7-dibromo and 2,4,7-tribromo derivatives of unguinol showed strong antibacterial activity (IC_{50} 1.03 and 1.15 µg/mL respectively) compared with unguinol (IC_{50} 6.1 µg/mL). Therefore, the bioassay results indicated that presence of halogen atoms is required for improved antibacterial activity. This demonstrates how key structural modifications can improve potency and selectivity of natural products, e.g. the antibacterial activity of vancomycin decreased by 70% when a single chlorine atom is replaced by hydrogen atom[112].

5.4 Antifungal activity of nidulin analogues

Antifungal activity testing was carried against *Candida albicans* and *Saccharomyces cerevisiae*, revealing that all the compounds were inactive against *Candida albicans*. Only two synthetic compounds, 2,7-dibromo-1′,2′-dihydrounguinol (**28**) and 2,4-diiodo-1′,2′-dihydrounguinol (**30**), showed activity against *Saccharomyces cerevisiae* (IC_{50} 1.73 and 4.7 µg/mL respectively). Among the natural depsidones, only 2-bromo-7-chlorounguinol (**17**), aspergillusidone D (**20**) and aspergillusidone F (**22**) showed activity against *Saccharomyces cerevisiae* (IC_{50} 2.5, 2.4 and 2.4 µg/mL respectively), while all isolated depsides were inactive against *Saccharomyces cerevisiae*. Antifungal activity of nidulin family depsidones has not been reported previously.

5.5 Cell cytotoxicity of nidulin analogues

Cell cytotoxicity was assessed against mouse NS-1 myeloma cells and all the semi-synthetic and natural compounds were inactive against this cell line.

5.6 Analysis of structure activity relationship of the nidulin pharmacophore

5.6.1 Effect of halogens on nidulin depsidone ring

For maximum antibacterial activity, the presence of halogen atoms on the aromatic rings is essential. Replacement of aromatic hydrogen with three bromine atoms or two iodine and bromine atoms increased the antibacterial activity of semi-synthetic compounds as compared with parent 1′,2′-dihydrounguinol (**27**). From the bioassay results, it was also revealed that the positions of the halogen atoms were also important for antibacterial activity. Halogenation at C-2 and C-7 resulted in improved antibacterial activity compared to C-4 and C-7 (Figure 5.1). From the literature, it was also revealed that when the C-2 position was chlorinated (2-chlorounguinol), the molecule showed antibacterial activity[113]. Therefore, of the three positions, C-2 is most important for antibacterial action.

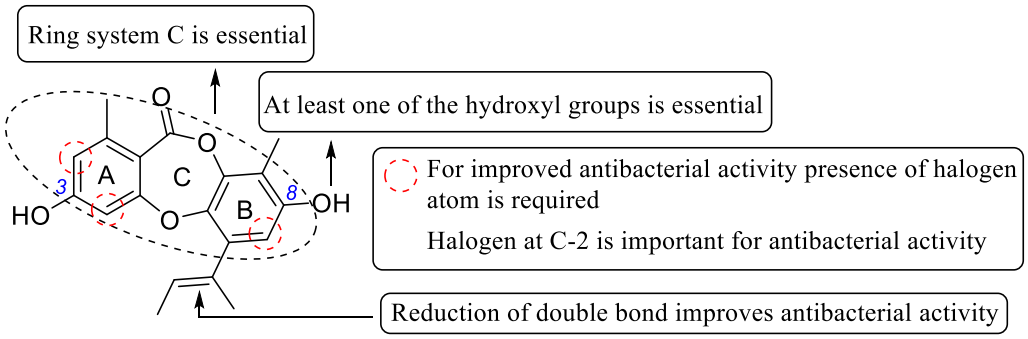

Figure 5.1: Summary of SAR studies of nidulin depsidone pharmacophore

5.6.2 Effect of replacement of hydroxyl groups

Unguinol (**3**) has underivatised hydroxyl groups at C-3 and C-8. Bioassay data revealed that when both hydroxyl groups were methylated or benzylated, the molecule lost its antibacterial activity. However, when only the C-3 hydroxyl group was derivatised, its antibacterial activity was unaffected. Given that nidulin (**1**) has one free hydroxyl group at C-3 and one methylated hydroxyl group at C-8, this indicates that at least one free hydroxyl group is essential for antibacterial activity.

5.6.3 Role of seven-membered C ring

All the nidulin depsidone analogues contain a seven-membered ring consisting of both an ester and an ether linkage. Antibacterial assays revealed that all the depsides that were isolated by directed biohalogenation process were inactive against test organisms. This result suggested that opening of ether linkage leads to loss of antibacterial effect. Recently, Yi Zhang and co-workers reported that aspergillusether A (ring-opened methyl ester derivative of nidulin) did not demonstrate significant effect (MIC >512 µg/mL) against methicillin-resistant *Staphylococcus aureus* (MRSA)[75]. This suggests that the seven-membered ring is essential for antibacterial activity of nidulin family depsidones. A summary of SAR studies of the nidulin pharmacophore is summarised in Figure 5.1.

5.7 Summary

This chapter described the bioassay profile of isolated natural compounds as well as semi-synthetic compounds. From the bioassay results revealed that nidulin family depsidones were selective against Gram-positive bacteria. However, among the all isolated new compounds, 2-bromo-7-chlorounguinol (**17**) showed significant antibacterial and antifungal activity. On the other hand, out of all the semi-synthetic compounds, 2,4-diiodo-1′,2′-dihydrounguinol (**30**) was found to be the most potent. Therefore, nidulin-family depsidones containing halogens, particularly iodine or mixed halogen, may be lead compounds for further drug development. Finally, this chapter also described the SAR of nidulin depsidone pharmacophore, which suggested that a seven-membered ring is essential for bioactivity of these depsidones.

5.8 Concluding remarks

Under laboratory conditions, the metabolic profile of microorganisms may be highly dependent on culture media and it was hypothesised that every single steps of biosynthesis of secondary metabolites is influenced by environmental factors either at the transcriptional level, or at the translational level or/and the enzyme level resulting in different metabolome[114]. Moreover, the influence of external stimuli, like changes in carbon and nitrogen sources, may lead to the activation of orphan gene clusters, which were silent under laboratory condition, to give new metabolites[115]. Genome mining of *Aspergillus nidulans* revealed that this organism is able to generate up to 32 polyketides, 14 ribosomal peptides and 2 indole alkaloids and out of these only 25 compounds have been described up to date. To access these silent gene products, modern molecular biology based techniques such as gene knock out (e.g. emericellamides A-F)[116] and epigenetic modulation (e.g. asperthecin)[117] have ushered in a new era of antibiotic discovery.

In the present study, it was observed that the fungus *A. unguis* produced increased amounts of chloro derivatives of depsidone (nidulin and nornidulin, chlorounguinol) when supplemented with NaCl in the media. Similarly, whenever this fungus was supplemented with KBr, it produced unnatural bromo depsidones and depsides as well as unique 'mixed' chlorine and bromine containing depsidone. Recently, Sureram and coworkers suggested that halogenation of marine-derived fungus *A. unguis* is from the activity of an $FADH_2$-dependent halogenase enzyme[85]. However, isolation of mixed Cl/Br depsidone from this fungus emphasised again how versatile the biosynthetic machinery of *A. unguis* is, which allowing the incorporation of different halogen atoms in two different aromatic rings in nidulin pharmacophore. Although mixed Cl and Br containing terpenes and polyketides have been isolated from red and brown algae, they are extremely rare from fungal sources[118].

Among the all nidulin family depsidones, nidulin (containing 3 chlorine atoms) showed highest antibacterial activity. This chlorinated depsidone showed selective antibacterial activity against Gram-positive bacteria. Other chlorodepsides, such as spiromastixones B–P from the deep sea fungus *Spiromastix* sp., also showed selective antibacterial activity against Gram-positive bacteria[119]. It was observed that an increasing number of chlorine atoms enhanced the antibacterial activity and spiromastixones J (containing four chlorines) showed better inhibitory activity against MRSA than levofloxacin[119]. Chlorinated depsidones are valuable lead compounds for further antibacterial drug development against resistant organisms. Moreover, in the present study, the structure activity relationship of the nidulin pharmacophore was proposed and utilising this knowledge affinity probes can be synthesised for subsequent mode of action studies using chemical proteomics approaches such as phage and yeast display[120].

6 Experimental

6.1 General experimental details

6.1.1 Material

All chemicals and reagents unless otherwise stated were purchased from Sigma-Aldrich (St. Louis, U.S.A) and used without further purification. TLC was performed with Merck Kieselgel 60 F254 plates with viewing under ultraviolet light (254 nm and 365 nm).

6.1.2 Equipment

^{1}H NMR and ^{13}C NMR spectra were recorded in 5 mm Pyrex tubes (Wilmad, USA) on either a Bruker Avance DPX-400 400 MHz or DRX-600K 600 MHz spectrometer. All spectra were obtained at 25 °C, processed using Bruker Topspin 3.5 software and referenced to residual solvent signals (DMSO-d_6 δ_H 2.49/ δ_C 39.5 ppm). High resolution electrospray ionisation mass spectra (HRESIMS) were obtained on a Q Exactive Plus hybrid quadrupole-Orbitrap mass spectrometer (Thermo Fisher Scientific, Bremen, Germany) by direct infusion. Electrospray ionisation mass spectra (ESIMS) were acquired on an Agilent 1260 UHPLC coupled to an Agilent 6130B single quadrupole mass detector.

Analytical HPLC was performed on a gradient Agilent 1260 Infinity quaternary HPLC system consisting of a G4212B diode array detector. The column was an Agilent Poroshell 120 EC-C_{18} (4.6 × 50 mm, 2.7 µm) eluted with a 1 mL/min gradient of 10-100% acetonitrile/water (0.01% TFA) over 8.33 min. Semi-preparative HPLC was performed on a gradient Agilent 1260 Infinity quaternary HPLC system consisting of a G4212B diode array detector. The column was Agilent Zorbax SB-C_{18} (9.4 × 250 mm, 5 µm) eluted with a 4.18 mL/min gradient of 10-100% acetonitrile/water (0.01% TFA) over 40 min. Preparative HPLC was performed on a gradient Shimadzu HPLC system comprising two LC-8A preparative liquid pumps with static mixer, SPD-M10AVP diode array detector and SCL-10AVP system controller with standard Rheodyne injection port. The column was hypersil C_{18} spring column (50 × 150 mm, 5 µm; Grace Discovery) eluted isocratically with acetonitrile at 60 mL/min.

6.2 Culture media optimisation

Culture media optimisation of *A. unguis* was performed on a range of agar, liquid and grain-based media. The agars: Glycerol casein agar, Czapek-Dox agar, Malt extract agar, Oatmeal agar, Yeast extract and sucrose agar; and the liquids: Glycerol casein, Czapek-Dox, Malt extract, Oatmeal, Yeast extract sucrose media; were prepared according to the recipes presented in the Supplementary Material. The grains: pearl barley, rice (Jasmine and Basmati) and cracked wheat; were prepared by hydration (~30 mL water in 250 mL flask) during sterilisation at 120 °C for 40 min. All the media were inoculated with a spore suspension of *A. unguis* and incubated at 24 °C for 14 days. The liquid

media were incubated both with shaking (150 rpm) and as static cultures. The cultures were sub-sampled (1 mL for liquid media and 1 g for agar and grain media) and extracted with methanol (2 mL) for a minimum of 1 h on a wrist shaker, centrifuged (15,700 × *g* for 5 min) and analysed by LCMS. The major metabolites were analysed by HPLC retention time, UV spectroscopy and mass spectrometry.

6.3 Cultivation, extraction and fractionation of *A. unguis*

Yeast extract sucrose media (4 L) was prepared according to recipe (presented in the Supplementary Material) and sterilised at 120 °C for 40 min. A spore suspension of a 7-day-old Petri plate of *A. unguis* was used to inoculate 70 × 250 mL Erlenmeyer flasks each containing 50 mL of sterile yeast extract sucrose media. The flasks were incubated at 24 °C for 14 days on a rotary shaker (150 rpm). By this time the culture has grown extensively and reached maximum metabolite productivity. The culture was transferred from individual flasks, extracted with acetone (2 × 1.5 L) and the combined extracts evaporated *in vacuo* to give an aqueous residue. The residue was then partitioned against ethyl acetate (2 × 1 L) and dried to give a crude extract (8.1 g). The crude extract was again partitioned against hexane and methanol with 10% water (2 × 1 L). The methanolic (4.6 g) and hexane fractions (3.4 g) were evaporated to dryness to give final crude extracts. The methanolic extract was further fractionated by preparative HPLC.

6.4 Precursor-directed biosynthesis with NaCl and KBr

Yeast extract sucrose media was prepared according to recipe presented in the Supplementary Material, and 50 mL of this media was transferred to three different 250 mL Erlenmeyer flasks. 2.5% NaCl, (1.25 g), 5% NaCl (2.5 g) and 10% NaCl (5.0 g) were added and the media was sterilised at 120 °C for 40 min. A spore suspension of a 7-day-old Petri plate of *A. unguis* was used to inoculate the flasks. The flasks were incubated at 24 °C for 14 days on a rotary shaker at 150 rpm. The cultures were sub-sampled (1 mL) and extracted with methanol (2 mL) for a minimum of 1 h on a wrist shaker, centrifuged (15,700 × *g* for 5 min) and analysed by LCMS. Precursor-directed biosynthesis experiments with lower salt (NaCl and KBr) concentrations (0.5%, 1% and 2%) were performed in the same fashion as described above. Here, 0.5% (0.25 g), 1% (0.5 g) and 2% (1 g) salt (NaCl and KBr) were added to YESL media. Experiments were performed in duplicate.

6.5 Cultivation, extraction and fractionation of *A. unguis* with KBr

Yeast extract sucrose media (4 L) was prepared according to recipe presented in the Supplementary Material. 1% KBr (40 g) was added and the media was sterilised at 120 °C for 40 min. A spore suspension of a 7-day-old Petri plate of *A. unguis* was used to inoculate 30 × 250 mL Erlenmeyer flasks each containing 50 mL of sterile yeast extract sucrose media. The flasks were incubated at 24

°C for 14 days. By this time the culture has grown extensively and reached maximum metabolite productivity. The culture was transferred from individual flasks, extracted with acetone (2 × 1.5 L) and the combined extracts evaporated *in vacuo* to give an aqueous residue. The residue was then partitioned against ethyl acetate (2 × 1 L) and dried to give a crude extract (3.1 g). The crude extract was again partitioned against hexane and methanol with 10% water (2 × 1 L). The methanolic (1.7 g) and hexane (0.9 g) fractions were evaporated to dryness to give final crude extracts.

The methanolic extract (1.7 g) was further fractionated by preparative HPLC. The fractions were subsampled and analysed by C_{18} analytical HPLC. The fractions containing comparable metabolite were combined and then evaporated to dryness, yielding 9 fractions. Fraction 4 (127 mg) was again purified by semi-preparative HPLC with isocratic 75% MeCN plus 0.01% TFA (flow rate 4.18 mL/min). After separation of this fraction, unguidepside A (**9**) (t_R = 18.7 min; 10.7 mg) was isolated. Fraction 6 (45.8 mg) was purified by semi-preparative HPLC with isocratic 80% MeCN plus 0.01% TFA (flow rate 4.18 mL/min). After separation of this fraction unguidepside B (**18**) (t_R = 20.8 min; 9.8 mg) was isolated. Fraction 7 (113.0 mg) was purified by semi-preparative HPLC with a gradient of 35% to 80% MeCN plus 0.01% TFA (flow rate 4.18 mL/min). After separation of this fraction, aspergillusidone F (**22**) (t_R = 22.8 min; 45.8 mg), 2-bromo-7-chlorounguinol (**17**) (t_R = 23.1 min; 8.1 mg) and aspergillusidone D (**20**) (t_R = 23.8 min; 24.7mg) were isolated. Fraction 9 (56.8 mg) was purified by semi-preparative HPLC with isocratic 50% MeCN + 0.01% TFA (flow rate 4.18 mL/min). After separation of this fraction, 5-bromoagonodepside B (**19**) (t_R = 20.1 min; 23.5 mg) was isolated.

6.6 Susceptibility of *A. unguis* to unnatural precursors by disc diffusion method

Sterile paper discs (9 mm diameter) were loaded with 6-methylsalicylic acid, 6-fluorosalicylic acid, 6-methoxysalicylic acid, 2,4-dihydroxybenzoic acid, orsellinic acid dimethyl ether, 3-methylorsellinic acid and 3-isopropylorsellinic acid (4 µL, 40 µg/mL in methanol for each). *A. unguis* was subcultured on malt extract agar medium at 24 °C for seven days. Following growth of the fungus, a spore suspension was made with sterile water. An aliquot (500 µL) of the spore suspension was added to each malt extract agar plate and streaked evenly with a spreader. Discs containing the test agents were applied to the surface of inoculated plates. Plates were inverted and incubated at 24 °C for 7 days to allow for fungal growth. Inhibition zone diameters (IZD) were measured in millimetres.

6.7 Precursor-directed biosynthesis with salicylic and orsellinic acids

Yeast extract sucrose media was prepared and inoculated with *A. unguis* in the same manner as described above. Five unnatural biosynthetic building blocks were selected, 6-methylsalicylic acid, 6-fluorosalicylic acid, 6-methoxysalicylic acid, orsellinic acid dimethyl ether, 3-methylorsellinic

acid. 50 mg of each precursor were dissolved in DMSO (200 µL) to give a final concentration of 0.5 mg/mL. From each of these solutions, 100 µL was added to each inoculated flask. The flasks were incubated at 24 °C for 14 days. The cultures were sub-sampled (1 mL) and extracted with methanol (2 mL) for 1 h on a wrist shaker, centrifuged (15,700 × *g* for 5 mins) and analysed by LCMS.

6.8 Semi-synthetic derivatives of unguinol

6.8.1 1′,2′-dihydrounguinol (27)

Unguinol (50 mg, 0.15 mmol) was dissolved in methanol (5 mL) and 10% palladium on carbon catalyst (3.2 mg) was added. The reaction mixture was stirred overnight under an atmosphere of H_2 (balloon) at room temperature. The reaction mixture was filtered through celite and the solvent was removed *in vacuo* to yield 1′,2′-dihydrounguinol (**27**) (50 mg, 100% yield), which was used without further purification. ESI-MS *m/z* $[M+H]^+$ 329.1374 (calculated for $C_{19}H_{21}O_5^+$ 329.1384). ^1H and ^{13}C NMR, see Table S7.

6.8.2 Bromination of 1′,2′-dihydrounguinol

1′,2′-dihydrounguinol (**27**) (10 mg, 30 µmol) was dissolved in chloroform (3 mL) and a solution of bromine in chloroform (2.1 M; 33 µL, 70 µmol) was added. The reaction mixture was stirred at room temperature for 6 h. The crude reaction mixture was washed with brine (3 × 3 mL) and the organic layer was dried over $MgSO_4$, filtered and reduced to dryness under N_2. The residue (9.1 mg) was purified by semi-preparative HPLC with isocratic 60% MeCN plus 0.01% TFA (flow rate 4.18 mL/min). After separation, 2,7-dibromo-1′,2′-dihydrounguinol (**28**) (t_R = 22.8 min; 1.64 mg, 16.4% yield) and 2,4,7-tribromo-1′,2′-dihydrounguinol (**29**) (t_R = 23.5 min; 1.9 mg, 19% yield) were isolated. HR-ESI(–)-MS *m/z* $[M–H]^–$ 482.9443 (calculated for $C_{19}H_{17}{}^{79}Br_2O_5^–$ 482.9443) and *m/z* $[M+H]^+$ 560.8553 (calculated for $C_{19}H_{18}{}^{79}Br_3O_5^+$ 560.8548) ^1H and ^{13}C NMR, see Tables S8 and S9 respectively.

6.8.3 Iodination of 1′,2′-dihydrounguinol

1′,2′-dihydrounguinol (10 mg, 30 µmol) was dissolved in acetic acid (3 mL) and NaI (130 mg, 88 µmol) was added. An aqueous solution of H_2O_2 (30%; 0.5 mL, 0.15 mmol) was added dropwise to the well-stirred solution, and the reaction mixture was stirred room temperature for 6 h. The mixture was treated with an aqueous sodium thiosulfate solution (2 × 3 mL) and extracted with ethyl acetate (3 × 3 mL). The organic layer was dried over anhydrous $MgSO_4$, and reduced to dryness under nitrogen. The residue was purified by silica flash chromatography using a SNAP-10g cartridge. The whole reaction product was dissolved in 1 mL *n*-hexane/ethyl acetate (50:50) and separated with *n*-hexane and ethyl acetate gradient system (7% to 60%), flow rate 12 mL/min, yielding 2,4-diiodo-1′,2′-dihydrounguinol (**30**) (t_R = 12.5 min, 5.6 mg, 56% yield). HR-ESI(–)-MS *m/z* $[M–H]^–$ 578.9172 (calculated for $C_{19}H_{17}I_2O_5^–$ 578.9166). ^1H and ^{13}C NMR, see Table S10.

6.8.4 3,8-di-*O*-methylunguinol (31)

Unguinol (10 mg, 31 µmol) was dissolved in acetone (3 mL) and iodomethane (50 µL, 0.77 mmol) and excess K_2CO_3 (5 mg) were added. The reaction mixture was stirred at room temperature overnight then filtered. The filtrate was reduced to dryness under nitrogen. The residue was purified by silica chromatography using a SNAP-10g cartridge. The whole reaction product was dissolved in 1 mL *n*-hexane/ethyl acetate (50:50). The mixture was separated with *n*-hexane and ethyl acetate gradient system (2% to 20%), flow rate 12 mL/min, yielding 3,8-di-*O*-methylunguinol (**31**) (3.0 mg, t_R = 13.5 min, 30% yield). HR-ESI(+)-MS *m/z* $[M+H]^+$ 355.1535 (calculated for $C_{21}H_{23}O_5^+$ 355.1546). ^1H and ^{13}C NMR, see Table S11.

6.8.5 Benzylation of unguinol

*6.8.5.1 3-O-benzylunguinol (**32**)*

Unguinol (10 mg, 31 µmol) was dissolved in tetrahydrofuran (3 mL) and benzyl bromide (51 µL, 0.43 mmol) and excess K_2CO_3 (5 mg) were added. The reaction mixture was stirred at 50 °C overnight. The crude reaction mixture was filtered and the filtrate was reduced to dryness under nitrogen. The product was purified by silica chromatography using a SNAP-10g cartridge. The whole reaction product was dissolved in 1 mL *n*-hexane and ethyl acetate (50:50). The mixture was separated with *n*-hexane/ethyl acetate gradient system (5% to 40%), flow rate 12 mL/min, yielding 3-*O*-benzylunguinol (**32**) (4.6 mg, t_R = 10.5 min, 46% yield). HR-ESI(+)-MS *m/z* $[M+H]^+$ 417.1689 (calculated for $C_{26}H_{25}O_5^+$ 417.1702). ^1H and ^{13}C NMR, see Table S12.

*6.8.5.2 3,8-di-O-benzylunguinol (**33**)*

Unguinol (10 mg, 31 µmol) was dissolved in acetone (3 mL) and benzyl bromide (102 µL, 0.86 mmol) and excess K_2CO_3 (5 mg) were added. The reaction mixture was stirred at room temperature overnight. The crude reaction mixture was filtered and the filtrate was reduced to dryness under nitrogen. The product was purified by silica chromatography and using a SNAP-10g cartridge. The whole reaction product was dissolved in 1 mL *n*-hexane/ethyl acetate (50:50). The mixture was separated with *n*-hexane and ethyl acetate gradient system (5% to 40%), flow rate 12 mL/min, yielding 3,8-di-*O*-benzylunguinol (**33**) (5.6 mg, t_R = 11.5 min, 56% yield). HR-ESI(+)-MS *m/z* $[M+H]^+$ 507.2162 (calculated for $C_{33}H_{31}O_5^+$ 507.2172). ^1H and ^{13}C NMR, see Table S13.

6.9 Preparation of microtitre plate for bioassay

All the isolated natural metabolites and semi-synthetic compounds were dissolved in DMSO to make stock solutions of 10,000 µg/mL. From each stock solution, 60 µL was transferred to the first lane of the rows B to G in a 96-well microtitre plate and two-fold serially diluted across the 12 lanes of the plate. Bioassay media was then added to the each of the wells to obtain a 100-fold dilution into the final bioassay. After this dilution, the final concentrations were 100 µg/mL to 0.05 µg/mL in 0.1%

DMSO across the plate. Rows A and H were used as negative control (0.1% DMSO) and positive control (no organism, 100% inhibition) respectively.

6.9.1 Antibacterial assays

The antibacterial activities of all the compounds were evaluated against two Gram-positive bacteria, *Bacillus subtilis* (ATCC 6633) and *Staphylococcus aureus* (ATCC 25923), and one Gram-negative bacterium, *Escherichia coli* (ATCC 25922). A bacterial suspension (50 mL in 250 mL flask) was prepared in nutrient media by cultivation for 24 h at 250 rpm, 28 °C. The suspension was diluted with sterile water to 0.01 absorbance units and an aliquot (10 µL) of this bacterial suspension was loaded into each well of the 96-well microtitre plate containing the test compounds dispersed in nutrient media with resazurin (120 µg/mL). The plates were incubated at 28 °C for 48 h during which time the negative control wells changed colour from blue to light pink. The absorbance was measured using a Spectromax plate reader at 605 nm and IC_{50} values were calculated using GraphPad Prism 7 (GraphPad Software, USA) by variable slope (four parameter) equation (Y=Bottom+(Top-Bottom)/(1+10^((LogIC_{50}-X) × HillSlope)). The experiments were performed in triplicate.

6.9.2 Antifungal assay

The antifungal activities of all the compounds were evaluated against the yeasts *Candida albicans* (ATCC 10231) and *Saccharomyces cerevisiae* (ATCC 9763). A yeast suspension was prepared in 1% malt extract broth by cultivation for 24 h at 250 rpm, 24 °C. This suspension was diluted with sterile water to give absorbances of 0.005 and 0.03 units for *C. albicans* and *S. cerevisiae* respectively. From these suspensions, 20 µL and 30 µL for *C. albicans* and *S. cerevisiae* respectively were loaded to the wells of a 96-well microtitre plate containing the test compounds dispersed in malt extract media and resazurin (120 µg/mL). The plates were incubated at 28 °C for 48 h during which the negative control wells changed colour from blue to yellow. The absorbance was measured using a Spectromax plate reader at 605 nm and IC_{50} values were calculated using GraphPad Prism 7 (GraphPad Software, USA) by variable slope (four parameter) equation (Y=Bottom+(Top-Bottom)/(1+10^((LogIC_{50}-X) × HillSlope)). The experiments were performed in triplicate.

6.9.3 Cell cytotoxicity activity

Cell cytotoxicity activity was evaluated using NS-1 (ATCC TIB-18) mouse myeloma cells. These cells were cultured in in DMEM (Dulbecco's Modified Eagle Medium + 10% fetal bovine serum (FBS) + 1% penicillin/streptomycin (Life Technologies)) and incubated at 37 °C (5% CO_2) for 48 h. From this culture, the cells (190 µL, 50,000/mL) were loaded in 96-well microtitre plates with resazurin (10 µL, 120 µg/mL) containing the test solution. The plates were incubated for 48 h at 37 °C (5% CO_2). The absorbance was measured using a Spectromax plate reader at 605 nm. The experiments were performed in triplicate.

7 References

1. Organization, W. H., *Antimicrobial resistance: global report on surveillance*. World Health Organization: 2014.

2. Coates, A.; Hu, Y.; Bax, R.; Page, C., "The future challenges facing the development of new antimicrobial drugs", *Nature Reviews Drug Discovery*, **2002**, *1*, 895-910.

3. Coates, A. R.; Hu, Y., "New Strategies for Antibacterial Drug Design", *Drugs in R & D*, **2006**, *7*, 133-151.

4. Levy, S. B.; Marshall, B., "Antibacterial resistance worldwide: causes, challenges and responses", *Nature Medicine*, **2004**, *10*, S122-S129.

5. Brown, E. D.; Wright, G. D., "Antibacterial drug discovery in the resistance era", *Nature*, **2016**, *529*, 336-343.

6. World Health Organization Antimicrobial Resistance Global Report on Surveillance. 2014.

7. Lewis, K., "Platforms for antibiotic discovery", *Nature Reviews Drug Discovery*, **2013**, *12*, 371-387.

8. Sabtu, N.; Enoch, D.; Brown, N., "Antibiotic resistance: what, why, where, when and how?", *British Medical Bulletin*, **2015**, *116*, 105-113.

9. Newman, D. J.; Cragg, G. M., "Natural products as sources of new drugs over the 30 years from 1981 to 2010", *Journal of Natural Products*, **2012**, *75*, 311-335.

10. Lam, K. S., "New aspects of natural products in drug discovery", *Trends in Microbiology*, **2007**, *15*, 279-289.

11. Cragg, G. M.; Newman, D. J., "Natural products: a continuing source of novel drug leads", *Biochimica et Biophysica Acta (BBA)-General Subjects*, **2013**, *1830*, 3670-3695.

12. Silver, L. L., "Challenges of antibacterial discovery", *Clinical Microbiology Reviews*, **2011**, *24*, 71-109.

13. Silver, L. L., "Natural products as a source of drug leads to overcome drug resistance", *Future Microbiology*, **2015**, *10*, 1711-1718.

14. Genilloud, O., "Current challenges in the discovery of novel antibacterials from microbial natural products", *Recent Patents on Anti-infective Drug Discovery*, **2012**, *7*, 189-204.

15. Payne, D. J.; Gwynn, M. N.; Holmes, D. J.; Pompliano, D. L., "Drugs for bad bugs: confronting the challenges of antibacterial discovery", *Nature Reviews Drug Discovery*, **2007**, *6*, 29-40.

16. Pham, V. H.; Kim, J., "Cultivation of unculturable soil bacteria", *Trends in Biotechnology*, **2012**, *30*, 475-484.

17. Ling, L. L.; Schneider, T.; Peoples, A. J.; Spoering, A. L.; Engels, I.; Conlon, B. P.; Mueller, A.; Schäberle, T. F.; Hughes, D. E.; Epstein, S., "A new antibiotic kills pathogens without detectable resistance", *Nature*, **2015**, *517*, 455-459.

18. Lok, C., "Mining the microbial dark matter", *Nature*, **2015**, *522*, 270-3.

19. Nichols, D.; Cahoon, N.; Trakhtenberg, E.; Pham, L.; Mehta, A.; Belanger, A.; Kanigan, T.; Lewis, K.; Epstein, S., "Use of ichip for high-throughput in situ cultivation of "uncultivable" microbial species", *Applied and Environmental Microbiology*, **2010**, *76*, 2445-2450.

20. Bertrand, S.; Bohni, N.; Schnee, S.; Schumpp, O.; Gindro, K.; Wolfender, J.-L., "Metabolite induction via microorganism co-culture: a potential way to enhance chemical diversity for drug discovery", *Biotechnology Advances*, **2014**, *32*, 1180-1204.

21. Moody, S. C., "Microbial co-culture: harnessing intermicrobial signaling for the production of novel antimicrobials", *Future Microbiology*, **2014**, *9*, 575-578.

22. Ueda, K.; Kawai, S.; Ogawa, H.-O.; Kiyama, A.; Kubota, T.; Kawanobe, H.; Beppu, T., "Wide distribution of interspecific stimulatory events on antibiotic production and sporulation among *Streptomyces* species", *The Journal of Antibiotics*, **2000**, *53*, 979-982.

23. Kurosawa, K.; Ghiviriga, I.; Sambandan, T.; Lessard, P. A.; Barbara, J. E.; Rha, C.; Sinskey, A. J., "Rhodostreptomycins, antibiotics biosynthesized following horizontal gene transfer from *Streptomyces padanus* to *Rhodococcus fascians*", *Journal of the American Chemical Society*, **2008**, *130*, 1126-1127.

24. Glauser, G.; Gindro, K.; Fringeli, J.; De Joffrey, J.-P.; Rudaz, S.; Wolfender, J.-L., "Differential analysis of mycoalexins in confrontation zones of grapevine fungal pathogens by ultrahigh pressure liquid chromatography/time-of-flight mass spectrometry and capillary nuclear magnetic resonance", *Journal of Agricultural and Food Chemistry*, **2009**, *57*, 1127-1134.

25. Schroeckh, V.; Scherlach, K.; Nützmann, H.-W.; Shelest, E.; Schmidt-Heck, W.; Schuemann, J.; Martin, K.; Hertweck, C.; Brakhage, A. A., "Intimate bacterial–fungal interaction triggers biosynthesis of archetypal polyketides in *Aspergillus nidulans*", *Proceedings of the National Academy of Sciences*, **2009**, *106*, 14558-14563.

26. Wright, P. M.; Seiple, I. B.; Myers, A. G., "The evolving role of chemical synthesis in antibacterial drug discovery", *Angewandte Chemie International Edition*, **2014**, *53*, 8840-8869.

27. Butler, M. S.; Blaskovich, M. A.; Owen, J. G.; Cooper, M. A., "Old dogs and new tricks in antimicrobial discovery", *Current Opinion in Microbiology*, **2016**, *33*, 25-34.

28. Rolinson, G., "Laboratory evaluation of amoxicillin", *Journal of Infectious Diseases*, **1974**, *129*, S139-S145.

29. Hiramatsu, K., "Vancomycin resistance in staphylococci", *Drug Resistance Updates*, **1998**, *1*, 135-150.

30. Boucher, H. W.; Wilcox, M.; Talbot, G. H.; Puttagunta, S.; Das, A. F.; Dunne, M. W., "Once-weekly dalbavancin versus daily conventional therapy for skin infection", *New England Journal of Medicine*, **2014**, *370*, 2169-2179.

31. Donadio, S.; Maffioli, S.; Monciardini, P.; Sosio, M.; Jabes, D., "Antibiotic discovery in the twenty-first century: current trends and future perspectives", *The Journal of Antibiotics*, **2010**, *63*, 423-430.

32. Kavanagh, F.; Hervey, A.; Robbins, W. J., "Antibiotic substances from Basidiomycetes VIII. *Pleurotus multilus* (Fr.) Sacc. and *Pleurotus Passeckerianus* Pilat", *Proceedings of the National Academy of Sciences*, **1951**, *37*, 570-574.

33. Egger, H.; Reinshagen, H., "New pleuromutilin derivatives with enhanced antimicrobial activity. II. Structure-activity correlations", *The Journal of Antibiotics*, **1976**, *29*, 923-927.

34. Yan, K.; Madden, L.; Choudhry, A. E.; Voigt, C. S.; Copeland, R. A.; Gontarek, R. R., "Biochemical characterization of the interactions of the novel pleuromutilin derivative retapamulin with bacterial ribosomes", *Antimicrobial Agents and Chemotherapy*, **2006**, *50*, 3875-3881.

35. Changhua, H.; Yi, Z., "Mutilins Derivatives: From Veterinary to Human-used Antibiotics", *Mini-Reviews in Medicinal Chemistry*, **2009**, *9*, 1397-1406.

36. Stein, G. E.; Craig, W. A., "Tigecycline: a critical analysis", *Clinical Infectious Diseases*, **2006**, *43*, 518-524.

37. Thiericke, R.; Rohr, J., "Biological variation of microbial metabolites by precursor-directed biosynthesis", *Natural Product Reports*, **1993**, *10*, 265-289.

38. Kirschning, A.; Taft, F.; Knobloch, T., "Total synthesis approaches to natural product derivatives based on the combination of chemical synthesis and metabolic engineering", *Organic & Biomolecular Chemistry*, **2007**, *5*, 3245-3259.

39. Kennedy, J., "Mutasynthesis, chemobiosynthesis, and back to semi-synthesis: combining synthetic chemistry and biosynthetic engineering for diversifying natural products", *Natural Product Reports*, **2008**, *25*, 25-34.

40. Brandl, E.; Margreiter, H., "Ein säurestabiles biosynthetisches Penicillin", *Oesterr Chem.-Ztg*, **1954**, *55*, 11.

41. Boecker, S.; Zobel, S.; Meyer, V.; Süssmuth, R. D., "Rational biosynthetic approaches for the production of new-to-nature compounds in fungi", *Fungal Genetics and Biology*, **2016**, *89*, 89-101.

42. Ritacco, F. V.; Graziani, E. I.; Summers, M. Y.; Zabriskie, T. M.; Yu, K.; Bernan, V. S.; Carter, G. T.; Greenstein, M., "Production of novel rapamycin analogs by precursor-directed biosynthesis", *Applied and Environmental Microbiology*, **2005**, *71*, 1971-1976.

43. Graziani, E. I.; Ritacco, F. V.; Summers, M. Y.; Zabriskie, T. M.; Yu, K.; Bernan, V. S.; Greenstein, M.; Carter, G. T., "Novel Sulfur-Containing Rapamycin Analogs Prepared by Precursor-Directed Biosynthesis", *Organic Letters*, **2003**, *5*, 2385-2388.

44. Berger, J.; Jampolsky, L.; Goldberg, M., "Borrelidin, a new antibiotic with antiborrelia activity and penicillin enhancement properties", *Archives of Biochemistry*, **1949**, *22*, 476-478.

45. Gao, Y.-M.; Wang, X.-J.; Zhang, J.; Li, M.; Liu, C.-X.; An, J.; Jiang, L.; Xiang, W.-S., "Borrelidin, a potent antifungal agent: insight into the antifungal mechanism against *Phytophthora sojae*", *Journal of Agricultural and Food Chemistry*, **2012**, *60*, 9874-9881.

46. Ishiyama, A.; Iwatsuki, M.; Namatame, M.; Nishihara-Tsukashima, A.; Sunazuka, T.; Takahashi, Y.; Omura, S.; Otoguro, K., "Borrelidin, a potent antimalarial: stage-specific inhibition profile of synchronized cultures of *Plasmodium falciparum*", *The Journal of Antibiotics*, **2011**, *64*, 381-384.

47. Wakabayashi, T.; Kageyama, R.; Naruse, N.; Tsukahara, N.; Funahashi, Y.; Kitoh, K.; Watanabet, Y., "Borrelidin is an angiogenesis inhibitor; disruption of angiogenic capillary vessels in a rat aorta matrix culture model", *The Journal of Antibiotics*, **1997**, *50*, 671-676.

48. Moss, S. J.; Carletti, I.; Olano, C.; Sheridan, R. M.; Ward, M.; Math, V.; Nur-E-Alam, M.; Braña, A. F.; Zhang, M. Q.; Leadlay, P. F., "Biosynthesis of the angiogenesis inhibitor borrelidin: directed biosynthesis of novel analogues", *Chemical Communications*, **2006**, 2341-2343.

49. Wang, Q.; Xu, L., "Beauvericin, a bioactive compound produced by fungi: a short review", *Molecules*, **2012**, *17*, 2367-2377.

50. Nilanonta, C.; Isaka, M.; Kittakoop, P.; Trakulnaleamsai, S.; Tanticharoen, M.; Thebtaranonth, Y., "Precursor-directed biosynthesis of beauvericin analogs by the insect pathogenic fungus *Paecilomyces tenuipes* BCC 1614", *Tetrahedron*, **2002**, *58*, 3355-3360.

51. Xu, Y.; Zhan, J.; Wijeratne, E. K.; Burns, A. M.; Gunatilaka, A. L.; Molnár, I., "Cytotoxic and antihaptotactic beauvericin analogues from precursor-directed biosynthesis with the insect pathogen *Beauveria bassiana* ATCC 7159", *Journal of Natural Products*, **2007**, *70*, 1467-1471.

52. Lam, K.; Gustavson, D.; Hesler, G.; Dabrah, T.; Matson, J.; Berry, R.; Rose, W.; Forenza, S., "Korkormicins, novel depsipeptide antitumor antibiotics from *Micromonospora* sp C39500: Fermentation, precursor directed biosynthesis and biological activities", *Journal of Industrial Microbiology*, **1995**, *15*, 60-65.

53. Clark, B. R.; Capon, R. J.; Lacey, E.; Tennant, S.; Gill, J. H., "Polyenylpyrroles and Polyenylfurans from an Australian Isolate of the Soil Ascomycete *Gymnoascus reessii*", *Organic Letters*, **2006**, *8*, 701-704.

54. Yamagishi, Y.; Matsuoka, M.; Odagawa, A.; Kato, S.; Shindo, K.; Mochizuki, J., "Rumbrin, a new cytoprotective substance produced by *Auxarthron umbrinum*. I. Taxonomy, production, isolation and biological activities", *The Journal of Antibiotics*, **1993**, *46*, 884-887.

55. Clark, B. R.; Murphy, C. D., "Biosynthesis of pyrrolylpolyenes in *Auxarthron umbrinum*", *Organic & Biomolecular Chemistry*, **2009**, *7*, 111-116.

56. Clark, B. R.; O'Connor, S.; Fox, D.; Leroy, J.; Murphy, C. D., "Production of anticancer polyenes through precursor-directed biosynthesis", *Organic & Biomolecular Chemistry*, **2011**, *9*, 6306-6311.

57. Pan, E.; Oswald, N. W.; Legako, A. G.; Life, J. M.; Posner, B. A.; MacMillan, J. B., "Precursor-directed generation of amidine containing ammosamide analogs: ammosamides E–P", *Chemical Science*, **2013**, *4*, 482-488.

58. Kreutzer, M. F.; Kage, H.; Herrmann, J.; Pauly, J.; Hermenau, R.; Müller, R.; Hoffmeister, D.; Nett, M., "Precursor-directed biosynthesis of micacocidin derivatives with activity against *Mycoplasma pneumoniae*", *Organic & Biomolecular Chemistry*, **2014**, *12*, 113-118.

59. Kage, H.; Kreutzer, Martin F.; Wackler, B.; Hoffmeister, D.; Nett, M., "An Iterative Type I Polyketide Synthase Initiates the Biosynthesis of the Antimycoplasma Agent Micacocidin", *Chemistry & Biology*, **2013**, *20*, 764-771.

60. Qin, Z.; Huang, S.; Yu, Y.; Deng, H., "Dithiolopyrrolone natural products: isolation, synthesis and biosynthesis", *Marine Drugs*, **2013**, *11*, 3970-3997.

61. Bouras, N.; Mathieu, F.; Sabaou, N.; Lebrihi, A., "Influence on dithiolopyrrolone antibiotic production by organic acids in *Saccharothrix algeriensis* NRRL B-24137", *Process Biochemistry*, **2007**, *42*, 925-933.

62. Bouras, N.; Merrouche, R.; Lamari, L.; Mathieu, F.; Sabaou, N.; Lebrihi, A., "Precursor-directed biosynthesis of new dithiolopyrrolone analogs by *Saccharothrix algeriensis* NRRL B-24137", *Process Biochemistry*, **2008**, *43*, 1244-1252.

63. Ratnayake, A. S.; Janso, J. E.; Feng, X.; Schlingmann, G.; Goljer, I.; Carter, G. T., "Evaluating Indole-Related Derivatives as Precursors in the Directed Biosynthesis of Diazepinomicin Analogues", *Journal of Natural Products*, **2009**, *72*, 496-499.

64. McAlpine, J. B.; Banskota, A. H.; Charan, R. D.; Schlingmann, G.; Zazopoulos, E.; Piraee, M.; Janso, J.; Bernan, V. S.; Aouidate, M.; Farnet, C. M., "Biosynthesis of diazepinomicin/ECO-4601, a *Micromonospora* secondary metabolite with a novel ring system", *Journal of Natural Products*, **2008**, *71*, 1585-1590.

65. Igarashi, Y.; Yabuta, Y.; Sekine, A.; Fujii, K.; Harada, K.-I.; Oikawa, T.; Sato, M.; Furumai, T.; Oki, T., "Directed biosynthesis of fluorinated pseurotin A, synerazol and gliotoxin", *The Journal of Antibiotics*, **2004**, *57*, 748-754.

66. Murphy, C. D.; Clark, B. R.; Amadio, J., "Metabolism of fluoroorganic compounds in microorganisms: impacts for the environment and the production of fine chemicals", *Applied Microbiology and Biotechnology*, **2009**, *84*, 617-629.

67. Wigley, L. J.; Mantle, P. G.; Perry, D. A., "Natural and directed biosynthesis of communesin alkaloids", *Phytochemistry*, **2006**, *67*, 561-569.

68. Moran, S.; Rai, D. K.; Clark, B. R.; Murphy, C. D., "Precursor-directed biosynthesis of fluorinated iturin A in *Bacillus* spp.", *Organic & Biomolecular Chemistry*, **2009**, *7*, 644-646.

69. Kurung, J. M., "*Aspergillus ustus*", *Science*, **1945**, *102*, 11-12.

70. Hogeboom, G. H.; Craig, L. C., "Identification by distribution studies VI. Isolation of antibiotic principles from *Aspergillus ustus*", *Journal of Biological Chemistry*, **1946**, *162*, 363-368.

71. Dean, F. M.; Robertson, A.; Roberts, J. C.; Raper, K. B., "Nidulin and 'Ustin': Two Chlorine-containing Metabolic Products of *Aspergillus nidulans*", *Nature*, **1953**, *172*, 344-344.

72. Dean, F.; Erni, A.; Robertson, A., "685. The chemistry of fungi. Part XXVI. Dechloronornidulin", *Journal of the Chemical Society (Resumed)*, **1956**, 3545-3548.

73. Dean, F.; Roberts, J. C.; Robertson, A., "The chemistry of fungi. Part XXII. Nidulin and nornidulin ("ustin"): chlorine-containing metabolic products of *Aspergillus nidulans*", *Journal of the Chemical Society (Resumed)*, **1954**, 1432-1439.

74. Beach, W. F.; Richards, J. H., "The structure and biosynthesis of nidulin1, 2", *The Journal of Organic Chemistry*, **1963**, *28*, 2746-2751.

75. Zhang, Y.; Mu, J.; Feng, Y.; Wen, L.; Han, J., "Four chlorinated depsidones from a seaweed-derived strain of *Aspergillus unguis* and their new biological activities", *Natural Product Research*, **2014**, *28*, 503-506.

76. Xu, Y.-J.; Chiang, P.-Y.; Lai, Y.-H.; Vittal, J.; Wu, X.-H.; Tan, B.; Imiyabir, Z.; Goh, S.-H., "Cytotoxic prenylated depsidones from *Garcinia parvifolia*", *Journal of Natural Products*, **2000**, *63*, 1361-1363.

77. Lang, G.; Cole, A. L.; Blunt, J. W.; Robinson, W. T.; Munro, M. H., "Excelsione, a depsidone from an endophytic fungus isolated from the New Zealand endemic tree *Knightia excelsa*", *Journal of Natural Products*, **2007**, *70*, 310-311.

78. Honda, N.; Pavan, F. R.; Coelho, R.; de Andrade Leite, S.; Micheletti, A.; Lopes, T.; Misutsu, M.; Beatriz, A.; Brum, R.; Leite, C. Q. F., "Antimycobacterial activity of lichen substances", *Phytomedicine*, **2010**, *17*, 328-332.

79. Kokubun, T.; Shiu, W. K.; Gibbons, S., "Inhibitory activities of lichen-derived compounds against methicillin-and multidrug-resistant *Staphylococcus aureus*", *Planta Medica*, **2007**, *73*, 176-179.

80. Shrestha, G.; Clair, L. L. S., "Lichens: a promising source of antibiotic and anticancer drugs", *Phytochemistry Reviews*, **2013**, *12*, 229-244.

81. Lohézic-Le Dévéhat, F.; Tomasi, S.; Elix, J. A.; Bernard, A.; Rouaud, I.; Uriac, P.; Boustie, J., "Stictic acid derivatives from the lichen Usnea articulata and their antioxidant activities", *Journal of Natural Products*, **2007**, *70*, 1218-1220.

82. Neamati, N.; Hong, H.; Mazumder, A.; Wang, S.; Sunder, S.; Nicklaus, M. C.; Milne, G. W.; Proksa, B.; Pommier, Y., "Depsides and depsidones as inhibitors of HIV-1 integrase: discovery of novel inhibitors through 3D database searching", *Journal of Medicinal Chemistry*, **1997**, *40*, 942-951.

83. Armaleo, D.; Sun, X.; Culberson, C., "Insights from the first putative biosynthetic gene cluster for a lichen depside and depsidone", *Mycologia*, **2011**, *103*, 741-754.

84. Sierankiewicz, J.; Gatenbeck, S., "A new depsidone from *Aspergillus nidulans*", *Acta Chem. Scand*, **1972**, *26*.

85. Sureram, S.; Kesornpun, C.; Mahidol, C.; Ruchirawat, S.; Kittakoop, P., "Directed biosynthesis through biohalogenation of secondary metabolites of the marine-derived fungus *Aspergillus unguis*", *RSC Advances*, **2013**, *3*, 1781-1788.

86. Feighner, S. D.; Salituro, G. M.; Smith, J. L.; Tsou, N. N., Unguinol and analogs are animal growth permittants. US Patent 5350763 A: 1994.

87. Kawahara, N.; Nakajima, S.; Satoh, Y.; Yamazaki, M.; Kawai, K.-I., "Studies on fungal products. XVIII: Isolation and structures of a new fungal depsidone related to nidulin and a new phthalide from *Emericella unguis*", *Chemical and Pharmaceutical Bulletin*, **1988**, *36*, 1970-1975.

88. Kawahara, N.; Nozawa, K.; Nakajima, S.; Kawai, K.-i.; Yamazaki, M., "Isolation and structures of novel fungal depsidones, emeguisins A, B, and C, from *Emericella unguis*", *Journal of the Chemical Society, Perkin Transactions 1*, **1988**, 2611-2614.

89. Hamano, K.; Kinoshita-Okami, M.; Hemmi, A.; Sato, A.; Hisamoto, M.; Matsuda, K.; Yoda, K.; Haruyama, H.; Hosoya, T.; Tanzawa, K., "Folipastatin, a new depsidone compound from *Aspergillus unguis* as an inhibitor of phospholipase A2. Taxonomy, fermentation, isolation, structure determination and biological properties", *The Journal of Antibiotics*, **1992**, *45*, 1195-1201.

90. Nielsen, J.; Nielsen, P. H.; Frisvad, J. C., "Fungal depside, guisinol, from a marine derived strain of *Emericella unguis*", *Phytochemistry*, **1999**, *50*, 263-265.

91. Cao, S.; Lee, A. S.; Huang, Y.; Flotow, H.; Ng, S.; Butler, M. S.; Buss, A. D., "Agonodepsides A and B: two new depsides from a filamentous fungus F7524", *Journal of Natural Products*, **2002**, *65*, 1037-1038.

92. Sureram, S.; Wiyakrutta, S.; Ngamrojanavanich, N.; Mahidol, C.; Ruchirawat, S.; Kittakoop, P., "Depsidones, aromatase inhibitors and radical scavenging agents from the marine-derived fungus *Aspergillus unguis* CRI282-03", *Planta Medica*, **2012**, *78*, 582-588.

93. Pawlowski, A. C.; Johnson, J. W.; Wright, G. D., "Evolving medicinal chemistry strategies in antibiotic discovery", *Current Opinion in Biotechnology*, **2016**, *42*, 108-117.

94. Fischbach, M. A.; Walsh, C. T., "Antibiotics for emerging pathogens", *Science*, **2009**, *325*, 1089-1093.

95. Gqaleni, N.; Smith, J. E.; Lacey, J.; Gettinby, G., "Effects of temperature, water activity, and incubation time on production of aflatoxins and cyclopiazonic acid by an isolate of *Aspergillus flavus* in surface agar culture", *Applied and Environmental Microbiology*, **1997**, *63*, 1048-1053.

96. Frisvad, J.; Samson, R., "Filamentous fungi in foods and feeds: ecology, spoilage and mycotoxin production", *Handbook of Applied Mycology*, **1991**, *3*, 31-68.

97. VanderMolen, K. M.; Raja, H. A.; El-Elimat, T.; Oberlies, N. H., "Evaluation of culture media for the production of secondary metabolites in a natural products screening program", *AMB Express*, **2013**, *3*, 1.

98. Larsen, T. O.; Smedsgaard, J.; Nielsen, K. F.; Hansen, M. E.; Frisvad, J. C., "Phenotypic taxonomy and metabolite profiling in microbial drug discovery", *Natural Product Reports*, **2005**, *22*, 672-695.

99. Silber, J.; Kramer, A.; Labes, A.; Tasdemir, D., "From Discovery to Production: Biotechnology of Marine Fungi for the Production of New Antibiotics", *Marine Drugs*, **2016**, *14*, 137.

100. Netzker, T.; Fischer, J.; Weber, J.; Mattern, D. J.; König, C. C.; Valiante, V.; Schroeckh, V.; Brakhage, A. A., "Microbial communication leading to the activation of silent fungal secondary metabolite gene clusters", *Frontiers in Microbiology*, **2015**, *6*.

101. Legaz, M. E.; Vicente, C.; de Armas, R., Bioproduction of depsidones for pharmaceutical purposes In *Drug Development – a Case Study Based Insight into Modern Strategies*, Rundfeld, C., Ed. Intech Open Access Publisher: 2011.

102. Rezanka, T.; Guschina, I. A., "Brominated depsidones from *Acarospora gobiensis*, a lichen of Central Asia", *Journal of Natural Products*, **1999**, *62*, 1675-1677.

103. Huneck, S.; Djerassi, C.; Becher, D.; Barber, M.; Von Ardenne, M.; Steinfelder, K.; Tümmler, R., "Flechteninhaltsstoffe—XXXI", *Tetrahedron*, **1968**, *24*, 2707-2755.

104. Sierankiewicz, J.; Gatenbeck, S., "The biosynthesis of nidulin and trisdechloronornidulin", *Acta Chem. Scand*, **1973**, *27*, 2710-2716.

105. Traber, R.; Hofmann, H.; Kobel, H., "Cyclosporins. New analogues by precursor directed biosynthesis", *The Journal of Antibiotics*, **1989**, *42*, 591-597.

106. Moussaïf, M.; Jacques, P.; Schaarwächter, P.; Budzikiewicz, H.; Thonart, P., "Cyclosporin C is the main antifungal compound produced by *Acremonium luzulae*", *Applied and Environmental Microbiology*, **1997**, *63*, 1739-1743.

107. Blasiak, L. C.; Drennan, C. L., "Structural perspective on enzymatic halogenation", *Accounts of Chemical Research*, **2008**, *42*, 147-155.

108. Wagner, C.; El Omari, M.; König, G. M., "Biohalogenation: Nature's Way to Synthesize Halogenated Metabolites", *Journal of Natural Products*, **2009**, *72*, 540-553.

109. Elix, J. A.; Wardlaw, J. H., "A new chloro-depside from the lichen Hypotrachyna leiophylla", *Australian Journal of Chemistry*, **2001**, *53*, 1007-1008.

110. Reddy, K. S. K.; Narender, N.; Rohitha, C.; Kulkarni, S., "Iodination of aromatic compounds using potassium iodide and hydrogen peroxide", *Synthetic Communications*, **2008**, *38*, 3894-3902.

111. Uchida, R.; Nakajyo, K.; Kobayashi, K.; Ohshiro, T.; Terahara, T.; Imada, C.; Tomoda, H., "7-Chlorofolipastatin, an inhibitor of sterol O-acyltransferase, produced by marine-derived *Aspergillus ungui* NKH-007", *The Journal of Antibiotics*, **2016**.

112. Harris, C. M.; Kannan, R.; Kopecka, H.; Harris, T. M., "The role of the chlorine substituents in the antibiotic vancomycin: preparation and characterization of mono-and didechlorovancomycin", *Journal of the American Chemical Society*, **1985**, *107*, 6652-6658.

113. Klaiklay, S.; Rukachaisirikul, V.; Aungphao, W.; Phongpaichit, S.; Sakayaroj, J., "Depsidone and phthalide derivatives from the soil-derived fungus *Aspergillus unguis* PSU-RSPG199", *Tetrahedron Letters*, **2016**, *57*, 4348-4351.

114. Bode, H. B.; Bethe, B.; Höfs, R.; Zeeck, A., "Big effects from small changes: possible ways to explore nature's chemical diversity", *ChemBioChem*, **2002**, *3*, 619-627.

115. Deepika, V.; Murali, T.; Satyamoorthy, K., "Modulation of genetic clusters for synthesis of bioactive molecules in fungal endophytes: A review", *Microbiological Research*, **2016**, *182*, 125-140.

116. Chiang, Y.-M.; Szewczyk, E.; Davidson, A. D.; Keller, N.; Oakley, B. R.; Wang, C. C., "A gene cluster containing two fungal polyketide synthases encodes the biosynthetic pathway for a polyketide, asperfuranone, in *Aspergillus nidulans*", *Journal of the American Chemical Society*, **2009**, *131*, 2965-2970.

117. Bok, J. W.; Chiang, Y.-M.; Szewczyk, E.; Reyes-Dominguez, Y.; Davidson, A. D.; Sanchez, J. F.; Lo, H.-C.; Watanabe, K.; Strauss, J.; Oakley, B. R., "Chromatin-level regulation of biosynthetic gene clusters", *Nature Chemical Biology*, **2009**, *5*, 462-464.

118. Gribble, G. W., "Naturally occurring organohalogen compounds--a survey", *Journal of Natural Products*, **1992**, *55*, 1353-1395.

119. Niu, S.; Liu, D.; Hu, X.; Proksch, P.; Shao, Z.; Lin, W., "Spiromastixones A–O, antibacterial chlorodepsidones from a deep-sea-derived Spiromastix sp. Fungus", *Journal of Natural Products*, **2014**, *77*, 1021-1030.

120. Piggott, A. M.; Karuso, P., "Identifying the cellular targets of natural products using T7 phage display", *Natural Product Reports*, **2016**, *33*, 626-636.

8 Supplementary Material

8.1 Recipes for microbiological media

Glycerol casein agar (GCA)	
Ingredient	Quantity
Glycerol	30 g
Casein peptone (Amyl)	2 g
K_2HPO_4	1 g
NaCl	1gm
$MgSO_4.7H_2O$	0.5 g
Trace element solution*	5 mL
Deionised water	1000 mL
Bacteriological agar[a] (Amyl)	20 g
Autoclave	121 °C

*Trace element solution	
$CaCl_2.2H_2O$	3 g
$FeC_6O_7H_5$	1 g
$MnSO_4$	0.2 g
$ZnCl_2$	0.1 g
$CuSO_4.5H_2O$	0.025 g
$Na_2B_4O_7.10H_2O$	0.02 g
$CoCl_2$	0.004
$Na_2MoO_4.2H_2O$	0.01
Deionised water	1000 mL
Filter sterilise	

Yeast Extract agar	
Ingredient	Quantity
Yeast Extract (Difco)	20 g
Sucrose (Amyl)	150 g
Bacteriological Agar[a] (Amyl)	20 g
Deionised water	1000 mL
Autoclave	121 °C

Malt extract agar	
Ingredient	Quantity
Bacteriological peptone (Difco)	3 g
Malt Extract (Amyl)	60 g
Bacteriological glucose (Amyl)	60 g
Distilled water	1000 mL
Adjust pH to 5.5	
Bacteriological agar[a] (Amyl)	20 g
Autoclave	121 °C

Czapeks Dox agar	
Ingredient	Quantity
Czapeks Dox Media (Oxoid)	45.4 g
Deionised water	1000 mL
Autoclave	121 °C

Oatmeal agar	
Ingredient	Quantity
Oatmeal	60 g
Agar[a]	12.5
Distilled water	1000 mL
Autoclave	121 °C

[a] Omit agar for liquid media

8.2 Tabulated NMR data

Table S1: NMR data for 7-carboxyfolipastatin (**7**) in DMSO-d_6

Position	δ_H, mult (J in Hz)	δ_C	^{1}H-^{13}C HMBC	COSY	ROESY
1		148.1			
2	6.55, s	111.4	3, 4, 11, 11a, 1″		2″, 4″
3		159.9[a]			
4		113.2			
4a		162.0[a]			
5a		139.5			
6		136.8			
7		114.6			
8		160.3			
9		114.0			
9a		143.8			
11		163.9			
11a		110.5			
1′		133.7			
2′	4.93, qq (6.7, 1.5)	119.6	6, 3′, 4′	3′	
3′	1.65, dq (6.7, 1.0)	13.9	1′, 2′	2′	4′, 4-Me
4′	1.81, dq (1.5, 1.0)	18.8	6, 1′, 2′		3′, 4-Me
1″		135.9			
2″	5.34, qq (6.7, 1.6)	123.5	1, 3″, 4″	3″	2
3″	1.64, dq (6.7, 1.0)	14.1	1″, 2″	2″	4″
4″	1.78, dq (1.6, 1.0)	17.5	1, 1″, 2″		2, 3″
4-Me	2.06, s	8.5	3, 4, 4a		3′, 4′
9-Me	2.03, s	9.0	8, 9, 9a		
3-OH					
8-OH					
7-CO_2H		169.7			

[a] Assignment interchangeable

Table S2: NMR data for unguinolic acid (**8**) in DMSO-d_6

Position	δ_H, mult (J in Hz)	δ_C	^{1}H-^{13}C HMBC	COSY	ROESY
1		114.9			
2		157.2			
3	5.76, d (2.3)	99.1	1, 2, 4, 5	5	4″, 4-OH
4		158.9			
5	6.22, d (2.3)	110.5	1, 3, 4, 1-CO_2H, 6-Me	3, 6-Me	6-Me, 4-OH
6		137.9			
1′		148.1			
2′		110.3			
3′		152.9			
4′	6.20, s	105.5	2′, 3′, 6′, 1″		4″, 3′-OH
5′		135.9			
6′		131.6			
1″		133.2			
2″	5.48, qq (6.8, 1.4)	124.0	5′, 3″, 4″	3″	
3″	1.56, dq (6.8, 0.9)	13.8	1″, 2″	2″	4″
4″	1.75, dq (1.4, 0.9)	16.6	5′, 1″, 2″		4′, 3″
6-Me	2.22, s	19.8	1, 5, 6	5	5
2′-Me	1.95, s	8.9	1′, 2′, 3′		3′-OH
4-OH	9.60, s		3, 4, 5		3, 5
1′-OH	8.52, br s				
3′-OH	9.14, s		2′, 3′, 4′		4′, 2′-Me
1-CO_2H	12.78, br s	169.0			

Table S3: NMR data for unguidepside A (**9**) in DMSO-d_6

Position	δ_H, mult (J in Hz)	δ_C	^{1}H-^{13}C HMBC	COSY	ROESY
1		108.3			
2		160.0			
3	6.22, d (2.4)	100.4	1, 2, 5		2-OH, 4-OH
4		161.1			
5	6.21, d (2.4)	109.8	3, 4, 7, 6-Me	6-Me	6-Me
6		140.3			
7		166.9			
1′		112.1			
2′		158.8			
3′		116.8			
4′		151.6			
5′	6.45, s	114.1	7, 1′, 3′, 4′, 1″		4″
6′		145.4			
1″		136.9			
2″	5.30, qq (6.7, 1.4)	121.5	6′, 3″, 4″	3″	
3″	1.65, dq (6.7, 1.1)	13.7	1″, 2″	2″	4″
4″	1.85, dq (1.4, 1.1)	18.2	6′, 1″, 2″		5′, 3″
6-Me	2.34, s	21.3	1, 5, 6	5	5
3′-Me	2.01, s	9.2	2′, 3′, 4′		
2-OH	10.34, s		1, 2, 3		3
4-OH	9.99, s		3, 4, 5		3
2′-OH	11.39, br s				
1′-CO_2H	13.63, br s	171.8			

Table S4: NMR data for 2-bromo-7-chlorounguinol (**17**) in DMSO-d_6

Position	δ_H, mult (J in Hz)	δ_C	^{1}H-^{13}C HMBC	COSY	ROESY
1		141.3			
2		113.0			
3		157.6			
4	6.58, s	105.1	2, 3, 4a, 11a		3′, 4′, 3-OH
4a		161.7			
5a		141.0			
6		135.9			
7		117.0			
8		149.7			
9		108.2			
9a		142.1			
11		160.5			
11a		119.2			
1′		130.7			
2′	5.25, qq (6.8, 1.1)	126.1	3′, 4′, 6	3′	
3′	1.85, dq (6.8, 1.1)	13.5	4′, 2′, 1′	2′	4
4′	1.86, s	17.1	1′, 2′, 3′, 6,		4
1-Me	2.38, s	18.2	1, 2, 11, 11a		
9-Me	2.17, s	10.5	8, 9, 9a		8-OH
3-OH	11.52, s				4
8-OH	9.28, s		7, 8, 9		9-Me

Table S5: NMR data for unguidepside B (**18**) in DMSO-d_6

Position	δ_H, mult (J in Hz)	δ_C	^{1}H-^{13}C HMBC	COSY	ROESY
1		106.9			
2		158.9			
3		96.1			
4		159.1			
5	6.50, s	110.9	1, 3, 4, 7, 6-Me	6-Me	6-Me, 4-OH
6		140.3			
7		167.8			
1′		112.8			
2′		158.5			
3′		116.6			
4′		151.0			
5′	6.57, s	114.0	1′, 3′, 4′, 1″	3′-Me	4″
6′		145.4			
1″		136.7			
2″	5.32, qq (6.8, 1.4)	121.7	6′, 3″, 4″	3″	
3″	1.65, dq (6.8, 1.0)	13.7	1″, 2″	2″	4″
4″	1.85, dq (1.4, 1.0)	18.1	6′, 1″, 2″		5′, 3″
6-Me	2.40, s	22.6	1, 5, 6, 7	5	5
3′-Me	1.99, s	9.3	2′, 3′, 4′	5′	
2-OH	11.16, s		1, 2, 3		
4-OH	11.13, s		3		5
2′-OH	11.31, br s				
1′-CO_2H	13.64, br s	171.6			

Table S6: NMR data for 5-bromoagonodepside B (**19**) in DMSO-d_6

Position	δ_H, mult (J in Hz)	δ_C	^{1}H-^{13}C HMBC	COSY	ROESY
1		113.1			
2		154.5[a]			
3		112.7			
4		154.2[a]			
5		103.2			
6		142.5			
7		166.0			
1′		112.0			
2′		159.0			
3′		116.9			
4′		151.6			
5′	6.30, s	113.7	1′, 3′, 4′, 1″, 1′-CO_2H		2″, 3″, 4″
6′		145.5			
1″		137.0			
2″	5.30, qq (6.5, 1.4)	121.5	6′, 3″, 4″	3″	3″
3″	1.65, dq (6.5, 1.0)	13.7	6′, 1″, 2″, 4″	2″	4″
4″	1.84, dq (1.4, 1.0)	18.2	6′, 1″, 2″		5′, 3″
1‴		136.0			
2‴	5.31, qq (6.5, 1.4)	123.9	6, 3‴, 4‴	3‴	3‴
3‴	1.66, dq (6.5, 1.0)	13.4	6, 1‴, 2‴, 4‴	2″	4‴
4‴	1.87, dq (1.4, 1.0)	17.2	6, 1‴, 2‴		3‴
3-Me	2.12, s	10.0	2, 3, 4, 6		2-OH, 4-OH
3′-Me	1.99, s	9.0	2′, 3′, 4′		
2-OH	9.69, s		1, 2		3-Me
4-OH	9.42, s		3, 4, 5		3-Me
2′-OH	11.41, br s				
1′-CO_2H	13.62, br s	171.7			

[a] Assignment interchangeable

Table S7: NMR data for 1′,2'-dihydrounguinol (**27**) in DMSO-d_6

Position	δ_H, mult (J in Hz)	δ_C	^{1}H-^{13}C HMBC	COSY	ROESY
1		144.7			
2	6.57, dd (2.4, 0.8)	115.6	3, 4, 11, 11a, 1-Me	4, 1-Me	1-Me, 3-OH
3		161.8			
4	6.54, d (2.4)	104.4	2, 3, 4a, 11a	2	3-OH
4a		163.1			
5a		141.0			
6		136.1			
7	6.49, s	108.0	5a, 8, 9, 1′		8-OH
8		152.9			
9		113.6			
9a		142.8			
11		162.5			
11a		111.6			
1′	3.25, m	32.9	5a, 6, 7, 2′, 3′, 4′		
2′	1.51, m	29.8	6, 1’, 3’, 4’,	3′	
3′	0.79, t (7.3)	12.1	1’, 2’	2′	4′
4′	1.11, d (7.0)	21.4	6, 1’, 2’		3′
1-Me	2.33, s	20.6	1, 2, 11, 11a		2
9-Me	2.03, s	9.1	8, 9, 9a		8-OH
3-OH	10.61, s		2, 3, 4		2, 4
8-OH	9.49, s		7, 8, 9		7, 9-Me

Table S8: NMR data for 2,7-dibromo-1′,2'-dihydrounguinol (**28**) in DMSO-d_6

Position	δ_H, mult (J in Hz)	δ_C	^{1}H-^{13}C HMBC	COSY	ROESY
1		143.5			
2		111.3			
3		158.6			
4	6.86, s	104.6			
4a		161.3			
5a					
6		134.0			
7					4′
8		149.9			
9		116.7			
9a		142.3			
11		161.7			
11a		113.2			
1′	3.74, br s	34.1			
2′	1.81, m	26.2	6, 3′	3′	
	1.99, m		6, 3′	3′	
3′	0.82, br s	12.7		2′	
4′	1.34, d (7.2)	18.0	6, 1′, 2′		7
1-Me	2.44, s	21.6	1, 2, 3, 11, 11a		
9-Me	2.16, s	10.7	8, 9, 9a		8-OH
3-OH	11.63, s				
8-OH	9.23, s		9		9-Me

Table S9: NMR data for 2,4,7-tribromo-1′,2'-dihydrounguinol (**29**) in DMSO-d_6

Position	δ_H, mult (J in Hz)	δ_C	^{1}H-^{13}C HMBC	COSY	ROESY
1		142.2			
2		114.1			
3		158.7			
4		100.4			
4a		156.0			
5a		143.4			
6		134.2			
7		108.4			
8		150.4			
9		116.7			
9a		141.8			
11		161.3			
11a		113.0			
1′	4.44, br s	33.6		4′	3′, 4′
2′	1.76, m	25.7	6, 1′, 3′, 4′	3′	
	2.00, m		6, 1′, 3′, 4′	3′	
3′	0.7, t (7.3)	12.3	1′, 2′	2′	1′
4′	1.30, d (7.2)	18.0	6, 1′, 2′	1′	1′
1-Me	2.41, s	22.3	1, 2, 4a, 11, 11a		
9-Me	2.19, s	10.7	5a, 8, 9, 9a		8-OH
3-OH	11.15, s				
8-OH	9.30, s		7, 8, 9		9-Me

Table S10: NMR data for 2,4-diiodo-1′,2'-dihydrounguinol (**30**) in DMSO-d_6

Position	δ_H, mult (J in Hz)	δ_C	^{1}H-^{13}C HMBC	COSY	ROESY
1		146.3			
2		92.3			
3		160.4			
4		76.9			
4a		162.1			
5a		142.1			
6		136.5			
7	6.52, s	108.3	5a, 8, 9, 1′		2′, 4′, 8-OH
8		153.4			
9		113.9			
9a		142.5			
11		163.0			
11a		113.9			
1′	3.98, m	32.9	5a, 6, 7, 2′, 3′, 4′	2′, 4′	2′, 3′
2′	1.49, m	29.8	6, 1′, 3′, 4′,	1, 3′	7, 1′, 3′, 4′
3′	0.79, t (7.3)	11.7	1′, 2′		1′ 2′, 4′
4′	1.05, d (6.9)	21.6	6, 1′, 2′	1	7, 2′, 3′
1-Me	2.45, s	28.2	1, 2, 3, 11, 11a		
9-Me	2.06, s	9.1	8, 9, 9a		
3-OH	10.47, br s				
8-OH	9.61, s		7, 8, 9		7

Table S11: NMR data for 3,8-di-*O*-methylunguinol (**31**) in DMSO-d_6

Position	δ_H, mult (J in Hz)	δ_C	^{1}H-^{13}C HMBC	COSY	ROESY
1		144.6			
2	6.78, d (2.5)	114.4	4, 11, 11a, 1-Me	4	1-Me, 3-OMe
3		162.8[a]			
4	6.42, d (2.5)	103.1	2, 3, 4a	2	3-OMe
4a		162.1[a]			
5a		141.2			
6		135.5			
7	6.57, s	107.2	5a, 8, 9, 1′		8-OMe
8		154.3			
9		116.4			
9a		142.8			
11		162.6			
11a		113.0			
1′		132.4			
2′	5.53, qq (6.8, 1.5)	125.6	6, 3′, 4′	3′, 4′	
3′	1.8, dq, (6.8, 1.2)	13.7	1′, 2′	2′, 4′	4′
4′	2.04, dq (1.5, 1.2)	17.7	6, 2′, 1′	2′, 3′	3′
1-Me	2.38, s	20.6	1, 2, 11, 11a		2
9-Me	2.07, s	9.0	8, 9, 9a		
3-OMe	3.77, s	55.7	3		2, 4
8-OMe	3.76, s	56.0	8		7

[a] Assignment interchangeable

Table S12: NMR data for 3-*O*-benzylunguinol (**32**) in DMSO-d_6

Position	δ_H, mult (J in Hz)	δ_C	^{1}H-^{13}C HMBC	COSY	ROESY
1		144.5			
2	6.87, d (2.6)	115.2	4, 11a, 1-Me,	4, 1-Me	1-Me, 1″
3		161.7[a]			
4	6.46, d (2.6)	103.8	2, 4a, 11,	2	
4a		162.2[a]			
5a		140.2			
6		135.2			
7	6.41, s	110.7	5a, 8, 9, 9-Me, 1′		
8		152.6			
9		114.7			
9a		143.1			
11		162.8			
11a		113.4			
1′		132.2			
2′	5.45, qq (6.7, 1.5)	125.1	6, 3′, 4′	3′	
3′	1.75, dq (6.7, 1.1)	13.7	1′, 2′	2′	4′
4′	1.93, dq (1.5, 1.1)	17.6	6, 1′, 2′		3′
1″	5.14, s	69.6	3, 3″, 7″		2
2″		136.1			
3″/7″	7.39, m	127.5			
4″/6″	7.38, m	128.5			
5″	7.32, m	128.1			
1-Me	2.38, s	20.6	1, 2, 11, 11a	2	2
9-Me	2.04, s	9.2	8, 9, 9a		
8-OH	9.62, br s				

[a] Assignment interchangeable

Table S13: NMR data for 3,8-di-*O*-benzylunguinol (**33**) in DMSO-d_6

Position	δ_H, mult (J in Hz)	δ_C	^{1}H-^{13}C HMBC	COSY	ROESY
1		144.6			
2	6.88, d (2.45)	115.4	3, 4, 11a, 1-Me	4, 1-Me	1-Me, 1″
3		161.8			
4	6.48, d (2.45)	103.9	2, 11, 11a	2	2′, 1″
4a		162.0			
5a		141.4			
6		135.3			
7	6.68, s	108.8	5a, 6, 8, 9, 1′		2′, 1‴
8		153.3			
9		116.9			
9a		142.9			
11		162.6			
11a		113.3			
1′		132.1			
2′	5.51, qq (6.8, 1.4)	125.7	6, 3′, 4′	3′	4, 7
3′	1.77, dq (6.8, 1.1)	13.8	6, 1′, 2′	2′	
4′	1.96, dq (1.4, 1.1)	17.6	6, 1′, 2′		
1″	5.15, s	69.6	3, 2″, 3″/7″		2, 4
2″		136.1			
3″/7″	7.39, m	127.5			
4″/6″	7.38, m	128.5			
5″	7.33, m	128.1			
1‴	5.08, s	69.9	8, 2‴, 3‴/7‴		7
2‴		137.0			
3‴/7‴	7.41, m	127.3			
4‴/6‴	7.38, m	128.4			
5‴	7.31, m	127.8			
1-Me	2.38, s	20.6	1, 2, 11, 11a,	2	2
9-Me	2.13, s	9.2	8, 9, 9a		

8.3 Antibacterial activity of nidulin derivatives against *Bacillus subtilis*

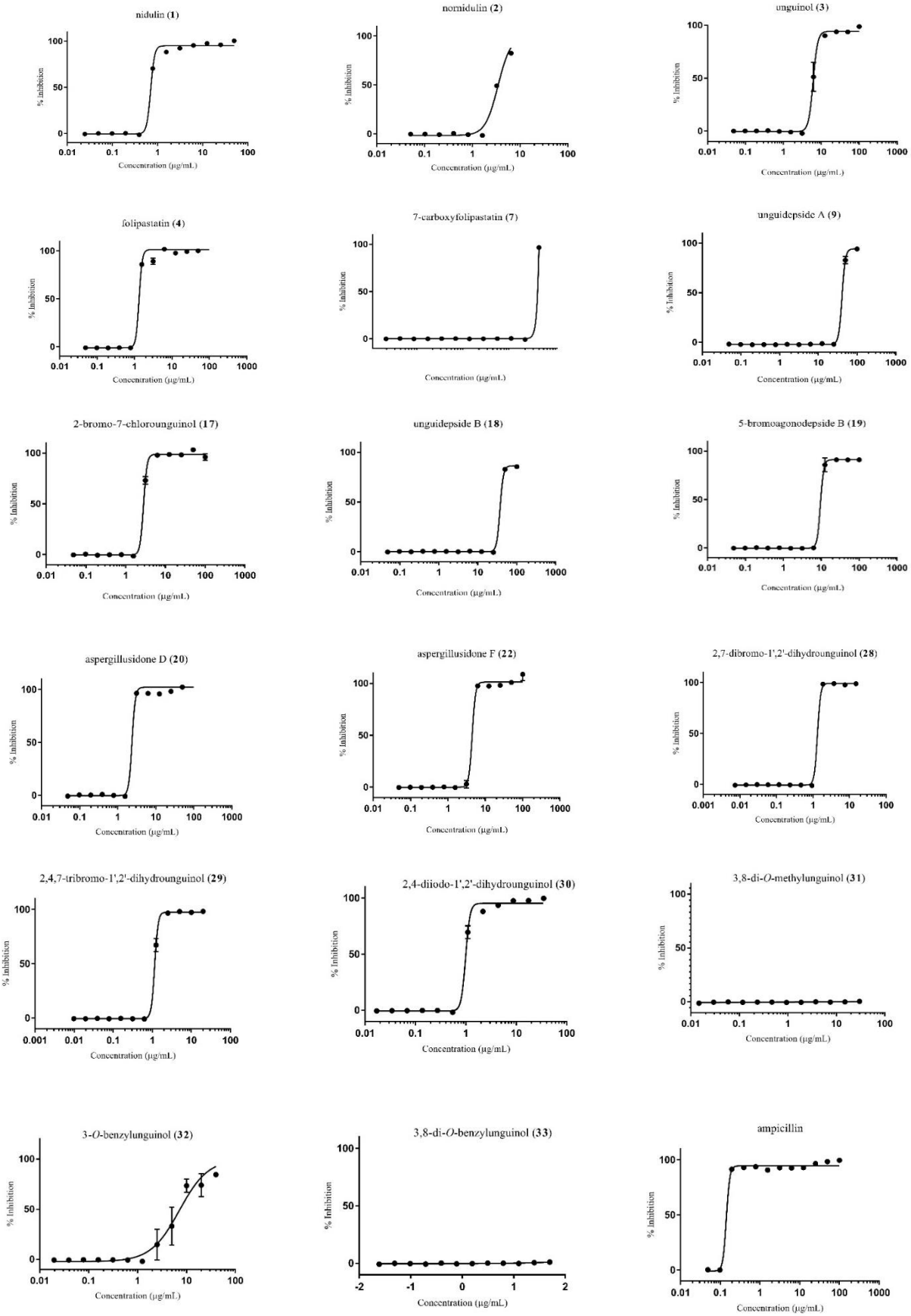

8.4 Antibacterial activity nidulin derivatives against *Staphylococcus aureus*

nidulin (**1**)

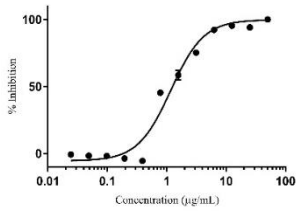

unguinol (**3**)

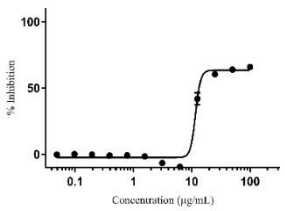

folipastatin (**4**)

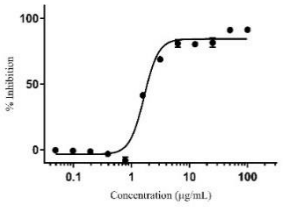

7-carboxyfolipastatin (**7**)

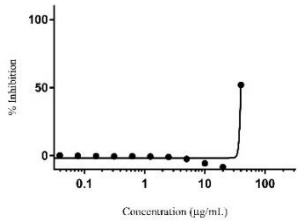

unguidepside A (**9**)

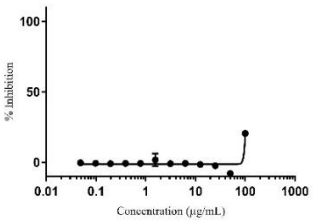

2-bromo-7-chlorounguinol (**17**)

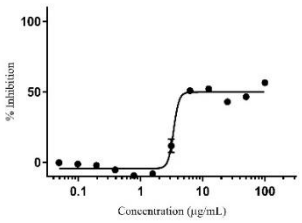

unguidepside B (**18**)

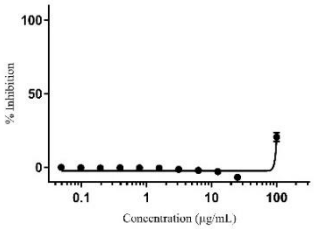

5-bromoagonodepside B (**19**)

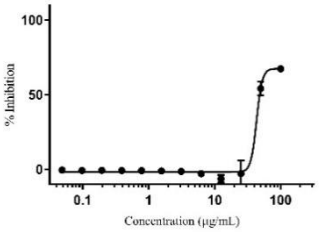

aspergillusidone D (**20**)

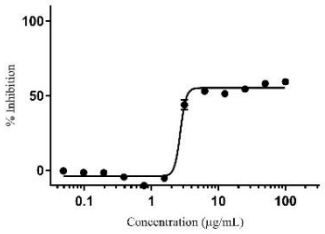

aspergillusidone F (**22**)

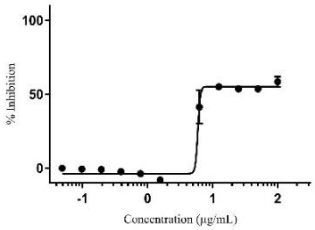

2,7-dibromo-1',2'-dihydrounguinol (**28**)

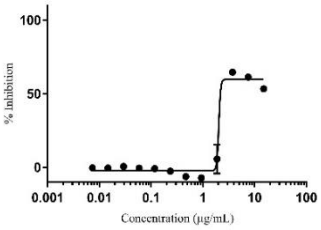

2,4,7-tribromo-1',2'-dihydrounguinol (**29**)

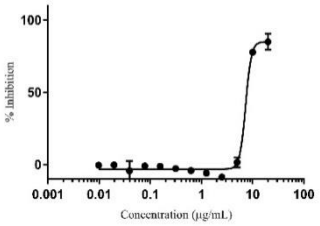

2,4-diiodo-1',2'-dihydrounguinol (**30**)

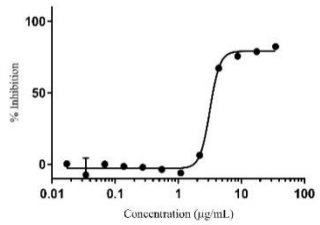

3,8-di-*O*-methylunguinol (**31**)

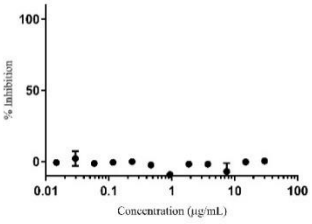

3-*O*-benzylunguinol (**32**)

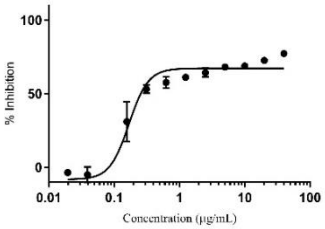

3,8-di-*O*-benzylunguinol (**33**)

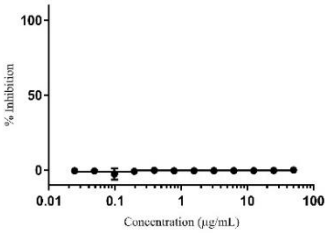

8.5 Antifungal activity of nidulin derivatives against *Saccharomyces cerevisiae*

nidulin (**1**)

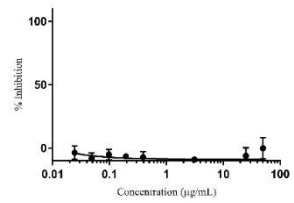

nornidulin (**2**)

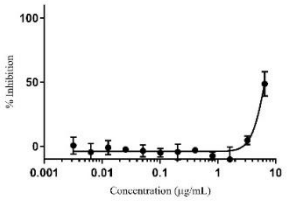

unguinol (**3**)

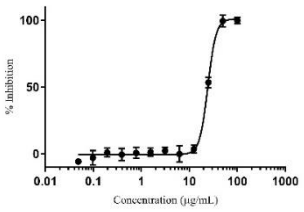

folipastatin (**4**)

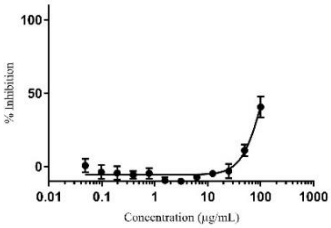

7-carboxyfolipastatin (**7**)

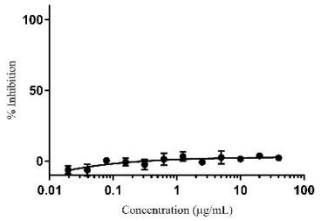

unguidepside A (**9**)

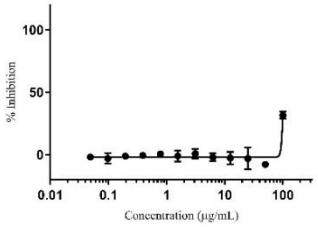

2-bromo-7-chlorounguinol (**17**)

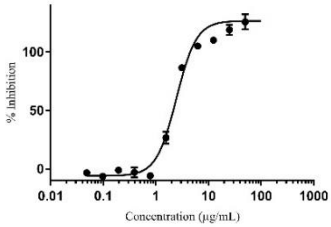

unguidepside B (**18**)

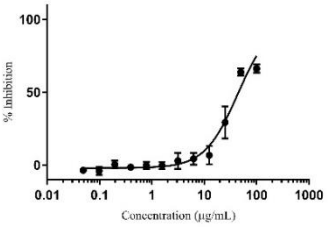

5-bromoagonodepside B (**19**)

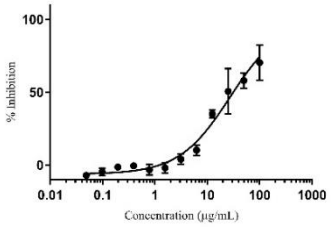

aspergillusidone D (**20**)

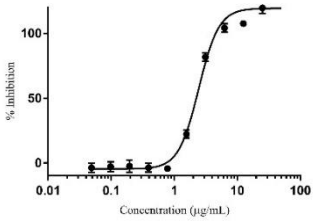

aspergillusidone F (**22**)

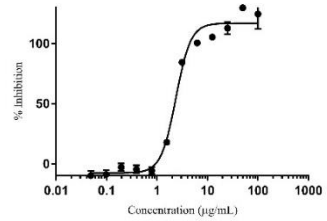

2,7-dibromo-1',2'-dihydrounguinol (**28**)

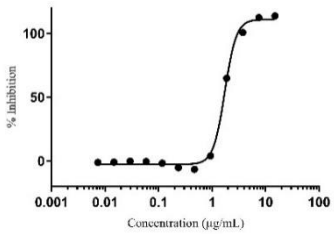

2,4,7-tribromo-1',2'-dihydrounguinol (**29**)

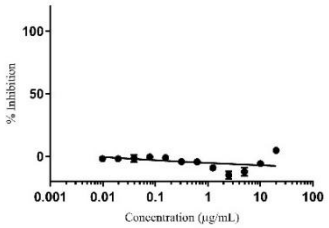

2,4-diiodo-1',2'-dihydrounguinol (**30**)

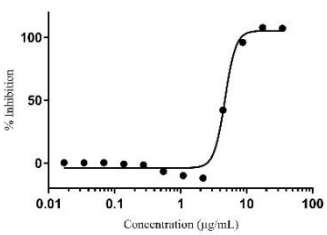

3,8-di-*O*-methylunguinol (**31**)

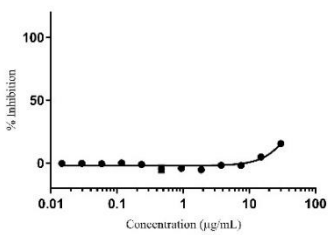

3-*O*-benzylunguinol (**32**)

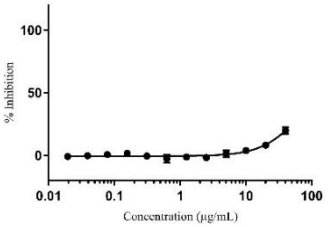

3,8-di-*O*-benzylunguinol (**33**)

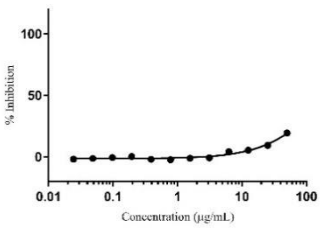

Clotrimazole